Vol. 6, №1, 2022 ISSN 2520-6133

KHAZAR JOURNAL OF SCIENCE AND TECHNOLOGY (KJSAT)

Hamlet Isayev/Isaxanli[1] *
Editor-in-Chief
Khazar University, Azerbaijan

[1] Also H. Issakhanly, H. Isakhanly, H. Isakhanli, H.A.Isayev, G.A.Isayev, or G.A.Isaev due to differences in transliteration. I use Hamlet Isayev in mathematics and science fields and Hamlet Isakhanli/Isaxanli in humanities.

Khazar University
41 Mehseti str., Baku AZ1096
Republic of Azerbaijan
Tel: (99412) 4217927
Website: **www.kjsat.com**

KHAZAR UNIVERSITY PRESS

Contents

Khazar Journal of Science and Technology Volume 6 №1 2022, 5-16
© Khazar University Press 2022 DOI: 10.5782/2520-6133.2022.6.1.5

Ecological Analyses of Subnivale Vegetation of Azerbaijan in the Context of Climate Change

Elman Yusifov
Institute of Botany of ANAS, Laboratory of Ethnobotany
Assos/ prof., PhD in Physics
yusifov_e@yahoo.com

Abstract

The study is devoted to the analysis of changes in the structure and distribution of vegetation in the subnivale landscapes of Azerbaijan in the context of climate change. As a result of the conducted research, it was found that the vegetation of the subnival landscapes of Azerbaijan consists of 136 species belonging to 28 families and 83 genera, and makes up 3% of the country's flora. Among the families, *Asteraceae* (25), *Poaceae* (15), *Caryophyllaceae* (13), *Brassicaceae* (8), *Saxifragaceae* (7), *Ranunculaceae* (6), *Lamiaceae* (5) are the richest and dominant ones. As a result of a comparative analysis of the data obtained with the data from the middle of the last century, it was found that 93 of these species previously lived in alpine-subalpine landscapes and only in the last 70 years have risen to subnival landscapes. The main reason for this upward shift is thought to be the impact of recent global warming. Out of these, 43 species, belonging to 11 families, were described at altitudes of 3000 - 3800 m at the beginning of the last century. The families that previously existed in the subnival landscapes *are: Poaceae, Apiaceae, Asteraceae Brassicaceae, Caryophyllaceae, Lamiaceae, Ranunculaceae, Rosaceae, Saxifragaceae, Scrophullariaceae, Valerianaceae* are "aborigene" taxa. The families that have risen to altitudes of 3500 m or more are relatively new ones: *Aspleniaceae, Boraginaceae, Cyperaceae, Juncaceae, Crassulaceae, Ericaceae, Fabaceae, Campanulaceae, Geraniaceae Gentianaceae, Papaveraceae, Orobanchaceae, Onagraceae, Liliaceae.* 85 endemic species (63 %) have been described in the territory.

Keywords: biodiversity, climate change, global warming, flora, subnivale, landscape

Introductıon

The biological diversity of subnival landscapes is particularly interesting from their biological, ecological and physiological point of view. These plants live in a relatively harsh climate, with reduced air density. Because their habitats are relatively small, changes in climatic factors are reflected in the size of the populations of these organisms. Subnival landscapes are under extreme pressure in this regard. Over the past 20 years, the melting of glaciers in Azerbaijan has led to a sharp change and warming of the climatic conditions of subnival creatures.

Sufficient research has been conducted on the vegetation and endemism of the upper alpine and subnival landscapes of the Middle and Eastern Caucasus (Abdulaev K.A. et al., 2011; Astamirova M.A et al., 2020; Taisumov M.A. et al. 2017; Murtazaliev R. A., 2012; Nakhutsrishvili G.Sh., 1998). However, there is no systematic research data on the vegetation of the subnival zone of the Southern part of the East Caucasus. Recent global warming and the rapid melting of glaciers have been leading to a dramatic change in the environmental conditions of vegetation in the area. Glacier inventories from 1960, 1986 and 2014 confirm this evidence. Thus, the total area of glaciers decreased by 28.8 ± 4.4% between 1960 and 2014 (Levan G. Tielidze and Roger D. Wheate. 2018).

Material and methods

High mountain subnival landscapes in Azerbaijan, mainly in the Greater Caucasus, cover areas from 3,200 to 3,500 m to 4,000 m, depending on the terrain and climatic features of the area. The average temperature of the hottest month is 0 - 5 ^{0}C and below, the temperature of the coldest month is 15 ^{0}C and below, and the average annual temperature is below 0 0 C. The average annual rainfall is 900-1200 mm (Geography of the Republic of Azerbaijan, 2015).

As the altitude increases, the density of the atmosphere decreases, leading to an increase in solar radiation. On the other hand, the fact that the long-wave radiation of the Earth's surface is higher than that of insolation, air temperature is sharply reduced here (Isachenko A. G., 1991).

The area is highly endemic. The main reason for this is that the alignment of mountain systems in the region creates a characteristic barrier effect of the terrain. These unique mountain barriers, which block the flow of air, play an important role in landscape creation. This configuration of mountains traps humid air currents, causing precipitation. As a result, a unique air and temperature regime is formed.

This, in turn, creates unique climatic conditions and high endemism. The landscape of the area belongs to the nival and subnival landscapes of high mountains (3000 - 4000 m) with cold, temperate-humid climate (Zernov A.S., 2006) .

The materials and information were collected by the author on the basis of expedition research and scientific literature of 2013-2020 period.

Here, mainly petrophytes: plants of rock substrates (hasmophytes), avalanches and moraine are predominant. The class Polypodiopsida is represented by the family Aspleniaceae . Monocotyledons are represented by the families Poaceae, Cyperaceae and Juncaceae . The class Magnoliopsida is represented by 24 chapters. As a result of the research, it was determined that 128 species belonging to 28 genera and 86 genera are distributed in the subnival landscapes of the flora of Azerbaijan.

Lamium tomentosum, Nepeta supina, Myosotis alpestris, Senecio karjaginii species are found on the avalanche deposits of clayey shales in the valley areas. On rocks, rocky and gravel slopes and on moraines are found the following species *Alopecurus dasyanthus*, *Silene humilis*, *S.lacera* and *Pseudovesicaria digitata*. *Taraxacum porphyranthum, Tripleurospermum caucasicum, Senecio karjaginii, Erigeron alpinus, Scrophularia minima* are widespread in Morens and wetlands .

Table 1 - shows the taxonomic structure and comparative indicators of flora diversity of subnival landscapes of Azerbaijan. Table 2 - presents the dominant genus of flora diversity of subnival landscapes of Azerbaijan, a comparative analysis of their characteristics.

For example, *Asteraceae* (25 species), *Poaceae* (15 species) and *Caryophyllaceae* (13 species) are the most diverse species in the landscape. This is 38% of the total number of species found in the subnival landscape. The chapters listed in Table 3 are the ones to be safe and under development because of their rich diversity. The taxonomic structure of dominant species is given in Table 4. Out of 83 plant species found in the area, 40 are represented by 3 or more species, which makes 48% of the species diversity in the belt. As can be seen from the table, the richest genus is Saxifragaceae, *which* is represented by 7 species.

However, 4 sensitive genus represented by 1 species have been identified in the area. These are *Geraniaceae (Geranium gymnocaulon), Liliaceae (Gagea sulfurea)*, *Onagraceae (Epilobium anagallidifolium), Violaceae (Viola minuta)*.

Table 1. Comparative analysis of the taxonomic structure of flora diversity of subnival landscapes of Azerbaijan with the general flora

№	Class	Families, n		%	Genera, n		%	Species, n		%
		Region	*Flora*		*Region*	*Flora*		*Region*	*Flora*	
1.	Polypodiopsida	1	6	17	2	24	4	2	55	3.6
2.	Liliopsida	3	25	12	14	213	6.5	21	958	2.2
3.	Magnoliopsida	24	95	25	67	771	8.7	113	3351	3.2
Total:		**28**	**133**	**21**	**83**	**1015**	**8.2**	**136**	**4388**	**3.0**

Table 2. Dominant families of flora diversity of subnival landscapes of Azerbaijan and their taxonomic structure

№	Families	Genera, n		Species, n		On landscape and genus %-with	
		Subnival	*Flora*	*Subnival*	*Flora*	*On the landscape*	*By genus*
Liliopsida							
1.	*Poaceae*	11	113	15	469	1.7	
Magnoliopsida							
2.	*Asteraceae*	14	121	25	572	6.8	
3.	*Caryophyllaceae*	5	34	13	191	8.6	
4.	*Brassicaceae*	5	82	8	245	5.5	
5.	*Saxifragaceae*	1	1	7	14	5.5	
6.	*Rosaceae*	3	33	6	216	4.7	
7.	*Ranunculaceae*	4	23	6	101	4.7	
8.	*Lamiaceae*	5	37	5	219	3.9	
9.	*Apiaceae*	5	70	5	182	3.9	
10.	*Scrophulariaceae*	2	2	5	58	3.9	

Table 3. Emerging species of flora diversity of subnival landscapes

№	Genera	The families to which it belongs	Number of species		
			In the belt	Florada	%-with
Liliopsida class: 3 genera; 21 species					
1.	*Alopecurus*	*Poaceae*	3	**13**	*23.0*
Magnoliopsida class: 66 genera, 109 species					
2.	*Saxifaga*	*Saxifragaceae*	7	**14**	*50.0*
3.	*Taraxacum*	*Asteraceae*	5	**23**	*21.7*
4.	*Gentiana*	*Gentianaceae*	3	**9**	*33.3*
5.	*Draba*	*Brassicaceae*	3	**12**	*25.0*
6.	*Cerastium*	*Caryophyllaceae*	5	**23**	*22.0*
7.	*Minuartia*	*Caryophyllaceae*	3	**17**	*17.6*
8.	*Sedum*	*Crassulaceae*	3	**18**	*16.7*
9.	*Senecio*	*Asteraceae*	3	**22**	*13.6*
10.	*Polygonum*	*Polygonaceae*	3	**29**	*10.3*
11.	*Ranunculus*	*Ranunculaceae*	3	**32**	*9.3*
12.	*Veronica*	*Scrophullariaceae*	3	**42**	*7.1*
13.	*Campanula*	*Campanulaceae*	3	**48**	*6.3*
Total			***43***	***279***	*15.0*

Of the 136 species of plants found in the area, 51 species are broad-leaved, and 85 species are endemic species of various categories distributed within limits in the Caucasus Ecoregion. Extensive area vegetation, mainly *Poaceae* (10 species), *Asteraceae* (10 species), *Saxifragaceae* (5 species), *Rosaceae* (4 species) chapters.

Endemism of subnival landscapes. As a result of the analysis, 85 endemic species with different habitats within the Caucasus Ecoregion were identified in the subnival landscapes of Azerbaijan. Of these, 8 species (3 genus, 6 genera) belong to the Liliopsida class, and 77 species (22 genera, 53 genera) belong to the Magnoliopsida class. Based on these findings, it has been determined that the originality of plant diversity in the subnival landscapes of Azerbaijan is 2% of the total flora, and 63% of the landscape flora. *Asteraceae (25; 15), Caryophyllaceae (12, 11), Brassicaceae (8; 6), Poaceae (15; 5), Apiaceae (5; 5), Lamiaceae (5; 5), Ranunculaceae (6; 4), Scrophullariaceae (5; 4)* chapters These are the dominant genus of endemic plant species found in the subnival landscapes of Azerbaijan (**Figure 2**).

Figure 2. Endemics of subnival landscapes with different statutes: A. North Caucasus and Transcaucasus: *Senecio sosnowskyi;* B. Caucasus, Turkey: *Cirsium tomentosum;* S. Caucasus, Turkey, Iran: *Sedum tenellum* ; D. Wide range: *Jurinea subacaulis*

Tablel 4. Distribution of dominant families of endemism of subnival landscapes by subregions

Subendem areas	Total number of species	Number of endemic species within families								
		Asteraceae	*Poaceae*	*Caryophyllaceae*	*Brassicaceae*	*Saxifragaceae*	*Rosaceae*	*Ranunculaceae*	*Apiaceae*	*Lamiaceae*
Wide range species	51	10	10	1	2	5	4	2	-	-
North Caucasus and South Caucasus	36	8	-	7	2	-	-	2	2	2
North Caucasus, South Caucasus, Turkey	26	5	-	3	3	2	1	-	-	1
North Caucasus, South Caucasus, Iran, Turkey	22	2	4	2	1	-	1	2	3	2

North Caucasus, South Caucasus, Iran	1	-	1	-	-	-	-	-	-	-
Total	***136***	***25***	***15***	***13***	***8***	***7***	***6***	***6***	***5***	***5***

Table 5. Caucasian endemics of subnival landscapes of Azerbaijan

№	Genus	Species
Magnoliopsida class: 31 species		
1.	*Apiaceae*	*Chaerophyllum humile (Ch.kiapazi), Symphyoloma graveolens*
2.	*Asteraceae*	*Aetheopappus caucasicus, Archanthemis sosnovskyana, Kemulariella rosea, Senecio karjagini, S.sosnowskyi, Taraxacum stevenii, T. tenuisectum*
3.	*Boraginaceae*	*Trigonocaryum involucratum*
4.	*Brassicaceae*	*Eunomia rotundifolia, Pseudovesicaria digitata*
5.	*Campanulaceae*	*Campa nula petrophila*
6.	*Caryophyllaceae*	*Cerastium multiflorum, C..kasbek, C.undulatifolium, Minuartia inamoena, M. oreina, Silene humilis, S.lacera*
7.	*Crassulaceae*	*Sedum stevenianum, Sempervivum caucasicum*
8.	*Fabaceae*	*Astragalus brachytropis*
9.	*Gentianaceae*	*Gentian angulosa*
10.	*Lamiaceae*	*Teucrium nuchense, Ziziphora puschkinii*
11.	*Ranunculaceae*	*Delphinium caucasicum, Ranunculus arachnoideus*
12.	*Scrophullariaceae*	*Scrophularia ruprechtii, Veronica caucasica, V.minuta*
13.	*Valerianaceae*	*Pseudobetckea caucasica*
14.	*Violaceae*	*Viola minuta*

As noted in previous studies, another reason for the high endemism here is the orographic nature of the area and the effect of the relief on solar radiation here. The combined effect of these two factors and orographic isolation is one of the factors contributing to the unique vegetation, high endemism (Zernov A.S., 2006). The highest endemism is found in the transitional ecotones at an altitude of 3200-3500 m, where the alpine belt with complex mountain systems passes into the subnuval zone.

Over the last 100 years, the average annual temperature in Azerbaijan has increased by 0.3-0.8 ° C (Safarov S. G., 2007). As a result of this change, the average annual rainfall decreased by 23% (Mamedov R.M., 2009). Hence, glaciers (Figure 2) in the

country are almost depleted, the level of high mountain lakes (Tufangol, Turfangol, etc.) has sharply decreased (Figure 3).

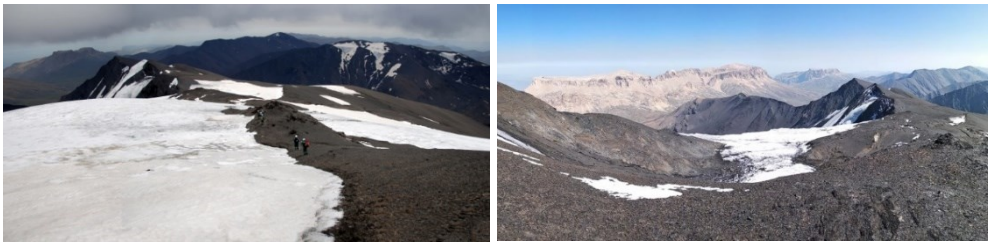

Picture 2 . Bazarduzu, the largest glacier in the country in the summer of 2003 and 2018

Picture 3. Tufangol and Turfangol mountain lakes

Results and discussions

A comparative analysis of data from the middle of the last century shows that 93 of the species distributed in subnival landscapes had previously been in alpine subalpine landscapes at altitudes of 1,800 to 2,200 m, and had only risen to subnival landscapes in the last 70 years (Aliyar Ibrahimov and Fatmakhanum Nabiyeva., 2013; Flora of Azerbaijan. 1950; Grossheyim A.A. 1936-1952). These are *Aspleniaceae, Boraginaceae, Cyperaceae, Juncaceae, Crassulaceae, Ericaceae, Fabaceae, Campanulaceae, Gentianaceae, Geraniaceae, Papaveraceae, Orobanchaceae, Liliaceae, Onagraceae, Polygonaceae, Primulaceae, Violaceae* species belonging to these genus (Table 6).

The remaining 43 species are aboriginal species and were previously distributed at altitudes of 3300-3700 m (Aliyar Ibrahimov and Fatmakhanum Nabiyeva., 2013; Flora of Azerbaijan. 1950; Grossheyim A.A. 1936-1952). These belong to

Aspleniaceae, Boraginaceae, Cyperaceae, Juncaceae, Crassulaceae, Ericaceae, Fabaceae, Campanulaceae, Gentianaceae, Geraniaceae, Papaveraceae, Orobanchaceae, Liliaceae, Onagraceae, Polygonaceae, Primulaceae and Violaceae genus (Table 7).

As found out, some plants have not changed their positions over the last 70-80 years, while others have risen to an average altitude of 300-500 m or more (Table 8). We believe that the phenological and other features of the relief, slopes, vegetation (thermophilic degree, etc.) play a key/crucial role here.

Table 6. Some species previously distributed in alpine-subalpine landscapes, only in the last 70 years have risen to subnival landscapes

№	Families	Species
1.	*Aspleniaceae*	*Athyrium distentifolium, Cystopteris fragilis*
2.	*Poaceae*	*Anthoxanthum odoratum, A.alpinum, Bromopsis variegate, Catabrosella variegate, Colpodium versicolor, Deschampsia flexuosa, Festuca montana, F.woronowii, Helictotrichon pubescens, Nardus stricta, Phleum alpinum, Poa alpine*
3.	*Cyperaceae*	*Carex tristis, C.micropodioides, Kobresia persica, K.schoenoides*
4.	*Juncaceae*	*Luzula spicata, L.stenophylla*
5.	*Apiaceae*	*Chamaesciadium acaule*
6.	*Asteraceae*	*Aetheopappus caucasicus, Anthemis melanoma, Anthemis sosnovskyana, Centaurea fischeri, Cirsium obvallatum, C. tomentosum, Kemulariella rosea, Leontodon hispidus, Senecio sosnowskyi, Taraxacum stevenii,*
7.	*Boraginaceae*	*Cynoglossum holosericeum, Myosotis alpestris, Trigonocaryum involucratum*
8.	*Brassicaceae*	*Didymophysa aucheri*
9.	*Campanulaceae*	*Campanula petrophila, C.saxifraga*
10.	*Caryophyllaceae*	*Arenaria lychnidea, Cerastium cerastioides, C.multiflorum, C.purpurascens, Gypsophila tenuifolia, Minuartia aizoides, M.caucasica, M.oriena,*
11.	*Crassulaceae*	*Sedum involucratum, S.tenellum, Sempervivum caucasicum*
12.	*Fabaceae*	*Astragalus brachytropis, Vavilovia Formosa*
13.	*Lamiaceae*	*Thymus nummuralis, Ziziphora puschkinii*
14.	*Orobanchaceae*	*Pedicularis crassirostri, P.nordmanniana*
15.	*Papaveraceae*	*Corydalis alpestris, C.conorhiza*
16.	*Polygonaceae*	*Oxyria digyna, Polygonum alpinum, P.carneum*
17.	*Ranunculaceae*	*Anemone speciosa,*
18.	*Rosaceae*	*Alchemilla caucasica, Potentilla nivea, Sibbaldia parviflora, S.semiglabra*

19.	*Scrophulariaceae*	*Veronica minuta*
20.	*Violaceae*	*Viola minuta*

Table 7. The main species distributed in subnival landscapes in earlier periods

№	Families	Species
1.	*Poaceae*	*Alopecurus dasyanthus, A.glacialis, A. textilis*
2.	*Apiaceae*	*Carum caucasicum, Chaerophyllum humile, Symphyoloma graveolens*
3.	*Asteraceae*	*Anthemis iberica, Antennaria caucasica, Erigeron alpinus, E.uniflorus, Jurinella subacaulis, Senecio karjaginii, S.sosnowskyi, Taraxacum porphyranthum, Tripleurospermum caucasicum*
4.	*Brassicaceae*	*Draba hispida, D.siliquosa, Eunomia rotundifolia, Murbeckiella huetii, Pseudovesicaria digitata*
5.	*Ranunculaceae*	*Ranunculus arachnoideus, Thalictrum alpinum*
6.	*Saxifragaceae*	*Saxifraga flagellaris, S.juniperifolia, S.moschata, S.pseudolaevis, S.sibirica*
7.	*Valerianaceae*	*Pseudobetckea caucasica, Valeriana alpestris*

Table 8. Cryophilic species found in subnival landscapes of Azerbaijan

№	Families	Species
21.	*Apiaceae*	*Chaerophyllum humile, Symphyoloma graveolens*
22.	*Asteraceae*	*Aetheopappus caucasicus, Anthemis iberica, Cirsium tomentosum, Jurinella subacaulis, Senecio karjaginii, S.sosnowskyi, S.taraxacifolius, Taraxacum stevenii, T.tenuisectum, Tripleurospermum caucasicum*
23.	*Boraginaceae*	*Myosotis alpestris*
24.	*Brassicaceae*	*Draba bryoides, D.siliquosa, Eunomia rotundifolia, Pseudovesicaria digitata*
25.	*Campanulaceae*	*Campanula petrophila*
26.	*Caryophyllaceae*	*Cerastium cerastioides, C.kasbek, C.multiflorum, C.polymorphum, C.undulatifolium, Minuartia aizoides, M. inamoena, M.caucasica, Silene humilis, S.lacera*
27.	*Crassulaceae*	*Sedum stevenianum, S.tenellum*
28.	*Cyperaceae*	*Carex tristis*
29.	*Gentianaceae*	*Gentian angulosa*
30.	*Juncaceae*	*Luzula spicata, L. stenophylla (L.pseudosudetica)*
31.	*Lamiaceae*	*Lamium tomentosum, Nepeta supina, Thymus nummuralis, Ziziphora puschkinii*

32.	*Plantaginaceae*	*Veronica minuta*
33.	*Poaceae*	*Agrostis gigantea, Alopecurus arundinaceus, A.glacialis, Catabrosa aquatic, Nardus stricta, Poa annua, Stipa ehrenbergiana*
34.	*Primulaceae*	*Androsace lehmanniana*
35.	*Ranunculaceae*	*Ranunculus arachnoideus*
36.	*Rosaceae*	*Alchemilla caucasica, A.sericea, Dryas caucasica, Potentilla gelida, P. cryptophila, Sibbaldia parviflora, S.semiglabra*
37.	*Saxifragaceae*	*Saxifraga exarata, S. flagellaris, S. juniperifolia, S.moschata, S.sibirica (S.mollis), S.pontica*
38.	*Scrophulariaceae*	*Verbascum georgicum, Scrophularia minima, Veronica caucasica, V.gentianoides, V.minuta (V.telefiifolia* subsp. *telephiifolia)*
39.	*Valerianaceae*	*Pseudobetckea caucasica, Valeriana alpestris*
40.	*Violaceae*	*Viola minuta*

The group of cryophilic plants include these edificator species *Alchemilla sericea*, *A. caucasica*, *Alopecurus glacialis, Anthemis iberica, Cirsium tomentosum, Nepeta supina, Sedum stevenianum, Silene humilis, Senecio sosnowskyi*.

References

Abdulaev K.A., Ataev Z.V., Bratkov V.V. (2011) Modern landscapes of mountainous Dagestan. Makhachkala, DSPU. 116 pp. (Rep. of Dag.) LBC 911.2 (470.67)

Aliyar Ibrahimov, Fatmakhanum Nabiyeva. (2013) Alpine vegetation of the Nakhchivan Autonomous Republic. LAP Lambert Academic Publishing. - 148 p.

Astamirova M.A-M, Taisumov M. A., Umarov M.U. and Magomadova R.S. (2020) Analysis of the plant cover of the Upper Alpine belt of the northern part of the Central and Eastern Caucasus. IOP Conf. Series: Earth and Environmental Science 579. 012078. doi:10.1088/1755-1315/579/1/012078

Ataev Z.V. (2011) Alpine landscapes of the Eastern Caucasus and their current ecological state. Young scientist. Monthly Scientific Journal. No. 12 (35). Volume I. December, p. 130-134.

Flora of Azerbaijan. (1950-1960) Publishing house of the Academy of Sciences of Azerbaijan. In 8 volumes. Baku. From AzFan.

Geography of the Republic of Azerbaijan. (2015) Regional geography. Volume III. Baku: Europe. 399 p.

George Sh. Nakhutsrishvili. (1998) The Vegetation of the Subnival Belt of the Caucasus Mountains. Arctic and Alpine Research, Vol. 30, No.3, pp. 222-226.

Grossheyim A.A. (1936-1952) Flora of the Caucasus. In 8 volumes. Baku. From AzFan.

Isachenko A. G. (1991) Landscape science and physical-geographical zoning: Textbook .. M .: Vyssh. school,. 366 p.: ill. c 80.

Levan G. Tielidze, Roger D. Wheate. (2018) The Greater Caucasus Glacier Inventory (Russia, Georgia and Azerbaijan). The Cryosphere, 12, 81–94. https://tc.copernicus.org/articles/12/81/2018/

Mamedov R.M., Safarov S.G., Safarov E.S. (2009) Modern changes in the atmospheric precipitation regime on the territory of Azerbaijan // Geography and Natural Resources. Novosibirsk. no. 4, p. 170-175. http://www.izdatgeo.ru/pdf/gipr/2009-4/170.pdf

Murtazaliev R. A. (2012) Analysis of endemic flora of the Eastern Caucasus and features of their distribution. Bulletin of the Dagestan Scientific Center. No. 47. p. 81–85. http://vestnikdnc.ru/IssSources/47/7.pdf

Safarov S. G. (2007) Changes in the temperature regime on the territory of Azerbaijan // Gidrometeorol. and ecol., No. 4. pp. 37–46.

Taisumov M.A., Magomadova R.S., Astamirova M.A-M., Israilova S.A., Khasueva B.A., Khanaeva Kh.R. (2017) Analysis of the endemism of the xerophyte flora of the Russian Caucasus. //South of Russia: Ecology, Development Vol. 12 N 1. P. 199-205.

Zernov A.S. (2006) Flora of the Northwestern Caucasus. Abstract of the dissertation for the degree of Doctor of Biological Sciences. Moscow. 32 p. https://static.freereferats.ru/_avtoreferats/01002937516.pdf

Khazar Journal of Science and Technology Volume 6 №1 2022, 17-22
© Khazar University Press 2022 DOI: 10.5782/2520-6133.2022.6.1.17

Evaluation of the Effectiveness of Disinfectants

Shalala Zeynalova*[1], Natig Guliyev[2], Hikmat Gahramanov[2], Tarana Azizova[2], Farid Manaflı[2], Naib Abayev[2]

[1]*Ministry of Agriculture of Azerbaijan*
[2]*"Saba" OJSC*
**Corresponding author: zeynalovaeddm@gmail.com*

Abstract

The disinfection process in poultry farming is the most important direction in the control of pathogens of infectious diseases. Currently, many farms carry out disinfection based on standard rules: manure transportation, dirty washing, clean washing, disinfection, fumigation. This study was conducted in order to determine whether disinfectants for poultry houses of poultry farming are effective for reducing bacteria, viruses and fungi. Poultry houses for breeding were selected for field tests. The disinfectants evaluated were chloride, glutaraldehyde and formalin. In order to determine the total number of aerobic and anaerobic bacteria, as well as the number of yeast and mold fungi, samples were inoculated into the nutrient medium. The tests were mainly carried out to determine *E.coli, Campylobacter spp.* and *Salmonella spp.* As a result of research conducted at the "Saba" poultry farming, a significant decrease in the number of microorganisms was observed. The results show that the percentage and type of disinfectants may vary depending on the type, degree of application, duration of storage and the strength of the effect of organic substances on common aerobic bacteria.

Key words: glutaraldehyde, Salmonella, E. coli, disinfection

Introduction

Poultry farming is a field of activity where poultry are kept for breeding and broiler types. The biggest obstacle to the development of the poultry industry is the presence of pathogens of bacterial, viral and fungal origin. Diseases cause serious damage to the farm at all stages of poultry development. In particular, the spreading of

pathogenic microorganisms in the technological process increases the likelihood of contamination of products going/ transferring to the consumer (Black, 1991; Bragg and Plumstead, 2003).

The disinfection process at poultry farms is the most important stage of the biosafety regulations. An important issue in maintaining the epizootic state of poultry farming is compliance with biosafety rules. There are several ways for installation of biosafety barriers: physical-decontaminators, chemical-disinfectants and logistical - this is a measure of the rules depending on the age of the bird and the status of the disease. One of the important parts of biosafety rules is disinfection. Due to disinfection, it is possible to minimize/ decline the number of microorganisms. *E.coli, Campylobacter* are usually found in poultry houses, where poultry is bred (Bender and Mallinson, 1991; Kitis, 2004)

Salmonella occurs in the environment and poses a danger to the health of birds in all phases of their development. Birds are kept in poultry houses until they are sent for slaughtering, and then, a large amount of feces accumulates. Here, cleaning of poultry houses in poultry farming from litter, which is mandatory for the reproduction of *Salmonella, E.coli* and other pathogens, occupies a major place/comes to the most prority in the prevention of diseases. The successful implementation of this process is the correct organization of the sanitary program. As a result, birds become healthier, productivity increases and the spread of pathogenic microorganisms is prevented (Corrier et al., 1992; Davies and Wray, 1995; Long, 1981). For the effective application of disinfectants, the dirty floor should be completely cleaned.

Aspergillosis, Candidiasis, Dactylios, Favus, etc., are related to fungus diseases of poultry. Fungal diseases, mycotoxins (contained in wheat and feed) or having an infectious nature cause significant economic damage to the poultry industry. Fungi cause to the occurrence of diseases, an increased mortality rate, especially an increase in growth in infected young birds, diarrhea and encephalitis (Kuldeep et al., 2013).

Disinfectants can be used in various forms such as: fumigation, spraying, misting, wet disinfection (Eckman, 1994). Usually the composition of disinfectants consists of alcohol, chlorine, aldehydes, phenol, halogens (Meroz and Samberg, 1995).

In Azerbaijan, poultry meat occupies an important place/plays a key role/is so crucial in meeting the needs for food. There are farms for the production of poultry meat and eggs in the country. Each of them has/faces with different risks depending on its location and direction.

The "Saba" poultry farming is located on the territory of the Shabran district. Here, an incubator, poultry houses for breeding, a slaughterhouse and a testing laboratory are located on the same territory. In a complex farm of this type, preventing the spread of pathogens is much more difficult. In addition, the Shabran district is under the migration routes of birds, which, in turn, is one of the risk factors for the occurrence of avian influenza.

The purpose of this investigation was the studying the effects of various disinfectants and determining the most effective.

Material and methods

Research area:

Length of each poultry house 77 m, width -18 m

Sampling plan:

After a dirty cleaning of the poultry house, a disinfectant was applied, and a smear sample was taken from 10 places. The samples were immediately sent to the testing laboratory. During the testing period, the samples were stored at a temperature of 4-8 ° C.

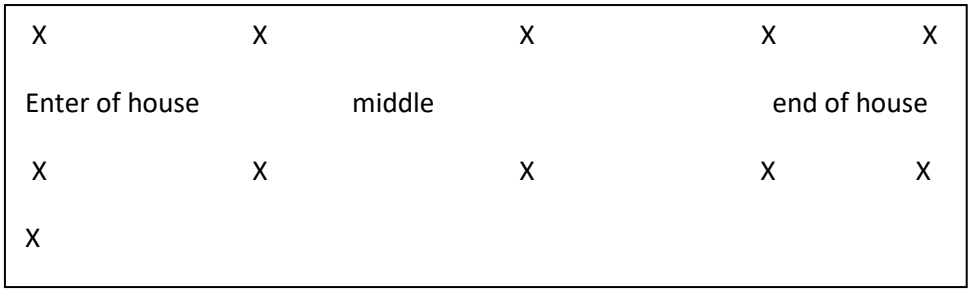

Graph 1. Sampling procedure from poultry houses

Laboratory tests

Using sterile swabs, smears were taken from 3 places of the poultry house. With the addition of PBS in a ratio of 1:10, the smears passed through a centrifuge. A 1 ml of sample taken from the supernatant was inoculated on MPA, End, Magconci agars. The inoculations in Petri dishes were kept for 2 days at a temperature of 37 °C. Colonies that gave growth were also taken and microscopized (SOP 02-V-2).

Result and discussion

The purpose of sanitation and disinfection is reducing or elimination the number of microbes that pose a danger to the health of the flock. All disinfectants - sprays, foams, aerosols or fumigants - act much better at temperatures above 20 °C.

Table 1. Test results of disinfectants

Name of substance	Percentage	Field of application	Period	Test results			
				GNM (number of colonies)	BCBG	Salmonella spp.	Yeast and mold fungi
Glutaraldehyde 15% Benzalconium chloride10%	2.75%	Breeding poultry houses	30 minutes	300	-	-	-
Glutaraldehyde Benzalconium chloride (GAC)	0.1-0.3%	Breeding poultry houses	30 minutes	450	-	-	-
Formalin - fumigation	%	Breeding poultry houses		-	-	-	-

Poultry houses for breeding are places where birds live from 0 day/from the day zero to slaughter (33-35 days). Disinfection works/measures in poultry houses are not carried out/taken before the birds are sent for slaughter. Field tests have shown a large number of common aerobic bacteria. After a clean wash (i.e. washing and rinsing with a foaming substance following waste disposal), disinfectants were applied in the 1st and 2nd sections. The exposure of all three substances was the same. According to the results, the bacteria *Campylobacter spp., Salmonella spp., E.coli* did not give growth.

The time of affection had a significant impact on the number of aerobic bacteria, because the mortality rate of organisms is affected by the duration of exposure to an antimicrobial agent (Black, 1996). Disinfectants are commercially available and care must be taken before choosing the appropriate remedy. Not all disinfectants are

classified as broad-spectrum; therefore, the selected substance must be effective for destroying the organism causing special problems. When mixing disinfectants, the correct proportions must be specified. It is important to follow the recommended procedures, the proportions of application - it is necessary to take some other factors into account such as water, temperature and the surfaces on which to be applied (Murray, 1991; Reiber et al., 1990).

The results of this study show that the area to be disinfected, the degree of application, as well as the duration of exposure, can affect populations of *aerobic bacteria, E.coli, Salmonella* on different surfaces. Along with this, it is important to ensure that all surfaces and empty organic materials are cleaned for field testing before applying the disinfectant.

Conclusion

Currently, disinfectants of various compositions are used. The basis of all disinfectants are chlorine compounds: sodium chloride, hypochlorite, hydrogen peroxide, iodine, acids. When choosing sanitation products, it would be better/it looks wise to change them periodically. This will help reduce the resistance of bacteria and other microbes on the farm. When using step-by-step cleaning methods, the microbial load on the farm can be minimized. This contributes to the fact that in the future a stable poultry farm will enjoy a working/an effective functional biosafety system.

References

Bender, F. E., Mallinson E. T. (1991) Healthy birds are lower cost birds. Broiler Ind. 54 (1): p.62–64.

Black, J. G., (1996) Microbiology Principles and Applications // 3rd ed. Prentice Hall, Englewood Cliffs.

Buhr R., Spickler J, A. Ritter D. V, Bourassa N. A. Cox, Richardson L.J., Wilson J.L. (2013) Efficacy of combination chemicals as sanitizers of Salmonella-inoculated broiler hatching eggshells// J. Appl. Poul., Res. 22: p.27–35.

Bragg R. R, Plumstead P. (2003) Continuous disinfection as a means to control infectious diseases in poultry. Evaluation of a continuous disinfection programme for broilers// Onderstepoort J Vet Res. Sep; 70(3):219-29.

Corrier D. E., A. Hinton, Jr., B. Hargis, and J. R. DeLoach. (1992) Effect of used litter from floor pens of adult broilers on Salmonella colonization of broiler chicks. Avian Dis. 36:897–902.

Cadirci S. (2009) Disinfection of hatching eggs by formaldehyde fumigation – a review// Arch. Geflügelk., 73 (2). p. 116–123

Castro Burbarelli MF, do Valle Polycarpo G, Deliberali Lelis K et al. (2017) Cleaning and disinfection programs against Campylobacter jejuni for broiler chickens: productive performance, microbiological assessment and characterization // Poult Sci. Sep 1;96 (9): p.3188-98

Davies R. H., Wray C. (1995) Observations on disinfection regimens used on Salmonella Enteritidis infected poultry units//Poult. Sci., 74: p. 638–47.

Eckman, M. K. (1994) Chemicals used by the poultry industry // Poult. Sci. 73: p.1429–32.

Kitis, M. (2004) Disinfection of wastewater with peracetic acid: Areview. Environ. Int. 30: p.47–55.

Kuldeep D., Sandip Ch., Amit K., Tiwari R. 4, Rajamani B., Amit K. (2013) Fungal/mycotic diseases of poultry-diagnosis, treatment and control: a review// Pak J Biol Sci., Dec 1;16(23): p.1626-40

Long, J. R., DeWitt W. F., Ruet J. L. (1981) Studies on Salmonella from floor litter of 60 broiler chicken houses in Nova Scotia// Can. Vet. J., 21: p.91–94.

Meroz M., Samberg Y. (1995) Disinfecting poultry production premises, Rev. sci. tech. Off. int. Epiz., 14 (2), p.273-291

Murray L. J. (1991) Salmonella in the environment// Rev. Sci.Tech., 10: p.765–785.

Reiber M. A., Hierholzer R. E., Adams M. H., Colberg M., Izat A. L. (1990) Effect of litter condition on microbiological quality of freshly killed and processed broilers// Poult. Sci., 69: p.2128–33.

Khazar Journal of Science and Technology Volume 6 №1 2022, 23-28
© Khazar University Press 2022 DOI: 10.5782/2520-6133.2022.6.1.23

Identification of Biological Risks While Manufacturing Food Products

Mahir Nasibov
Ministry of Agriculture of the Republic of Azerbaijan
Veterinary Scientific Research Institute,
Chief scientific officer, PhD in agricultural sciences
mahirnasibov.64@gmail.com

Abstract

Over the last 5 years, a growing trend in the number of cases of parasitosis has been observed in the territory of Khachmaz district, reaching 338 cases per year. Regular monitoring of information on biological risk factors in the production and processing of livestock products is necessary to prevent or minimize the risk situation based on the analysis of information on morphophysiological characteristics of causative agents of parasitic diseases. Being as peroral zoonoses, among biohelminthiasis, these are echinococcosis (hydatidose and alveolar) opisthorchis, trichinellosis and fasciolosis. Among geohelminthiasis, these are ascaridosis and trichocephalosis. Strongyloidosis belongs to geohelminthic anthroponoses with a percutaneous invasion way (the larva penetrates through the skin or mucous membranes during the contact with long-contaminated soil, water, aquatic plants). The group of contagious helminthioses, oral anthroponoses, includes hymenolepidosis and enterobiosis. This is an article on how pathogens negatively affect food.

Keywords: biological risks, parasites, livestock products

Introduction

High sensitivity to forces is typical for eggs of *Numeroleris nana*, tissue stages of *Tochorlasma gondii;* medium - for eggs and larvae of *Strogoides stercoralis,* eggs of *Enterobius vermicularis*, plerocercoids of the *Diphyllobothrium* genus; low – for cysts of *Entamoeba histolytica* and *Lamblia intestinalis*, metacercariae of opisthorchids and helminth eggs of *Echinososinae* subfamilies, *Trichocephalus trichiuris, Ascaris Iumbricoides, Fasciola spp;* for oocytes of *Toxoplasma gondii;* very low - for oocysts of *Cryptosporidium parvum*, for larvae of helminths of the

Trichinella genus, for eggs of *Taepiaghupshis saginatus* and *Taenia solium (*Callejón, 2015). In order to ensure the food safety for humans, analysis conduction is necessary not only for the biological risks that cause diseases, but also on veterinary, raw materials and technological risks that arise at the stages of production and sale of finished products (Kozak, 2013).

In the territory of Khachmaz district, the number of invasive diseases of people is growing annually. A general trend of an increase in the number of cases has been observed over the past 10 years, which during this period reached 340 cases per year. Considering the characteristics of parasites, it is necessary to regularly monitor information about biological risk factors in order to prevent or minimize the risk situation based on the collection and analysis of information on the morphophysiological characteristics of causative agents.

Materials and methods

The analysis of medical and veterinary statistics has been performed. The normative and technical documentation of scientific articles and guidelines have been considered (Callejón, 2015).

Research outcomes

In the production of livestock products, the most significant biological risk factors among the protozoa are *Toxoplasma gondii*, *Cryptosporidium parvum*, *Entamoeba histolytica*, *Giardia intestinalis*. The main mechanism of transmission of all the protozoa presented is fecal-oral (Sbareta J, 2012).

For *C. parvum, E. histolytica*, *G. intestinalis*, the predominant route of transmission is aquatic, while for *T.*gondii is alimentary. For human, both asexual and sexual stages of *T.gondii* development are invasive. Causative agents of toxoplasmosis can get into the human body with milk and meat from invasive intermediate hosts (tachyzoites and bradyzoites), and from the external environment (oocysts from feces of felines) as well. Oocysts of *C. parvum* and cysts of *E.histolytica, G.intestinalis* can contaminate food when washed with contaminated water, and while food is being cooked by a person infected with these species (GOST, R 51901.1, 2002).

In recent years, there has been recorded an increase in the spread of helminths among people. As a consequence of large-scale hydraulic engineering, the risk of infection

with opisthorchides and diphyllobothrides increases. The situation worsens with helminthiasis, in which the larval stages are localized in the muscles of farm animals (trichinellosis, teniidosis).

In the Republic of Azerbaijan, one of the most common parasites are trematodes from the family of *Opisthorchidae (Opisthochis felineus, Clonorchis sinensis, Pseudamphistomum truncatum, etc.), Fascila hepatica, F.gigantika;* cestodes of the *Echinoccinae (E.grnulosus, E.multilocularis)* subfamily, *Diphyllobothrium latum, Taeniarhynchus saginatus, Taenia solium, Hymenolepis:* nematodes of *Ascaris lumbricoides, Trichocephalus trichiuris, Strongyloides stercoralis, Enterobius vermicularis, Trichinella spiralis, Ascaridosis, Fasiola*.

The biological features of helminths consist of the stages of development, different ecological needs at different stages of development, features of reproduction in the adult and larval stages, long duration of ontogenesis and high adaptability. The life cycles of helminths are extremely diverse, but the main stages of development have common patterns. Helminths go through a number of successive stages: eggs (except trichinella) → larvae → eugamic (Lysenko, 2002).

Depending on the peculiarities of the helminth, a different number of hosts are required for the completion of development cycle: for nematodes (with the exception of trichinella), dwarf tenia requires one host: for trichinella, bovine and pork tenia, echinococci, fascioles-two hosts; for opisthorchids and broad tapeworm - three hosts.

Pathogens of most helminthiasis are well adapted to the protective mechanisms of the host organism. Infection occurs mainly when eggs or larvae of helminths get into the body. The mechanism of infection and transmission factors determines the division into geohelminths and biohelminthiasis and contagious helminthiasis (Abdel-Hafeez et.al., 2009; Dorny et.al, 2015).

Using the classification of Pokrovsky V. I. (Pokrovsky, 2007), teniarynchosis, teniosis, diphyllobothriosis are referred to the group of biohelminthiasis, which are peroral anthroponoses (passive, when an egg or larva of a helminth gets into the digestive tract with food, water or is brought into the mouth with dirty hands). Being as peroral zoonoses, among biohelminthiasis, these are echinococcosis (hydatidose and alveolar) opisthorchis, trichinellosis and fasciolosis. As geohelminthiasis, oral anthroponoses are ascaridosis and trichocephalosis. Strongyloidosis belongs to geohelminthic anthroponoses with a percutaneous invasion way (the larva penetrates through the skin or mucous membranes during the contact with long-contaminated soil, water, aquatic plants). Hymenolepidosis and enterobiosis are related to the group of contagious helminthioses, oral anthroponoses.

Sources of infection with biohelminths are meat and fish, with geohelminths contaminated with larvae and eggs are vegetables, berries, fruits: transmission factors are soil, water used in raw form for drinking, washing vegetables, fruits, dishes; mechanical carriers are flies or other insects. Contagious helminthiasis is transmitted through household items. The figure (Figure1) shows possible routes of getting risk factors of parasitic etiology into food products (New Food Security Doctrine Adopted**,** 2020).

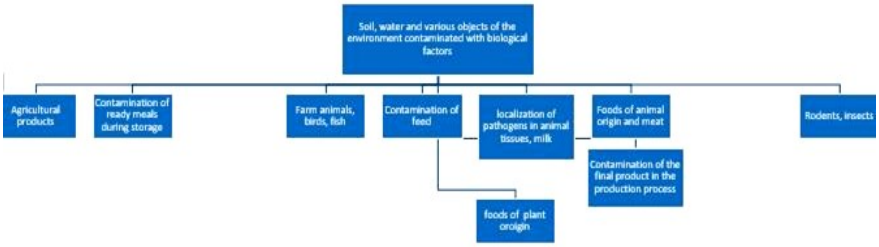

Figure 1. Routes of getting biological risk factors into food products

For a detailed assessment of biological risk factors, it is necessary to take some factors into account, including pathways of pathogen transmission, parameters of resistance in the external environment, persistence in food products, sensitivity to physical influences and disinfectants, as ways for prevention a risky situation.

The highest resistance in the external environment is peculiar to cysts of *Entamoeba histolytica, Lamblia intestinalis*, oocytes of *Cryptosporidium parvum*, *Toxoplasma gondii,* eggs of *Ascaris lumbricoides, Trichocephalus trichiuris, Diphyllobothrium spp., Opisthorchidae* и *Fasciola spp.*

The sensitivity of biological risk factors to physical influences plays an important role in the disinfection of premises in which it is either undesirable to use chemicals, or they are used in low concentrations that do not act on all types of pathogens, or risk factors have very high resistance to chemical agents, and disinfection is carried out mainly by physical methods. Sensitivity to drying can be both the main (spices, tea, dried fruits, dried meat and fish, etc.) and additional (dry fruit concentrates, milk powder, personal powder, etc.) risk reduction measure in the processing of products (Min, 2018).

Sensitivity to temperature conditions is the main criterion for preventing biological risks. Low temperatures play an important role not only in the disinfection of products, but also during their storage, since some risk factors remain viable at

temperatures close to zero. The use of high or low temperatures is the basis of disinfection in the technological processes of products processing (Pozio, 2008; Gould, 2013).

High sensitivity to physical influences is typical for *Hymenolepis nana* eggs, tissue stages of *Toxoplasma gondii.*

Average sensitivity to physical influences is typical for eggs and larvae of *Strongyloides stercoralis*, eggs of *Enterobius vermicularis*, plerocercoids tapeworms of the *Diphyllobothrium* genus.

Low sensitivity to physical impacts is typical for cysts of *Entamoeba histolytica* and *Lamblia intestinalis*, opisthorychid metacercariae and helminth eggs of the *Echinososinae*, *Trichocephalus trichiuris*, *Ascaris lumbricoides*, *Fasciola spp*. Subfamilies, *Toxoplasma gondii* oocytes.

Very low sensitivity to physical influences is tychapical for oocytes of *Cryptosporidium parvum*, larvae of helminths of the *Trichinella* genus, eggs of *Taeniarhynchus saginatus* and *Taenia solium (*Lysenko, 2002; Sbareta, 2012).

The sensitivity of biological risk factors to chemical influences (disinfectants) is also an important criterion in determining measures for reduction of biological risks by disinfection of water (chlorination and other methods), food (pickling, salting), anti-parasitic treatment of equipment, livestock facilities, agricultural equipment and other premises (Kozak,2013; Youn, 2009).

Low sensitivity to chemical influences is characteristic for *Entamoeba histolytica* cysts and *Cryptosporidium parvum* oocytes, helminths of the *Opisthorchis* genus, eggs of *Enterobius vermicularis* and helminths of the *Echinococcinae* subfamily, larvae of helminths of the *Trichinella* genus and plerocercoids of the *Diphyllobothrium* genus. Very low sensitivity to chemicals was recorded for *Lamblia intestinalis* cysts, eggs of helminths of the *Fasciola, Taeniarhynchus saginatus, Trichocephalus trichiuri, Taenia solium, Ascaris lumbricoides* genus (Wadamori, 2017).

Conclusions

In order to ensure the food safety for humans, analysis conduction is necessary not only for the biological risks that cause diseases, but also veterinary, raw materials and technological risks that arise through the stages of production and sale of finished products.

References

Abdel-Hafeez EH, Kamal AM, Abdelgelil NH, Abdel-Fatah M.J. (2015) Parasites Transmitted to human by ingestion of different types of meat, El-minia city governorate, Egypt// Egypt Soc Parasitol. Dec; 45(3):671-80.

Callejón, R.M, Rodríguez-Naranjo M.I, Ubeda C, Hornedo-Ortega R, Garcia-Parrilla M.C, Troncoso A.M. (2015) Reported foodborne outbreaks due to fresh produce in the United States and European Union: trends and causes Foodborne Pathog Dis. Jan; 12(1):32-8.

Djurković-Djaković O, Bobić B, Nikolić A, Klun I, Dupouy-Camet J, (2013) Pork as a source of human parasitic infection//. Clin. Microbiol Infect. Jul; 19(7):586-94.

Dorny P, Praet N, Deckers N, Gabriel S. (2009) Emerging food-borne parasites// Vet Parasitol. Aug 7; 163(3):196-206.

GOST, R 51901.1 (2002) "Risk management. Risk analysis of technological systems" M. IPK publishing house of standards.

Gould L.H, Walsh KA, Vieira AR, Herman K, Williams IT, Hall AJ, Cole D, (2013) Surveillance for foodborne disease outbreaks - United States, 1998-2008// Centers for Disease Control and Prevention.MMWR Surveill Summ. Jun 28; 62(2):1-34.

Kozak, G.K, MacDonald D, Landry L, Farber, (2013) Foodborne outbreaks in Canada linked to produce: 2001 through 2009// JM. J Food Prot. Jan;76(1):173-83.

Lysenko, A.Y., Clinical parasitology/ Gebeva, 2002, p.752.

Min Li, Christopher Baker A et al. (2018) Identification of Biological Hazards in Produce Consumed in Industrialized Countries: A Review/ Food Prot, 81 (7): 1171–1186.

New Food Security Doctrine Adopted (2020)/ USA

Pokrovsky V.I, **S.G. Pak, Brico N.I., Danilkin B.K.**, (2007) Infectous disease and epidemiology/ GEOTAR media, p.816.

Pozio E., (2008) Epidemiology and control prospects of foodborne parasitic zoonoses in the European Union// Parassitologia. Jun; 50(1-2):17-24

Sbareta J. (2012) Gryptosporidiosis and Gryptosporidium species in animals and humans: A thirty colour rainbow / Int J parasitology, p.957-970.

Sivapalasingam S, Friedman C.R, Cohen L, Tauxe R.V, (2004) Fresh produce: a growing cause of outbreaks of foodborne illness in the United States, 1973 through 1997.//. J Food Prot. Oct; 67(10):2342-53

Wadamori Y, Gooneratne R, Hussain M.A., (2017) Outbreaks and factors influencing microbiological contamination of fresh produce//J Sci Food Agric. 97(5):1396-1403.

Youn H. (2009) Review of zoonotic parasites in medical and veterinary fields in the Republic of Korea// J Parasitol. Oct; 47 Suppl (Suppl): S133-41.

Khazar Journal of Science and Technology Volume 6 №1 2022, 29-39

DOI: 10.5782/2520-6133.2022.6.1.29

Carbon Dots Dye-Sensitized Solar Cells Application

Babak Emdadi
Institute of Physics & Electronic of Khazar University, Azerbaijan
emdadi.babak2021@khazar.org

Abstract

Carbon dots (CDs) are a series of non-dimensional carbon-based little particles, endowed with great photoluminescence, water-dissolved, good bio adaptability, and small toxicity. Carbon dots (CDs) are a unique class of fluorescent Nano materials, whose emissions can be tuned by manipulating the reaction conditions of their formation. Moreover, CDs act a significant duty in the transfer of electrons. On the one hand, the appropriate energy band value of CDs assists the charge segregation and transfer after the carbon point is excited. In addition, carbon dots depict explicit electrical conductivities analogous to graphene. An excellent utilization amount of fossil vigorhas led to the crisis of energy as well as the surroundings. Thus, it is an immediate duty to research renewable scavenging energy to dissolve these issues. In this paper, I've strived to classify the application of carbon dots in dye-sensitized solar cells in recent years and explained the mechanisms of improving the performance of carbon dots. Among them, solar energy is reliable to be the most promising renewable energy resource due to its fascinating properties such as being inexhaustible and environmentally friendly. The growth of solar cells is already in the third stage, and investigation focuses contain dye-sensitized solar cells. Dye-sensitized solar cells make use of a similar sense, and light to electric power transformation efficiencies above 10% have been reached with DSCs.

Keywords: Dye-Sensitized Solar Cells, Solar Cells, Renewable energy, Carbon dots, solar energy

Introduction

Carbon Dots, a recent genre of functional nanocarbon family, have ushered in an expansion boom insomuch as they were firstreported (Xu et al., 2004) in 2004. Carbon dots (CDs) area series of non-dimensional carbon-based little particles, endowed with greatphotoluminescence, water-dissolved, good bio adaptability, and

small toxicity (Tang et al., 2012; Gupta et al., 2011; Liu et al., 2012; Limet al., 2015; Yuan et al., 2018; Baker et al., 2010; Gao et al., 2020). According to their excellent characteristics, these nanoparticles have obtained lots of profit for a broad span of applications including sensors (Zhu et al., 2013; Zhu et al., 2012), drug delivery (Karthik et al., 2013; Wang et al., 2013; Feng et al., 2016), light-emitting diodes (Yuan et al., 2018; Sun et al., 2015). Combinatorial approaches to carbon dots canbe organized into two classes: Top-Down and Bottom-Up methods (Zheng et al., 2015; Liu et al., 2011; Wu et al., 2018). Top-down ways, scatter huge carbon structures into small Nano scale carbon materials, including Arc-discharge, laser ablation electrochemicaloxidation. Bottom-up means using approaches such as microwave synthesis, thermal decomposition, hydrothermal treatment to compound CDs, which suggest exciting chances to control CDs with a good-defined molecular measure, form. Figure 1 demonstrates some joint provision ways and carbon dot topography.

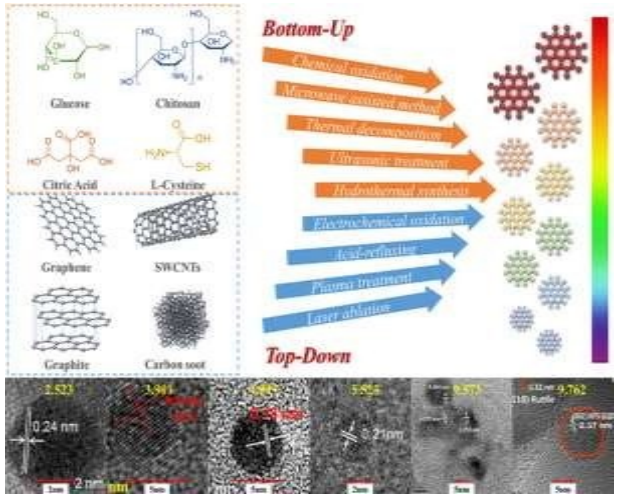

Figure 1. Precursors and preparation methods of carbon dots

Albeit, there are some significant problems in usual CDs procurement, practical measures have been suggested to unravel them. Carbonaceous aggregation during carbonization can be avoided by using electrochemical combinations, confined pyrolysis, or solution chemistry procedures (Gao et al., 2020). In conflict, with other nano carbons, carbon dots trait a high inherent photo- luminescence and premier photochemical attributes (Arcudi et al., 2017). Hence, the observed photoluminescence answer is not a singlesolution but a composition of at least two mechanisms from several sources. In terms ofcore factors, carbon dots have natural quantization effects. CDs and semiconductor oxide surfaces and on the electron

forwardingcharacteristics; Moreover, CDs act a significant duty in the transfer of electrons.

On the one hand, the appropriate energy band value of CDs assists the charge segregation and transfer after the carbon point is excited,thereby gaining a better photocurrent; On theother hand, the CDs can repress dark currentin the battery and impede electrons from being transferred from the semiconductor oxide to the electrolyte, therefore decreasingthe mixture of electrons and redox couples. Carbon Dots are small nanoparticles compounded of sp2- or sp3-carbon spheres and wealthy in oxygen- and nitrogen containing functional groups (Stepanidenko et al., 2021). CDs evenfound some applications in agriculture, where they were used to ameliorate plantdevelopment and efficiency (Li et al., 2020). Due to the single visual and electronic attributes, water- solubility, good bio-adaptability, small toxicity, and strong chemical inertness (Lim et al., 2015; Ge et al., 2014; Baker., 2010; Liu et al., 2009; Zhao et al., 2008).

In addition, thin-film solar cells use materials with a great molarabsorptivity and straight energy bandstructure (Figure. 2).

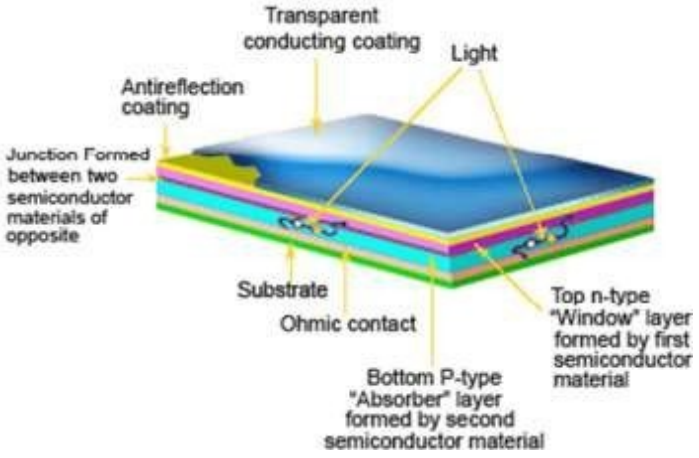

Figure 2. Structure of thin film solar cells

The benefits of these thin-film solar cells aretheir small thickness, low-cost (Gao et al., 2020). Now, the growth of solar cells is already in the third stage, and investigation focuses contain dye-sensitized solar cells (DSSCs), polymer solar cells,

perovskite solar cells, and quantum dot solar cells. As shown in Figure 3, it demands three substantial steps totransform sunlight into electricity:

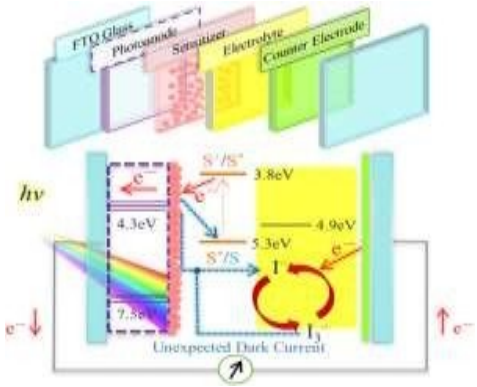

Figure 3. Structure and schematic diagram of chargetransfer in dye-sensitized solar cells.

Materials and methods

Carbon dots depict explicit electrical conductivities analogous tographene. With a quick expenditure of fossilfuels in the last years and resulting energy deficiencies, environmental contamination, and hothouse the result, tolerable energy transformation machines/technologies have gradually become usual themes of universal public extension. Great conductivities and electron tank properties permit CDs to serve as electron acceptors of light-attraction materials and interfacial modifiers for increased charge draw out/transport in solar cells (Hui et al., 2020). The concern in CDs is principally due to their optical characteristics. These nanomaterials do not importantly act as classical quantum dots and as such their optical attributes can be fully multiple. Indeed, their fluorescence is mostly related to the pioneers, response parameters, and combination scheme (Wen et al., 2016; Li et al., 2014). CDs may be organized from an abundance of pioneers andcombination paths all of which straightly impact their chemical, physical and optical characters. Considering the microwavecombination of CDs, polarization rules the interplay among the precursors and solvents permitting the probability of organizing hydrophilic, hydrophobic, or amphiphilic bits (de Medeiros et al., 2019).

Energy is a fundamental subject and problemthat all generations should be confronted withat present and in the future (Wu et al., 2015). For decades,emerging of novel systems and technologies to produce, supply, and usefully use solar power has been a persuasion to study recent procedures for the generation of pure power. Sun is a full, secure, inexpensive, and clean provenance of the vigor that can be straightly

altered to electricity without generatingcontamination and environmentaldifficulties. An excellent utilization amount of fossil vigor has led to the crisis of energy as well as the surroundings. Thus, it is an immediate duty to research renewable scavenging energy to dissolve these issues. Among them, solar energy is reliable to be the most promising renewable energyresource due to its fascinating properties suchas being inexhaustible and environmentally friendly.

A solar cell is an electronic system that straightly changes sunlight into electricity. Glory righting on the solar cell products both a current and a voltage to produce electric energy. This procedureneeds in the first step, a material in which theattraction of light increases an electron to a superior vigor case, and secondly, the motionof this premier force electron from the solar cell into an outer circuit. A diversity of solar cells have been improved and sections ofthem have been realized the industrial production.

Usually, solar cells can be organized into three generations according tothe materials and technological improvement(Wu et al., 2015, Wu et al., 2017). The prominent usage of solar energy is solar photovoltaic transformation, which ismeant by the transformation of solar energy into electrical vigor using solar cells. Due to some important errors in crystalline silicon solar cells, people started to check thin-film solar cells, and so solar cells entered thesecond phase of expansion.

Recently, the third race solar cells mostly contain dye-sensitized solar cells (DSCs), organic/polymer solar cells (OSCs), perovskite solar cells (PSCs), and quantum dot (QD) based solar cells (Grätzel, M. 2009; Cheng et al., 2009; Günes et al., 2007; Carey et al., 2015; Nozik et al., 2010; Kojima et al., 2009; Hodes, 2013; Lee et al., 2012; Hagfeldt et al., 2010). In the previous two decades, third-generation solar cells have absorbed great investigation concern and undergone rapid progress (Figure. 4).

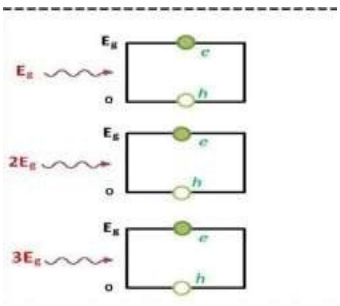

Figure 4. Schematic illustration of the generation of carriers under the excitation of photon energy traditional solar cell.

The utilization of solar vigor is boosting in homes as well. Residential appliances caneasily use electricity generated through solarpower. Besides this solar energy is running solar stoves to reserve hot water in residentialplaces. In many places, solar energy is used for ventilation targets. It aids in running bathfans, floor fans, and ceiling fans in houses. Fans run mostly every time in a building to control humidity and odor and in homes to take the warmth out of the galley. It is possible to increase a serious amount of utility bills, to decrease these bills solar energy is used for ventilation aims. Subsequent-generation solar cells are possibly unlimitedly more helpful thanks to arecently discovered nanotube structure able of carrying electrical charges 100 million times more than precedent measured.

The majority of solar cells recently use silicon to suck up light, however, inefficiencies in the material have led erudite to foster carbonnanotubes that can be implemented to boost the light attraction abilities of common cells. Checking the third generation solar cells, of special interest, was concentrated on QD-based solar cells (Carey et al., 2015; Nozik et al., 2010; Kramer et al., 2011; Kamat et al., 2010; Kramer et al., 2014).

Dye-sensitized solar cell (DSSCs) is the first third-generation that has engrossed much consideration due to their low construction cost and great performance, flexibility in color, shape, and clear. Dye-sensitized solar cells (DSSCs) are a kind of solar cells that transform the sun's energy to electric vigor using a sensitizing dye (Wei, 2010; Ye et al., 2015). DSSCs based on natural dyes though are environmentally friends usually haverelatively low efficiencies. DSSCs fabricated using synthetic dyes on the other hand have relatively higher solar-to-electric energy conversion efficiency yet dyes frequently contain certain metals that are not environment friendly. Solar cells can be builtof one single layer of light-absorbing material (single-junction) or use numerous physical shapes (multi-junction) to catch the benefit from diverse absorption and charge segregation mechanisms. Solar cells can be organized into first, second, and third-generation cells.

Dye-Sensitized solar cells (DSSC), also somewhen referred to as dye- sensitized cells (DSC), are third-race photovoltaic (solar) cell that changes any seeming glory into electrical power. This novel category of progressed solar cells can be likened to artificial photosynthesis due to the way in which it imitates nature’s attraction of light vigor (Figure. 5).

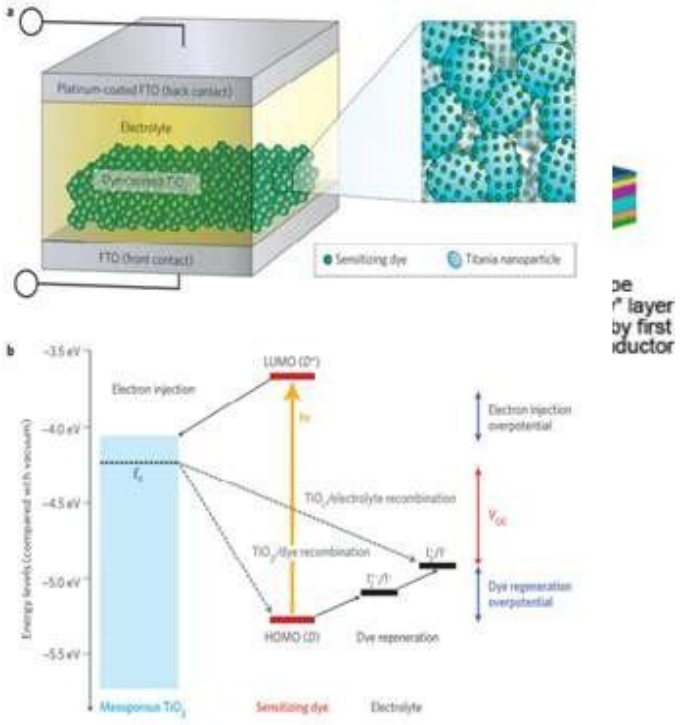

Figure 5. Dye-sensitized solar cell device schematicand operation

Conclusion

As a conclusion, we can obtain these prominent outcomes that, Carbon dots (CDs) are a type of null-dimensional carbon-based nanoparticles with excellent light-trapping capability, high optical absorption ability, and great inherent catalytic activity. Due to these beneficial characteristics, they have received eager regard from scholars in the field of optical devices. Carbon dots (CDs) are an important class of carbon-based phosphors. The application of carbon dots in dye-sensitized solar cells has boosted with constant steps recently. CDs may be organized from an abundance of pioneers andcombination paths all of which straightly impact their chemical, physical and optical characters. CDs emit in different colors in terms of morphology and optical properties of the resulting nanoparticles, with a focus on the synthetic approaches allowing them to shift their emission to longer wavelengths. We further consider the formation of CD-based composite materials. The use of CDs in the field of optoelectronics is of great interest currently and has high development potential. Alongside the well-recognized advantages of CDs as cheap, nontoxic, environmentally friendly materials, a wide variety of the available synthetic

methods opens up an opportunity to produce CDs with the desired optical and electrical properties. Considering the microwavecombination of CDs, polarization rules the interplay among the precursors and solvents permitting the probability of organizinghydrophilic, hydrophobic, or amphiphilic bits. Solar energy is reliable to be the most promising renewable energy resource due to its fascinating properties such as beinginexhaustible and environmentally friendly. A solar cell is an electronic system that straightly changes sunlight intoelectricity. The utilization of solar vigor is boosting in homes as well. Residential appliances can easily use electricity generated through solar power. Dye- Sensitized solar cells (DSSC), alsosome when referred to as dye-sensitized cells(DSC), are third-race photovoltaic (solar) cellthat changes any seeming glory into electricalpower.

References

Arcudi, F., Strauss, V., Đorđević, L., Cadranel, A., Guldi, D. M., & Prato, M. (2017). Porphyrin antennas on carbon nanodots: excited state energy and electron transduction. Angewandte Chemie International Edition, 56(40), 12097-12101.

Baker, S. N., & Baker, G. A. (2010). Luminescent carbon nanodots: emergent nanolights. Angewandte Chemie International Edition, 49(38), 6726-6744.

Baker, S. N., & Baker, G. A. (2010). Luminescent carbon nanodots: emergent nanolights. Angewandte Chemie International Edition, 49(38), 6726-6744.

Carey, G. H., Abdelhady, A. L., Ning, Z., Thon, S. M., Bakr, O. M., & Sargent, E. H. (2015). Colloidal quantum dot solar cells. Chemical reviews, 115(23), 12732-12763.

Cheng, Y. J., Yang, S. H., & Hsu, C. S. (2009). Synthesis of conjugated polymers for organic solar cell applications. Chemical reviews, 109(11), 5868-5923.

de Medeiros, T. V., Manioudakis, J., Noun, F., Macairan, J. R., Victoria, F., & Naccache, R. (2019). Microwave-assisted synthesis of carbon dots and their applications. Journal of Materials Chemistry C, 7(24), 7175-7195.

Feng, T., Ai, X., An, G., Yang, P., & Zhao, Y. (2016). Charge-convertible carbon dots for imaging-guided drug delivery with enhanced in vivo cancer therapeutic efficiency. ACS nano, 10(4), 4410-4420.

Gao, N., Huang, L., Li, T., Song, J., Hu, H., Liu, Y., & Ramakrishna, S. (2020). Application of carbon dots in dye-sensitized solar cells: a review. Journal of Applied Polymer Science, 137(10), 48443.

Ge, J., Lan, M., Zhou, B., Liu, W., Guo, L., Wang, H., ... & Han, X. (2014). A graphene quantum dot photodynamic therapy agent with high singlet oxygen generation. Nature communications, 5(1), 1-8.

Grätzel, M. (2003). Solar cells to dye for. Nature, 421(6923), 586-587.

Grätzel, M. (2009). Recent advances in sensitized mesoscopic solar cells. Accounts of chemical research, 42(11), 1788-1798.

Günes, S., Neugebauer, H., & Sariciftci, N. S. (2007). Conjugated polymer-based organic solar cells. Chemical reviews, 107(4), 1324-1338.

Gupta, V., Chaudhary, N., Srivastava, R., Sharma, G. D., Bhardwaj, R., & Chand, S. (2011). Luminscent graphene quantum dots for organic photovoltaic devices. Journal of the American Chemical Society, 133(26), 9960-9963.

Hagfeldt, A., Boschloo, G., Sun, L., Kloo, L., & Pettersson, H. (2010). Dye-sensitized solar cells. Chemical reviews, 110(11), 6595-6663.

Hodes, G. (2013). Perovskite-based solar cells. Science, 342(6156), 317-318.

Hui, W., Yang, Y., Xu, Q., Gu, H., Feng, S., Su, Z., ... & Huang, W. (2020). Red-carbon-quantum-dot-doped SnO2 composite with enhanced electron mobility for efficient and stable perovskite solar cells. Advanced Materials, 32(4), 1906374.

Kamat, P. V., Tvrdy, K., Baker, D. R., & Radich, E. J. (2010). Beyond photovoltaics: semiconductor nanoarchitectures for liquid-junction solar cells. Chemical reviews, 110(11), 6664-6688.

Karthik, S., Saha, B., Ghosh, S. K., & Singh, N. P. (2013). Photoresponsive quinoline tethered fluorescent carbon dots for regulated anticancer drug delivery. Chemical Communications, 49(89), 10471-10473.

Kojima, A., Teshima, K., Shirai, Y., & Miyasaka, T. (2009). Organometal halide perovskites as visible-light sensitizers for photovoltaic cells. Journal of the american chemical society, 131(17), 6050-6051.

Kramer, I. J., & Sargent, E. H. (2011). Colloidal quantum dot photovoltaics: a path forward. ACS nano, 5(11), 8506-8514.

Kramer, I. J., & Sargent, E. H. (2014). The architecture of colloidal quantum dot solar cells: materials to devices. Chemical reviews, 114(1), 863-882.

Lee, M. M., Teuscher, J., Miyasaka, T., Murakami, T. N., & Snaith, H. J. (2012). Efficient hybrid solar cells based on meso-superstructured organometal halide perovskites. Science, 338(6107), 643-647.

Li, X., Zhang, S., Kulinich, S. A., Liu, Y., & Zeng, H. (2014). Engineering surface states of carbon dots to achieve controllable luminescence for solid-luminescent composites and sensitive Be2+ detection. Scientific reports, 4(1), 1-8.

Li, Y., Xu, X., Wu, Y., Zhuang, J., Zhang, X., Zhang, H., ... & Liu, Y. (2020). A review on the effects of carbon dots in plant systems. Materials Chemistry Frontiers, 4(2), 437-448.

Li, Y., Zou, X., & Zhao, C. (2015, September). Mg-Doped CdTeO3 Quantum Dot Sensitized Solar Cells. In International Conference on Advances in Energy, Environment and Chemical Engineering (pp. 848-854). Atlantis Press.

Li, Y., Zou, X., & Zhao, C. (2015, September). Mg-Doped CdTeO3 Quantum Dot Sensitized Solar Cells. In International Conference on Advances in Energy, Environment and Chemical Engineering (pp. 848-854). Atlantis Press.

Lim, S. Y., Shen, W., & Gao, Z. (2015). Carbon quantum dots and their applications. Chemical Society Reviews, 44(1), 362-381.

Lim, S. Y., Shen, W., & Gao, Z. (2015). Carbon quantum dots and their applications. Chemical Society Reviews, 44(1), 362-381.

Liu, R., Wu, D., Feng, X., & Müllen, K. (2011). Bottom-up fabrication of photoluminescent graphene quantum dots with uniform morphology. Journal of the American Chemical Society, 133(39), 15221-15223.

Liu, R., Wu, D., Liu, S., Koynov, K., Knoll, W., & Li, Q. (2009). An aqueous route to multicolor photoluminescent carbon dots using silica spheres as carriers. Angewandte Chemie International Edition, 48(25), 4598-4601.

Liu, S., Tian, J., Wang, L., Zhang, Y., Qin, X., Luo, Y & Sun, X. (2012). Hydrothermal treatment of grass: a low-cost, green route to nitrogen-doped, carbon-rich, photoluminescent polymer nanodots as an effective fluorescent sensing platform for label-free detection of Cu (II) ions. Advanced materials, 24(15), 2037-2041.

Nozik, A. J., Beard, M. C., Luther, J. M., Law, M., Ellingson, R. J., & Johnson, J. C. (2010). Semiconductor quantum dots and quantum dot arrays and applications of multiple exciton generation to third-generation photovoltaic solar cells. Chemical reviews, 110(11), 6873-6890.

Stepanidenko, E. A., Ushakova, E. V., Fedorov, A. V., & Rogach, A. L. (2021). Applications of Carbon Dots in Optoelectronics. Nanomaterials 2021, 11, 364.

Sun, C., Zhang, Y., Sun, K., Reckmeier, C., Zhang, T., Zhang, X., ... & Rogach, A. L. (2015). Combination of carbon dot and polymer dot phosphors for white light-emitting diodes. Nanoscale, 7(28), 12045-12050.

Tang, L., Ji, R., Cao, X., Lin, J., Jiang, H., Li, X., ... & Lau, S. P. (2012). Deep ultraviolet photoluminescence of water-soluble self-passivated graphene quantum dots. ACS nano, 6(6), 5102-5110.

Tian, J., & Cao, G. (2013). Semiconductor quantum dot-sensitized solar cells. Nano reviews, 4(1), 22578.

Wang, Q., Huang, X., Long, Y., Wang, X., Zhang, H., Zhu, R., & Zheng, H. (2013). Hollow luminescent carbon dots for drug delivery. Carbon, 59, 192-199.

Wei, D. (2010). Dye-sensitized solar cells. International journal of molecular sciences, 11(3), 1103-1113.

Wen, Z. H., & Yin, X. B. (2016). Excitation-independent carbon dots, from photoluminescence mechanism to single-color application. RSC advances, 6(33), 27829-27835.

Wu, J., Lan, Z., Lin, J., Huang, M., Huang, Y., Fan, L., & Luo, G. (2015). Electrolytes in dye-sensitized solar cells. Chemical reviews, 115(5), 2136-2173.

Wu, J., Lan, Z., Lin, J., Huang, M., Huang, Y., Fan, L., & Luo, G. (2015). Electrolytes in dye-sensitized solar cells. Chemical reviews, 115(5), 2136-2173.

Wu, J., Lan, Z., Lin, J., Huang, M., Huang, Y., Fan, L., ... & Wei, Y. (2017). Counter electrodes in dye-sensitized solar cells. Chemical Society Reviews, 46(19), 5975-6023.

Wu, X., Ma, L., Sun, S., Jiang, K., Zhang, L., Wang, Y., ... & Lin, H. (2018). A versatile platform for the highly efficient preparation of graphene quantum dots: photoluminescence emission and hydrophilicity–hydrophobicity regulation and organelle imaging. Nanoscale, 10(3), 1532-1539.

Xu, X., Ray, R., Gu, Y., Ploehn, H. J., Gearheart, L., Raker, K., & Scrivens, W. A. (2004). Electrophoretic analysis and purification of fluorescent single-walled carbon nanotube fragments. Journal of the American Chemical Society, 126(40), 12736-12737.

Ye, M., Wen, X., Wang, M., Iocozzia, J., Zhang, N., Lin, C., & Lin, Z. (2015). Recent advances in dye-sensitized solar cells: from photoanodes, sensitizers and electrolytes to counter electrodes. Materials Today, 18(3), 155-162.

Yuan, B., Guan, S., Sun, X., Li, X., Zeng, H., Xie, Z & Zhou, S. (2018). Highly efficient carbon dots with reversibly switchable green–red emissions for trichromatic white light-emitting diodes. ACS applied materials & interfaces, 10(18), 16005-16014.

Zhao, Q. L., Zhang, Z. L., Huang, B. H., Peng, J., Zhang, M., & Pang, D. W. (2008). Facile preparation of low cytotoxicity fluorescent carbon nanocrystals by electrooxidation of graphite. Chemical Communications, (41), 5116-5118.

Zheng, X. T., Ananthanarayanan, A., Luo, K. Q., & Chen, P. (2015). Glowing graphene quantum dots and carbon dots: properties, syntheses, and biological applications. small, 11(14), 1620-1636.

Zhu, A., Qu, Q., Shao, X., Kong, B., & Tian, Y. (2012). Carbon-dot-based dual-emission nanohybrid produces a ratiometric fluorescent sensor for in vivo imaging of cellular copper ions. Angewandte Chemie International Edition, 51(29), 7185-7189.

Zhu, S., Meng, Q., Wang, L., Zhang, J., Song, Y., Jin, H & Yang, B. (2013). Highly photoluminescent carbon dots for multicolor patterning, sensors, and bioimaging. Angewandte Chemie, 125(14), 4045-4049.

Khazar Journal of Science and Technology Volume 6 №1 2022, 40-52
© Khazar University Press 2022 DOI: 10.5782/2520-6133.2022.6.1.40

Brain Tumor Area Segmentation of MRI Images

Behnam Kiani Kalejahi
Faculty of Engineering and Applied Sciences,
Khazar University, Azerbaijan
bkiani@khazar.org

Abstract

Accurate and timely detection of the brain tumor area has a great impact on the choice of treatment, its success rate, and following the disease process during treatment. The existing algorithms for brain tumor diagnosis have problems in terms of good performance on various brain images with different qualities, low sensitivity of the results to the parameters introduced in the algorithm, and also reliable diagnosis of tumors in the early stages of formation. In this study, a two-stage segmentation method for accurate detection of the tumor area in magnetic resonance imaging of the brain is presented. In the first stage, after performing the necessary preprocessing on the image, the location of the tumor is located using a threshold-based segmentation method, and in the second stage, it is used as an indicator in a pond segmentation method based on the marker used. Placed. Given that in the first stage there is not much emphasis on accurate detection of the tumor area, the selection of threshold values over a large range of values will not affect the final results. In the second stage, the use of the marker-based pond segmentation method will lead to accurate detection of the tumor area. The results of the implementations show that the proposed method for accurate detection of the tumor area in a large range of changes in input parameters has the same and accurate results.

Keywords: Brain tumor, MRI images, Tumor segmentation, Brain MR Images.

Introduction

A brain tumor is a hard, solid neoplasm inside the brain or the central spinal canal. In simpler terms, a brain tumor is an abnormal mass in the brain that may be cancerous (malignant) or noncancerous (benign) in nature. The degree of threat of a tumor depends on a set of factors such as type, location, size, life, and how it spreads and develops. The brain is completely covered by the skull. This makes rapid and

early detection of brain tumors possible only if paraclinical instruments and appropriate diagnostic devices are available to assess the condition of the intracranial cavity in the early stages of tumor formation. Even with these tools, it is very difficult to accurately diagnose brain tumors due to their variety of shapes, sizes, and appearances. In addition, in most cases, brain tumors are diagnosed in the advanced stages of the disease and when its presence causes unexplained signs and symptoms in the patient. Magnetic resonance imaging is commonly used to visualize details of the internal structure of the body. In this imaging method, differences in the magnetic properties of the fabric are used to form the image. The magnetic moment of the nucleus of some elements in the presence of a strong magnetic field is also aligned with it. The amplitude of the received signal in magnetic resonance imaging depends on two factors, the density of the protons and the rest times T1 and T2. The rest time T1 is the temporal period at which 63% of the longitudinal magnetic moment of a proton returns from the direction perpendicular to the field to the parallel direction of the field after excitation. The resting time of T2 is also the length of time that the transverse magnetic moment of a proton decreases to 37% of its initial value after excitation. Pathological processes increase T1 and T2 rest periods Compared to the natural textures around them in T1-Weighted images, the signal amplitude is lower (darker image) and T2-Weighted images produce a larger signal amplitude (brighter image). According to the above, it is possible to diagnose a brain tumor with a bandage image in terms of uniformity of light intensity. Manually isolating the tumor area in images of magnetic resonance imaging of the brain is a time-consuming and quite difficult process. Today is progressing image segmentation algorithms have also been enabled to automatically detect brain tumors. Automated brain tumor detection methods, while reducing operator work and human error, also make it easy to store tumor growth status during treatment (Faisal et al. 2013). However, due to the variety in the shape, size, and appearance of tumors, it is very difficult to achieve high accuracy in detecting tumors in a wide range of images. Also, the proper performance of many of the algorithms presented for the segmentation of magnetic resonance imaging of the brain depends on the proper selection of the input parameters of the algorithm as an example.

The KIFCM method presented in (Faisal et al., 2013), plays an important role in the exact banding of the tumor in the magnetic resonance imaging of the brain. In addition, for selecting the values of the input parameters, a large range of values cannot be selected by the user. For example, in (Harati et al., 2011) the user may not even be mentally aware of the appropriate value of the parameter used in the algorithm, and in (El-Dahshan et al., 2014.) according to the author the success of using the PCNN method to segment to properly adjust various network parameters such as communication parameter, (β) thresholds, (Θ) The disappearance time constants (αθ) and the internal connection matrices M and W depend on the fact that

the user may not have a reasonable amount of the parameters used in this method. In this paper, an effective two-step algorithm for accurate segmentation of the brain tumor area in magnetic resonance imaging is presented. The proposed two-stage segmentation method is organized in such a way that in the first stage the ability to reduce the sensitivity of the algorithm results in the selection of parameters and thus increase the range of selectable numbers for the parameters is available and in the second stage to improve the results. In the first stage, a threshold-based segmentation method was used to locate the tumor, and in the second stage, a pond-based segmentation method was used to accurately detect the shape of the tumor (Guo et al., 2012). The results of the implementation show that the proposed two-step method has a precise function in tumor detection on a large range of selected input parameters and on a wide range of magnetic resonance imaging images of the brain.

Related Works

The segmentation of the image is done by different methods. Clustering is one of the common methods in this field. In (Abdel-Maksoud et al., 2015), a combined clustering system is presented which includes the three main stages of preprocessing, clustering, extraction, and contouring. The image obtained from the preprocessing stage is clustered by the K-means clustering technique with the Fuzzy C-means algorithm and then by the thresholding method.

The cluster, the area of the tumor is extracted, or in other words, the initial location. In the last step, the leveling algorithm is applied to the image and provides a more accurate segmentation. The dependence of the output on the parameters such as the number of clusters, maximum replication, and the closing parameter are the disadvantages of this method. In Reference (Harati et al., 2011), Vida Herati et al. Have proposed a method based on an improved fuzzy communication algorithm for brain tumor segmentation (Havaei et al., 2017). In this method, first, a point of seed is automatically selected from inside the tumor. For adjacent pixels, the amount of brightness based on the sum of the mean intensity is corrected in a certain range in the original image and the main image derivative to improve the performance of the fuzzy communication algorithm at weak limits. In the next step, the amount of fuzzy communication for each new pixel is calculated based on comparing the similarity of that pixel with the characteristics of the tumor area. Finally, the tumor site is extracted by astringency. The similarity index for this method is 89.92%. In (El-Dahshan et al., 2014), FPCNN pulsed buccal neoplasm feedback has been used to define the area in question by segmentation of MRI images of the brain. Neural network feedback with pulse coupling consists of three main parts: acceptance,

modulation, and pulse generation. The main difference between this model and PCNN is that the input is replaced by the input drive and output feedback to modify the input. According to the author, the success of using the FPCNN method for segmentation depends on the proper adjustment of various network parameters such as connection parameters (β), thresholds (θ), time-disappearing constants (αθ) and internal connection matrices M and W.

In (Sachdeva et al., 2012), a content-based active boundary model is used for tumor segmentation. In this system, the primary cantilever is first radiologically marked in the tumor area and then the tissue properties and severity are estimated and using it, the tumor is formed and energy is formed. External contour deformation is used. In the next step, the static motor field and the dynamic motor field are generated to guide the macro center to the tumor margins. Contour deformation is stopped by limiting the number of repetitions or reaching fixed criteria. Not completely automatic is one of the problems of this method. Segmentation and diagnosis of tumor lesions and stroke have also been implemented by optimization algorithms.

Noshin Nabizadeh et al. (Nabizadeh et al., 2014) used a histogram-based gravity optimization algorithm. This algorithm is divided into two separate sections, including the histogram-based brain segmentation algorithm and the n-dimensional optimal optimization algorithm. This algorithm uses histogram-based techniques to determine the initial set of brain segments, and then apply the gravitational optimization algorithm to reduce the number of sections to the user's desired number and finally use the threshold to identify waste Tumor or stroke. Appropriate determination of input parameters such as the selection of the number of parts of the brain, the number of first-generation, the number of repetitions, and the like are some of the problems of this method. Also, in (Arakeri and Reddy, 2013), a combination of wavelet analysis and modified FCM MFCM is suggested for tumor segmentation. In this system, first, the removal of the skull is done by the method of astringency and preservation of the largest connected component, in the next stage of properties, the weave is revealed by the application of discrete wavelet transform. In the next part, the number of peaks in the brain histogram is used to detect the presence of a tumor in MRI images. The image containing the tumor is then clustered into four sections: CSF, GM, WM, and abnormal, by the MFCM algorithm, and the cluster with the highest value of the cluster center is selected as the abnormal region. Finally, the number of peaks in the histogram of the abnormal area is used to determine the presence of a swollen area associated with the tumor. If there is a swollen area, the abnormal area is clustered into two tumor clusters and the swollen area by the MFCM algorithm. This study seeks a fully automated method with low sensitivity to input parameters that can accurately detect the tumor area.

Implementation of the proposed method

The proposed method includes four stages of initial preprocessing, skull removal, marking positioning using the threshold-based segmentation method, and finally marker-based pond conversion. In this section, in addition to introducing the data set to be used, the implementation details of each of these steps are stated.

Data collection

In this paper, the BRATS2018 standard data set has been used (http://www2.imm.dtu.dk/projects/BRATS2018/). This dataset contains FLAIR, T2, T1, and T1C images for each patient.

Pre-processing

The initial preprocessing step includes image normalization in terms of size and brightness values, noise cancellation and image sharpening. At this stage, the input MRI image is first converted to a gray surface image, the brightness values between zero and one are normalized and the image dimensions are changed to 250 × 250. Noise removal is done using the middle filter. To repair the details lost during the noise removal and sharpening of the brain image, the image details are extracted using a high-pass filter and added to the original image.

The skull, skin, and other non-brain tissues in some methods may be misaligned or at least increase processing time due to their strong resemblance to the brain structure, so they need to be removed. In this system, skull removal is performed by a method based on measuring the properties of the image areas.

This method works in such a way that initially the average brightness of the image is calculated and a fuzzy system specifies the threshold value for the image. By applying this amount of threshold on the image, the tumor tissue and the skull (as two attached components) are identified. Then a set of different properties is calculated for each connected component (object) in the binary image, and based on these properties, an attached component is selected as the skull component. In other words, any component attached to an image that has certain properties is known as a skull and is removed. For example, the number of pixels in each component will have a "hard" property, which indicates the percentage of a region being thicker, for the skull component. Therefore, the largest area with low stiffness can be considered as a component of the skull.

Threshold-based segmentation

Thresholding is a simple but effective technique for image segmentation. The thresholding technique is based on dividing the image into separate regions (object and background) in such a way that one part contains pixels with a higher intensity equal to or equal to the threshold value, and the other part contains pixels with a smaller value. It will be the amount. Finding the right threshold value to separate the desired object from the background is an important step in processing the machine image and vision (Zhou, 2018).

If T is the value of the threshold and (f (x, y) the brightness of the point (x, y) in the gray image, the threshold image is calculated as follows:

$$g(x,y) = \begin{cases} 1 & f(x,y) \geq T \\ 0 & f(x,y) < T \end{cases}$$

In order to perform accurate thresholding and to obtain a binary image that includes the desired details, parallel thresholding has been used. This technique uses two methods of fuzzy thresholding and adaptive thresholding in parallel. In the first method, the threshold value is selected through a fuzzy system in proportion to the intensity of the image. In the fuzzy thresholding method, a fuzzy system with three trapezoidal membership functions for low, medium, and high modes receives the average light intensity of the image as input and the threshold value as output. The fuzzy rules used are such that the threshold value is selected from the low, medium, and high values for the threshold value depending on the average value of the image, which is low, medium, or high, respectively (Ain et al., 2014).

Adaptive thresholding is also applied to the image based on the mean value and the variance of the image according to Equation (Jaccard, 1912).

$$f_{Th}(x,y) = \frac{1}{e^{-\frac{(f(x,y)-Mean(f(x,y)))}{Var(f(x,y))}}}$$

In the two methods mentioned, the threshold value is determined automatically and is obtained from the heart of the image. One advantage of using the parallel thresholding technique is that if the threshold value is set incorrectly and the segmented image is inappropriate, another method corrects the final image using sharing. But the correction itself consists of two modes: the first mode occurs when, for example, the first method fails to determine the appropriate threshold value and divides the tumor area larger than its actual size, in which case the second method

Properly operated, the output image is modified by sharing two images (Chang et al., 2018.).

But in the second case, if the area of the tumor is smaller than the actual size of that section, in the output image, the size of the tumor will also be smaller. The final will not be created. Because the output of the parallel thresholding stage is used as an indicator for the pond conversion algorithm in the final stage (Rezaei et al., 2017.).

In fact, the cause of error at this stage is the segmentation of the tumor area is larger than the actual size because it will cause the pond conversion algorithm to be mistaken and the smaller segmentation of the tumor area will not cause a problem in the final exit. In other words, the implementation of this step is done with the aim of reducing the dependence of the algorithm on the selection of input parameters (including threshold values) and accuracy is not a priority at this stage. Using the pond segmentation method based on the marker will then be used to accurately detect the tumor area (Yang et al., 2018.).

The pond conversion algorithm is a zone-based segmentation method that performs segmentation based on the image intensity. The visual idea of this method is taken from geography and immersed by imagining an image as a three-dimensional map.

This map is implemented in a lake of water with holes drilled in the local minima of this map. Water rises in different ponds with the same rate of increase and reaches the same points. Vertical dams are placed at these points to prevent the pools from joining water continuously. After the highest point of the map is submerged in water, the dams divide the map into separate areas. These dams are in fact the same lines they are ponds (Zijdenbos et al., 1994; Jaccard., 1912).

To zoning the image using the pool conversion, first, the intensity of the image brightness gradient is calculated and then the pool conversion is applied to it. In the light intensity gradient image, the values for the edge points are higher than the values for the other points. Therefore, the pond lines are located around the edges. This is suitable for image zoning. The pond conversion algorithm, in addition to all its advantages, suffers from a major problem of additional bandwidth, which occurs due to a large number of local minimums and causes the number of detected areas to be larger than the number of objects. In the proposed system, in order to eliminate the effect of most of the bandage zone, the method of segmentation of the pool-based indicator has been proposed (Kong et al., 2018.). The area of the tumor located in the threshold stage is determined in parallel with the application of a series of minimization operations as internal markers (tumor). Black areas are also considered as backgrounds, but ideally, we do not want the background markers to be too close to the edges of the objects we are trying to segment (internal markers). This will be

done by thinning the background by calculating SKIZ from the binary image foreground (Alex et al.,2017.).

Evaluation

In this paper, the threshold value and σ value in the step of calculating the gradient are considered as input parameters and the effect of changes in these parameters on the output results is investigated. The results of the proposed algorithm with the application of different threshold values are shown in Figure 1

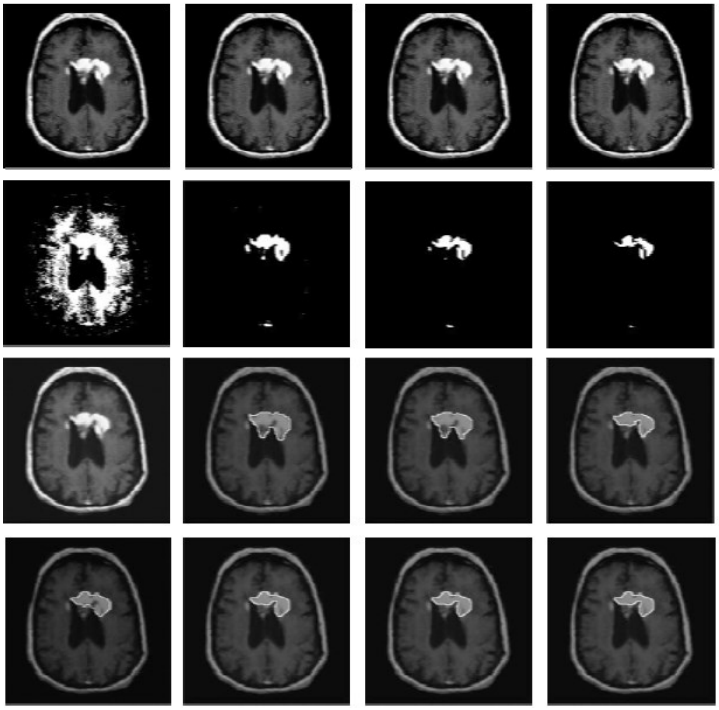

Figure 1. The results of the proposed algorithm by applying different threshold values. (a) Original image. (b) Threshold output. (c) Results of the single-indicator pool-based algorithm. (d) The results of the proposed algorithm

In this system, the selection of the threshold value in the parallel thresholding stage was completely automatic, but to evaluate the system and check the sensitivity of the algorithm results to the input parameters, the threshold value in the parallel thresholding stage is about 0.3 to large. 0.9 has been selected. As can be seen, by

changing this parameter in a relatively large body and the inappropriate output of the parallel threshold stage, the output of the proposed algorithm has the least change and still accurately performs the banding of the tumor area.

Also, to approximate the image gradient, image convolution with a Gaussian-oriented filter has been used. In this two-dimensional symmetric filter, the parameter σ is the standard deviation of the Gaussian function. σ determines the width of Gauss and its increase is removed by removing more details. The effect of changes in this parameter on the output results has also been investigated.

Similarly, the value of the parameter σ in the image gradient calculation step is changed in the range of 0.5 to 3, which is a large range of values for the parameter σ, to investigate the effect of changes in this parameter on the output results. It is observed that with the changes of σ, the output results of the proposed algorithm have the least change, and also the banding of the tumor area is done properly.

To further ensure the proper performance of the proposed algorithm, a quantitative evaluation of the results of the algorithm for the standard data set has also been performed. In order to quantitatively evaluate the performance of the proposed method, T1C images of the BRATS 2012 dataset and its reference images were used. The following five criteria were used to quantitatively compare the location of the extracted tumor and its position in the reference images stored as binary.

$$\begin{aligned}
Sensitiviy &= \frac{TP}{TP+FN}\times 100 \\
Specificiy &= \frac{TN}{TN+FP}\times 100 \\
Accuracy &= \frac{TP+TN}{TP+TN+FN+FP}\times 100 \\
Dice\ Similarity\ Score &= \frac{2(TP)}{2(TP)+FN+FP}\times 100 \\
Jaccard\ Similarity\ Index &= \frac{TP}{TP+FN+FP}\times 100
\end{aligned}$$

In the above equation, FP, TN, TP, and FN, respectively, represent the number of pixels that have been correctly identified as part of the tumor, the number of pixels that have been correctly identified as the year texture, and the number of pixels that have been incorrectly identified as Part of the tumor has been identified and the number of pixels that have been mistakenly identified as healthy tissue.

Dice's similarity score actually measures the ratio of properly segmented tumor tissue to the total area of tumor tissue in both the reference and segmented images. DSS values range from zero to one, and the proximity of this value to an indicator

The segmentation is more accurate (Zijdenbos et al., 1994). Also, the value of one for the Jacquard similarity index (Jaccard, 1912) indicates the existence of complete similarity between the two sets and the value of zero indicates the non-similarity between the two sets. The two Dice similarity score criteria and the Jaccard similarity index show both degrees of overlap between the actual tumor and the extracted tumor. Figure 2 shows the results of this implementation. The performance of the proposed algorithm in the brain tumor segmentation for the 2012 BRATS dataset is shown in Table 1.

Table 1. Results of tumor segmentation by the proposed algorithm on the images shown in Figure 7 of the BRATS 2012 dataset

Image number	DSS	Sensitivity	Specificity	Accuracy	JSI
1	95/83	94/85	99/89	99/70	92/00
2	96/22	98/91	99/82	99/79	92/72
3	90/68	96/77	99/91	99/89	91/08
4	94/53	96/82	99/92	99/89	89/63
5	93/89	98/00	99/81	99/78	88/48
6	95/22	97/53	99/88	99/84	90/88

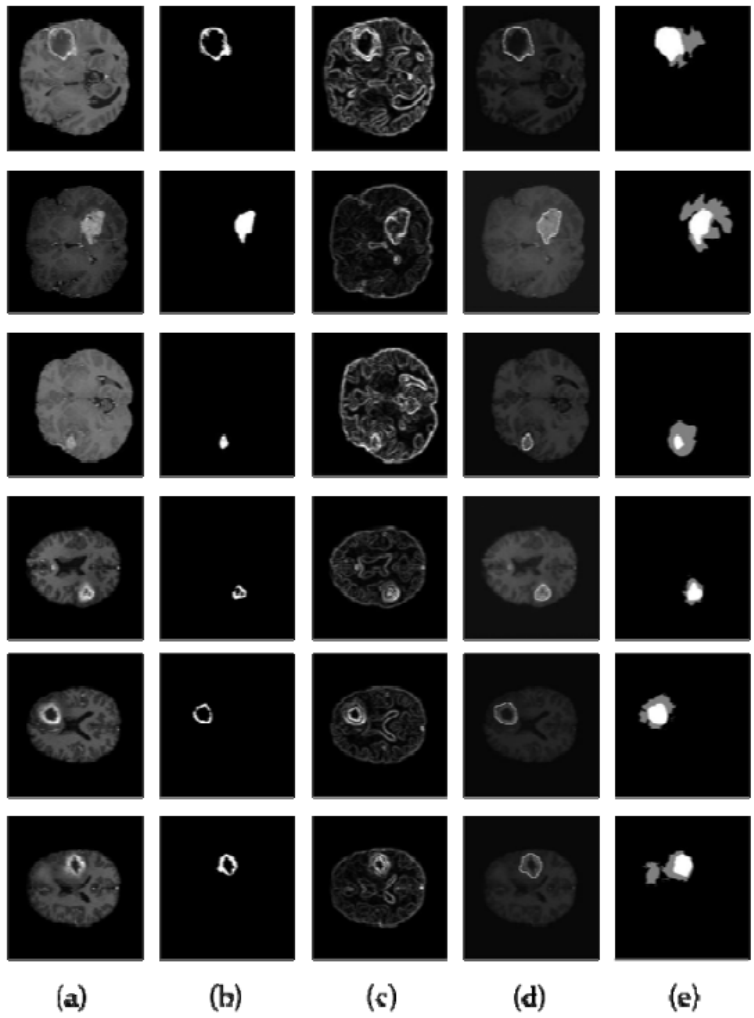

Figure 2. Results of implementation of the proposed method on the data set BRATS 2012
(a) Original image (b) Parallel threshold output with morphological processing (c) Rotation of the original image (d) Tumor area (e) Reference image

Conclusion

The two-stage segmentation algorithm proposed in this paper is a combination of two threshold-based segmentation methods and an indicator-based pond segmentation method. Each of these methods alone has one drawback. The results of the threshold-based segmentation method are highly dependent on the choice of

input parameters, and for each image, a different threshold value is needed from the other image, in other words, it is not an automated method. The pond section also has the problem of creating additional areas.

However, the reason for choosing these two methods is that they are able to cover each other's weaknesses. Threshold-based segmentation the problem of additional areas covers the pond sealing section and the pond sealing section covers the problem of low-precision threshold-based segmentation. In addition, because in the threshold-based segmentation method the goal is to locate the tumor area and not to accurately detect it, the input parameters of this step can be selected in a large range of values.

Also, the proposed algorithm is able to provide accurate output for tumors of different shapes, sizes and appearances in various images. This is despite the fact that the input parameters of the algorithm were fixed for all images. The implementations show that the proposed hybrid algorithm, in addition to being automated, has yielded accurate results on a wide range of images.

References

Abdel-Maksoud, E., Elmogy, M., and Al-Awadi, R., (2015) "Brain tumor segmentation based on a hybrid clustering technique," Egypt. Informatics J.

Ain, Q., Jaffar, M. A., and Choi, T. S. (2014) "Fuzzy anisotropic diffusion-based segmentation and texture-based ensemble classification of brain tumor," Appl. Soft Comput., vol. 21, no. 2014, pp. 330–340, Aug.

Alex V., Safwan M. Krishnamurthi, (2017) Brain tumor segmentation from multi modal MR images using fully convolutional neural network, Medical Image Computing and Computer Assisted Intervention - MICCAI 1—8.

Arakeri, M. P. and Reddy, G. R. M., (2013) "Computer- aided diagnosis system for tissue characterization of brain tumor on magnetic resonance images," Signal, Image Video Process., Apr.

Chang H., Lu J., Yu F., Finkelstein A., (2018) Pairedcyclegan: asymmetric style transfer for applying and removing makeup. IEEE Conference on Computer Vision and Pattern Recognition (CVPR).

El-Dahshan, E. S. a., Mohsen, H. M., Revett, K., and Salem, A. B. M. (2014) "Computer-aided diagnosis of human brain tumor through MR I: A survey and a new algorithm," Expert Syst. Appl., vol. 41, no. 11, pp. 5526–5545, Sep.

Faisal, A., Parveen, S., Badsha, S., Sarwar, H., and Reza, A. W., (2013) "Computer assisted diagnostic system in tumor radiography," J. Med. Syst., vol. 37, no. 3, pp. 1-10.

Guo, X., Tang, C., Zhang, H., and Chang, Z., (2012) "Automatic thresholding for defect detection," ICIC Express Lett., vol. 6, no. 1, pp. 159–164.

Harati, V., Khayati, R., and Farzan, A., (2011) "Fully automated tumor segmentation based on improved fuzzy connectedness algorithm in brain MR images," Comput. Biol. Med., vol. 41, no. 7, pp. 483–492.

Havaei M., Davy A., Warde-Farley D. et al. (2017) "Brain tumor segmentation with deep neural networks," Medical image analysis, vol. 35, pp. 18–31.

Jaccard P. (1912) "The distribution of the flora in the alphine zone," New Phytol., vol. XI, no. 2, pp. 37–50.

Kong X., Sun G., Wu Q., Liu J., Lin F., (2018) Hybrid pyramid U-Net model for brain tumor segmentation, in: International Conference on Intelligent Information Processing, Springer, pp. 346—355.

Multimodal Brain Tumor Segmentation Challenge, Web: (2012) data available at http://www2.imm.dtu.dk/projects/BRATS2012/

Nabizadeh, N., John, N., and Wright, C., (2014) "Histogrambased gravitational optimization algorithm on single MR modality for automatic brain lesion detection and segmentation," Expert Syst. Appl., vol. 41, no. 17, pp. 7820–7836, Dec.

Rezaei M., Harmuth K., Gierke W., Kellermeier T., Fischer M., Yang H., Meinel C., (2017) A conditional adversarial network for semantic segmentation of brain tumor, in: International MICCAI Brainlesion Workshop, Springer, pp. 241-252.

Sachdeva, J., Kumar, V., Gupta, I, Khandelwal, N, and Ahuja, C. K., (2012) "A novel content- based active contour model for brain tumor segmentation," Magn. Reson. Imaging, vol. 30, no. 5, pp. 694–715.

Yang X., Xu Z., Luo J., (2018) Towards perceptual image dehazing by physics-based disentanglement and adversarial training, The Thirty-Second AAAI Conference on Artificial Intelligence (AAAI-18).

Zhou, C., Chen, S., Ding, C., Tao, D.: (2018) Learning contextual and attentive information for brain tumor segmentation. In: International Conference on Medical Image Computing and Computer Assisted Intervention (MICCAI 2018). Multimodal Brain Tumor Segmentation Challenge (BraTS 2018). BrainLes 2018 workshop. LNCS, Springer.

Zijdenbos A.P., Dawant B. M., Margolin R. A., and Palmer A. C. (1994) "Morphometric analysis of white matter lesions in MR images: method and validation.," IEEE Trans. Med. Imaging, vol. 13, no. 4, pp. 716–24.

Khazar Journal of Science and Technology Volume 6 №1 2022, 53-57

DOI: 10.5782/2520-6133.2022.6.1.53

Application of NGN and NG-SDH Technologies

Asiman Teymurlu
Azerbaijan Technological University
asiman_t@outlook.com

Abstract

The article provides information on the applications of development of NGN and NG-SDH (New Generation Synchronous Digital Hierarchy) technologies. The article covered the possibilities of using this technology, the main strategies for the development of modern broadcasting systems. Reader can find main directions and purposes of applications of this technology out. Why Telecommunication area needs to improve traditional SDH technology? There is a comparison table of traditional SDH and NG SDH technologies. The transport network revolution, which began with WDM technology, and a number of other ancillary technologies are shown. The issue of economic evaluation of the mentioned technologies was also touched upon.

Keywords: communication, information, NGN, SDH, telecommunications, network.

Introduction

World telecommunications has undergone many scientific and technological revolutions. Its first revolution was entirely technological in nature and was associated with the transition from the principle of analog transmission and switching to the principle of number. A century has passed since this revolution, which began all over the world in the 1960s, and in the 1990s led to the emergence of completely new technologies. Its main features are that until the last moment it did not cover the whole society and was applied only in the telecommunications sector (Verdiyev & Məmmədov, 2018).

The second revolution in telecommunications is due to the emergence of mobile communication systems. What distinguishes it from the first revolution is that it covers the entire human civilization. The idea that any two people can communicate with each other anywhere, at any time, mobile communication has become one of the intangible values of society. Such deep support from the population did not lead

to a stormy new revolution. As a result, the percentage of "mobilization" of communication networks in many European countries today significantly exceeds the coverage of "classic" services of wired communication (Verdiyev & Məmmədov, 2018).

The third revolution, which has just begun and is growing rapidly, is the transition to a global information society (GIC). This revolution is radically different from the previous two revolutions, it not only covers the whole society, but also changes the foundations of its structures, in general, changes directions, values and so on. For example, information resources are strategic in parallel with the process of AIDS transition to the global information society, mercury, oil and gas resources. The sphere of communications is not the basis for business development, their economic model and production models are more virtualized (Məmmədov, 2022).

Main directions and purposes

One of the directions of application of new virtual technologies in life is to provide the population with the widest possible access to the information resources of society and the whole world civilization. Thus, it is necessary to modernize all modern communication systems. A new revolution is emerging in the practice of the world and the country, which is called the New Generation Network (NGN) (Zingerenko, 2013).

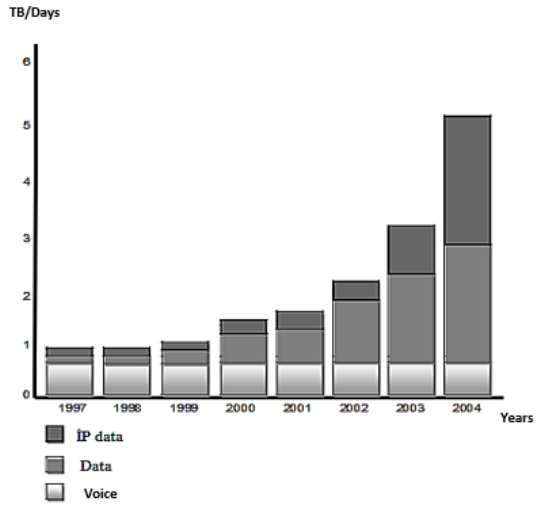

Figure 1. One of the qualitative assessments of the development of three traffic groups in networks

The NGN revolution is based on a shift in priority from voice traffic, data traffic from switching channels, and packet switching. Indeed, the share of data transmission traffic is currently growing dynamically and is gradually dominating in modern communication systems (*Ivanov, 1999*). Evaluation of qualitative and quantitative indicators shows that the dynamics of growth of voice traffic is stable on average worldwide. In this case, the level of voice traffic remains unchanged. On the contrary, the share of data traffic, and especially the share of IP traffic, is growing significantly. From 2003 to 2004, data traffic was preferred in European networks, and from 2004 the share of IP traffic exceeded the share of voice traffic (José, 2005).

Comparison of traditional SDH and NG SDH

This table (Table 1) consist comparison of main functions of Traditional and New Generation SDH technologies (José, 2005):

Table 1. Main functions of Traditional and New Generation SDH technologies

Functions	**Traditional SDH**	**NG-SDH**
Basic appointments	To provide the first network channel between two points	Provide a corridor for IP traffic between the two points
Network channel settings	Standard channel at PDH E1, E3 and E4 level	nxVC-12 capacity corridor
Ability to release	Registration	Registration
Input interface settings	PDH interfaces in accordance with G.703 recommendations	Different interfaces, maximum 10/100/1000 Base T

Conclusion

As a result, the NGN revolution is ideologically grounded and sets new requirements for next-generation SDH systems: NGSDH technology must support packet traffic transmission and be maximally adapted to all levels of packet traffic transmission, primarily IP traffic (José, 2001).

If NGSDH allows you to connect different segments of access networks, then it can fully claim its place among NGN transport networks. The advantages of this system arise when the following three conditions are met:

1. The NGSDH system is already deployed and used by the operator to solve classic SDH problems. The solution is only viable if it optimizes the use of existing SDH transport;

2. The NGSDH system has sufficient spare capacity to create a corridor of the required width;

3. The NGSDH system itself successfully connects to the segments via the Ethernet / GE interface (ITU-T Rec. G.703).

One of the main requirements of NGN's transport networks is the transmission of different types traffics. Sources of such traffic are ESCON (Optical Fiber Channel Interface), FICON (Channel Sequence of Data Transmission), DVB (Digital Video Broadcasting), Ethernet, RPR, as well as leased channel (Private Lines) technologies (ITU-T Rec. G.783). All of these technologies are interrelated with NGSDH at the channel level or MAC level. This is equivalent to the channel level of NGN networks. These technologies transmit traffic consisting of various applications.[10]

For these applications, the NGSDH system must form interconnected channels with fixed or variable throughput. Thus, the network layer functions are defined in the NGSDH model. At the bottom of the model is the level of the transmission system. Thus, the network layer functions are defined in the NGSDH model (ITU-T Rec. G.781).

References

Huub van Helvoort. (2005). Next Generation SDH/SONET: Evolution or Revolution? 1st Edition, 256s.

Ivanov, A.B. *(1999). fiber optics. Moscow.*

ITU-T Rec. G.703, Physical/electrical characteristics of hierarchical digital interfaces.

ITU-T Rec. G.781, Synchronization layer functions.

ITU-T Rec. G.783, Characteristics of synchronous digital hierarchy (SDH) equipment functional blocks.

José, M. (2005). Caballero-Artigas, SONET/SDH and NG-SONET/SDH. 145s.

José, M. (2001). Caballero and Andreu Guimerà, Jerarquías Digitales de Multiplexión, PDH y SDH, Sincronización de Redes, L&M Data Communications.

Mammadov I.M. (2022). Optik rabitə, Ali məktəblər üçün dərslik. Ganja, 435s.

Verdiyev S.Q., & Məmmədov I.M. (2018). Optik rəqəmli telekommunikasiya sistemləri və şəbəkələri. Dərs vəsaiti, Ganja 2018- 292 s.

Zingerenko, S.A. (2013). Optical digital telecommunication systems and networks of synchronous digital hierarchy. St. Petersburg: Textbook. - St. Petersburg: NRU ITMO, 393 p.

Khazar Journal of Science and Technology Volume 6 №1 2022, 58-62
DOI: 10.5782/2520-6133.2022.6.1.58

Effective Method of Industrial Waste Treatment

Narmin Rakida
Baku State University, Z. Khalilova 23, AZ 1148
nararakida@mail.ru

Abstract

According to our study, the use of special coagulant, flogulyant, extragent, and the use of conditions can result in the efficient disposal of oil spills from the oil spill mixture. In addition to thoroughly cleaning oil spills, up to 100 percent of dependent substances have been cleaned and black rice has been fully dissolve. In the study, from 1ml petroley effects (from 40 to 70 degrees Fahrenheit [40 to 70°C] in gasoline fractions), from $Al_2 (SO_4)_3$, The optimal use of 2 ml 5% H_2SO_4 acid as a flogulyant, 1ml 5% $NaHCO_3$ solution to have pH=7-7.5 when required. This chemical method is based on the scientific basis for the possibility of cleaning up NMTG-based industrial wastewater at a maximum of 25-30 degrees Celsus in the industry.

Keywords: wastewater, industry, coagulant, ecological, effective, flogulyant, chemical, petroleum products, waste mixture

Introduction

In the oil industry, technological advances are complex and complex, so they are shaped by a stream of water that differs from one another. Because the industrial wastewater that occurs during this time is not separately cleaned, it is mixed with the facility's general sewage system and enters the refinery's refinery. In those refineries, industrial wastewater is first cleaned up in mechanical and biological cleaning stages, as well as in ecological standards. During these processes, some of the clean water is used in the recycling water system at oil refineries, while part of it is flowing into reservoirs. That is why the oil refinery industry is considered one of the sources of hydrosphere pollution.

Currently, despite the use of new technological processes, installations, and the results of many research projects in the developed world, the wastewater industry has not been fully cleaned of wastewater.

Based on the results of a long-term study carried out by our mission, it is noteworthy that the number of wastewaters that is the most complex component of the oil spill is specifically the use of optimal conditions, coagulants, flogulyants. Using chemical technology for the use of extragents, up to 100 percent of NMTQ-dependent substances can be used to ensure that the wastewater is not fully transparent.

This newly used method (Rakida, 2020; Burenin, 2015; Tulemann and Sherbel, 2011; Xutoryanski, 2011; Shapkin et al., 2012; Shamilov et al., 2020; Hajiyeva et al., 2021; Bayramov et al., 2019) has been compared to the methods used in publications (Rakida, 2020; Burenin, 2015; Tulemann and Sherbel, 2011; Xutoryanski, 2011; Shapkin et al., 2012) and has been compared to the methods used in some institutions by mechanical thermal, physical, and chemical methods (extraction, evap) based on several new scientific research of oil-producing industrial waters although oration, azeotropic, ionization, adsorption, absorption, coagulation) and finally biological cleaning methods have been used in the final phase, up to 100 percent of those industrial flows have not been able to be cleaned of NMTQs and dependent substances.

Materials and methods

For a long time, various substances such as $FeCl_3$, $FeSO_4$, $Fe_2(SO_4)_3$, $Al_2(SO_4)_3$ have been used to clean up the oil industry's wastewater samples in a number of ways. At the same time, a new optimal technological regime has been developed using a fraction of 40 to 70 degrees Fahrenheit [40 to 70°C] of petroleum $_2SO_4$ acidic acid, as well as an extragent.

The highest score at the time of the study was obtained when using 5 percent of $Al_2(SO_4)_3$ as a coagulant. Therefore, we provide the following explanation for the experimental part of the method used. A liter of TS samples from NMTQ at a rate of 1,000mg/l are placed at a separator of 5-20°C and are mixed with a petroleum effect of up to 0.1 percent (1ml) for a minute. Up to 0.5 percent of the TS sample is mixed for 1 minute with a 5 percent $Al_2(SO_4)_3$ and 2 ml 5% H_2SO_4 acid is added to accelerate the coagulation process. The maximum process of coagulation is completed in 15-20 minutes. In the separator lock, the upper part of the three phases (NMTQ+extra) was separated by a small amount of mechanical mixtures, including water and salts. The separation of water layers, water layers, and debris (Shapkin et al., 2012) is completed by known methods. The amount of a separated phase has been refined in a gravitational way.

The study found that the TS sample, which was refined, was about zero in the amount of NMTG and dependent matter. Thus, using chemical reactors-coagulant, flogulyant, and extraterrestrogen - a special optimal technological regime has been used to clean up NMTQ, 100 percent of the dependent substances, and full transparency of the color.

The method mentioned in the bible uses up to 10 percent of the water that is extracted from the NMTG because of the $_3$ and salt mixture of SO_4 ions. At the same time, it has been made clear that up to 3 percent of the TS, which is collected in the cleaning process instead of extragents, can be used to clean up to 100 percent of the NMTQ, dependent substances, and fully discontinue the color.

Result and discussion

The problem of deep cleanup of wastewater, which contains high NMTQ emissions, is still ongoing because of frequent changes in the oil industry, its very complex physical characteristics, and its high flow speed.

Experimental research and scientific, technological, and technological research have found that the use of extragent, coagulant, and flogular wastewater from economic and ecological activities can also be used to clean up 100 percent of NMTQs, dependent substances, and fully transparent. As the data show, this method is now considered scientifically valid because it has a very important ecologically and economically important technology.

When using various percentages, density, and specialized coagulants in various directions, it has been proven that the highest coagulating chemical reaction is $Al_2(SO_4)_3$ substance. During this time, the use of petroleum reactors, such as H_2SO_4 acid, and extragents, has been identified as a floguliant and the use of optimal and technological regimes.

The following scientific explanations can be used in publications to describe the progress of the coagulation process (Novruzov, 1991; Patent, 2021) in the chemical ecological efficiency of wastewater samples that have been developed in the oil industry.

The environment of wastewater is shaped by neS, often changing pH=9-10, and in some cases even pH=10-11. That is why when using $Al_2(SO_4)_3$ as a coagulant during the cleaning of TS_4 5 percent H_2SO is added to the TS that is cleaned as a flogulyant and neutralizing TS.

Previously, up to 0.1 percent of the TS sample is mixed with petrole effects. During the extraction process, the combination of i-C_5H_{12}, n-C_5H_{12}, and i-C_6H_{14}, n-C_6H_{14} is extracted from the main NMTG and other organic compounds contained in the TS.

The mixture of NMTG emissions and the full extraction of NMTG occurs when the mixture is mixed with a mixture of up to 0.5 percent of that water and a 5 percent $Al_2 (SO_4)_3$. Meanwhile, $al_2 (SO_4)_3$ hydrogen peroxide and becomes colloidal dispersion $_3$ Al(OH) (Novruzov, 1991):

$$Al_2(SO_4)_3 + 6H_2O = 2Al(OH)_3 + 3H_2SO_4$$

The SO_4^{-2} aniones of sulfuric acid, such as sulfuric acid, and (Shapkin et al., 2012) sulfuric acid, are reacted to by NaOH, $Ca(HCO_3)_2$, and so on.

$Al_2 (SO_4)_3$ coagulant is hydrogenated as soon as it is added to the TS mixture, and when it is transformed into a colloidal shape $Al(OH)_3$ the TS environment is likely to be loaded because it is pH=9-11, and the loaded colloids contained in that water are likely to be adsorbed and coagulated. Meanwhile, when Al(OH) $_3$ collapses at its own expense, the TS mechanically crushes clay, soil, and other particles that are dependent on the environment and accumulates them in an organic layer, which has a positive effect on the complete extraction process.

The aforementioned explanations show that regardless of the amount of NMTG in manufacturing and the volume of TS, it is possible to clean up 100 percent of that water.

Finally, it should be noted that the NES's disposal of wastewater that is shaped by the production process will prevent TS from being released into a million cubic feet [1 million cubic meters] of water in those institutions, and drinking water can be saved at that rate, which is very important in ecological value.

References

Bayramov G.I., Samadova A.A., Jafarova N.M. (2019). Methods of analysis of harmful substances in industrial wastewater obtained in the oil industry // Laman Publishing Polygraphy. MMC. 22

Burenin V.V. (2015). Protection of water bodies from pollution by oily wastewater. // Ecology of production. Scientific and technical journal. M. 2: 54–62

Hajiyeva S.R., Bayramov G.I., N.T.Shamilov, Rakida N.M. (2021). Ecologic effektive treatment of industrial waste water formed in the oil – producing industry by coagulation method // Azerbaijan chemical journal. 63-67.

Novruzov S.A. (1991). General chemical tecnology and industry ecology ekologiyası. Baku: Maarif, 340–345

Patent. (2021) "Method of treatment of industrial wastewater", 7: 5

Rakida N. (2020). Development of the method of deep ecological effective chemical treatment of industrial wastewater generated in the oil industry. // International Journal of Scientific Engineering Research, 11: 6: 880–886

Shamilov N.T., Hajiyeva S.R., Bayramov G.I., Kadirova E.M. (2020). Problems of toxic organic substances for aquatic systems // "Materials of the VIII International Scientific Conference "Chemistry of Coordinating Compounds" dedicated to the 85th anniversary of the Department of "Analytical Chemistry" Baku- BSU, 22-23 december 3 (113-115)

Shapkin N.P. and oth. (2012). Wastewater treatment method. Patent 2440931, Russia. MPK CO 2F 1/465. Chapter. 3.

Tulemann I., Sherbel V.S. (2011). Wastewater treatment at refineries // Ecology of production. Scientific and technical journal, 4:28–30.

Xutoryanskiy F.M. (2011). Trapped water-oil emulsions: removal of mechanical impurities and dehydration. // Journal. The world of petroleum products. Chapter. Ecology and industrial safety. 4:25–28

Khazar Journal of Science and Technology Volume 6 №1 2022, 58-62
© Khazar University Press 2022 DOI: 10.5782/2520-6133.2022.6.1.58

Artificial Intelligence Using a Neural Network System to Support Human Resources in the Workplace

Mohammad Ali Alqudah
Department of Computer Science, Khazar University, Azerbaijan
mohammad.ali@khazar.org

Abstract

Artificial neural networks mirror the behaviour of the human brain, allowing computer programs to recognize patterns and solve common problems in the fields of artificial intelligence, machine learning, and deep learning and from it an attempt to represent human behaviour according to learning algorithms; These artificial networks target cognitive and cognitive activities associated with brain function. The current study aims mainly to reveal the nature of the relationship between human resources and the smart organization through the neural network system and the level of its practices, the neural network resembles the sources of human mental activity as an effective resource in the functional environment, and to identify the most important what these super-intelligent applications can add to organizational behaviour. The data was analyzed using The simulation system for neural networks through mean clustering tests and to indicate the level of influence of inputs and outputs to reach the proposed model, as well as tests of accuracy and performance of the model, the level of error in training neural networks, then the strength of the relationship between layer nodes, the weights of the effect of hidden neurons (layer hidden) and the relative importance The dimensions of the inputs over the outputs of the final model. The results of the study showed that the practice of smart organizations has a greater impact on the human resources elements The study recommended that decision centres should realize the importance of the simulation system in neural networks in providing solutions for to administrative problems because of the time, effort, and money it saves, in addition to the accuracy of the results, in addition to the need to continue to Disseminate and adopt human resources because it is the basis on which to achieve an important strategic competitive advantage and The necessity of compatibility of the objectives set by the Bank with the economies of knowledge, electronic commerce, and mutual communication and innovative knowledge.

Keywords: neural networks, artificial intelligence, human resource, organizational behaviour

Introduction

The knowledge industry, its possession, and then its transmission and dissemination, has become a feature closely related to scientifically advanced, technologically, and technically advanced societies. The concept of knowledge has become closely related to the concept of power, even if the dimensions and goals of this power are numerous. Concepts that were adopted from knowledge as rooted in their formation, such as the concept of "knowledge society, knowledge economy, knowledge management, knowledge capital ... etc." For a concept that is self-contained, studied by disciplines, dealt with my studies, and in which research and fields are deepened, it gains its weight from the weight of knowledge, because it is the industry of the future, and the wealth of nations looking forward to tomorrow, controlling the initiative, and proactive for excellence and eager for it; In the midst of all this, the concept of knowledge technology emerged, within the enormous information and communication technology tide, which the post-modern stage knew at a high level of expectation.

The huge scientific development that followed the information revolution of information technology and communication media, allowed the emergence of the concept of simulating human knowledge; That is, searching for models that can represent the amount of knowledge that distinguishes humans from skills, experiences, and acquisitions; As a person has tried to search for ways to transfer his knowledge experience to smart media, which saves him time and effort in his daily life dealings, no matter how different aspects of these transactions are, and their goals are numerous. These systems are based on advanced pillars to turn into super-intelligent networks, whose interactive environment is represented by the computer and its accessories, and their technological capabilities are researched; So, the human mental capacity, including its trilogy; Thinking, Awareness and Perception, looking at the possibility of simulating human intelligence with its complex mental functions through computing, thus what is known as artificial intelligence appeared.

Artificial intelligence, like a quantum leap in the world of advanced and accurate technology, has opened the way for the search for an exceptional alternative to human intelligence, with the possibility of applying this alternative intelligence in several areas based on data and data, most of which are digital, based mainly on smart systems technology, and branches of engineering and abstract mathematics. and specializations from the humanities, and gave a strong impetus to the emergence

of designs parallel to the design of the human brain, as the main source of various cognitive mental processes, and the most important of these designs are what is known as artificial neural networks, which derive their name from the representation of the human vital neural network, which depends on precise mathematical programming using Computing is an attempt to simulate the functioning of the neurons of the human brain, which are the source of various voluntary cognitive functions (mental) that distinguish humans from other organisms. One of the most important areas that can benefit from the skills of artificial intelligence techniques, such as neural networks, is the field of management, as it is a vital field that includes within its organizational environment human resources that seek to develop their management methods and raise the level of their tasks, in an attempt to improve the efficiency of their performance for their various functions, by introducing technology in The management and management process, depending on what is known as management by technology, through our research paper; We seek to research the possibility of using artificial neural networks as an alternative to performing some human resource tasks, as energies that need support and cognitive refinement, through a behavioural simulation of their organizational behaviour within the work environment, by asking the following question: Can artificial neural networks perform administrative functions based on a modelled simulation of resource behaviour Human in his organizational environment? As solving some administrative problems or predicting organizational phenomena? We have dealt with this problem, and tried to answer it by adopting a number of elements that we have clarified in our next study.

Artificial Intelligence and Simulated Technology

There were many definitions that tried to approximate the concept of Artificial Intelligence as a unique simulated technology experiment that seeks to create highly advanced techno-technological systems, simulating human biological systems, most notably the bio-neural system, and focusing more on intelligence as the most prominent human activity characterized by complexity and privacy.(Dick, 2019) This is because the concept of artificial intelligence is closely related to several sciences and disciplines. From linguistics and linguistics to mathematics(Thierer et al., 2017)

And logic, to computer and software engineering, to neurosciences and genetic algorithms, without forgetting the active role of psychological sciences, especially cognitive psychology and its great contribution to the search for ways to develop

learning and comprehension activities, all of which have to do with human cognitive functions(Vinuesa et al., 2020).

Artificial intelligence is defined in its simplest concepts as: “A computer simulation of the cognitive processes that humans use in performing actions that we consider intelligent, and these actions vary widely in nature; they may be understanding a spoken or written linguistic text, playing chess, solving a puzzle or a mathematical problem. Or writing a poem, or making a medical diagnosis, or inferring a way to move from one place to another. The researcher in the science of artificial intelligence begins his work first by choosing one of the activities agreed upon as intelligent and then makes some assumptions about the information that a person uses when performing this activity. and inferences, then enters them into a computer program and then observes the behaviour of this program(Khrais, 2020).

The roots of artificial intelligence as a fertile field of knowledge for research go back to the forties of the last century, a period that witnessed an increase in research and studies related to the development of computing applications based on computers of various generations.(Chui, 2017)This is the name for artificial or neuron neural networks; Where did the research actually begin in the possibility of simulating the work of the human brain, while in the sixties began to pay attention to the field of Heuristic search, which is one of the research techniques in artificial intelligence, while in the seventies the research was based on what is known as systems based on knowledge representation and processing, to be Paying attention to the eighties and beyond, when Japan announced the implementation of a program for the development of fifth-generation computers; This generation was known for its performance efficiency, speed of implementation and response compared to previous generations, and the generation that paved the way for the emergence of what is known as smart computers, with knowledge-based computing systems based on knowledge bases, to make a qualitative leap in the development of artificial intelligence research and the emergence of what is known as machine learning(Butcher & Beridze, 2019).

Artificial intelligence programs seek a realistic simulation of human knowledge, relying on inferential operations, and not only work with binary machine language (0,1), but go beyond it to use non-numeric symbols, and on languages based on the interpreter and not the translator, which makes them able to visualize concepts At its different levels, given that human knowledge is multi-level, and these programs are also characterized by their ability to make decisions in the absence of data and complete information available about these decisions, or their conflict, and this is similar to a close extent, the process of human reasoning towards finding solutions and making decisions based on intuition. In the absence of data and facts about these

decisions or their contradictions, and these programs have the ability to learn from mistakes by acquiring the ability to infer symmetry, and access to generalities. Cognitive psychology has also contributed to the development of these programs to identify the methodology of the work of human intelligence (Nishida et al., 2017).

From the foregoing, it can be said that artificial intelligence, as a broad scope that includes among its cognitive innovations the innovations of symmetry, has given way to the emergence of the concept of technology simulating not only human knowledge but its material and moral assets, and the emergence of the concept of artificial neural networks and their connection to the field of technology (computing technology), evidence of the integration between The triad of experiential sensory knowledge, abstract knowledge, and mental knowledge, it is a reconstruction and design of the system from interactive thinking between the existing innovative development or known as Technology Innovation, and what the human experience must reach from innovative patterns that enhance the simulation of human life(Wall, 2018).

Artificial Neural Networks

The definition a neural network

Artificial neural networks are one of the most controversial areas of artificial intelligence among researchers and scholars of this discipline. Which largely reflects the extent to which this precise technological trend has developed, as it is closely related to an attempt to simulate the activities of the most important vital organ of the human organs, the brain, despite the complex structure of the latter, and the specificity of its vital processes(Silva Araújo et al., 2019).

Artificial Neural Networks can be defined as ANN, or what are also called Simulated Neural Networks. It is an interconnected group of virtual neurons, created by computer programs to resemble the work of a biological neuron or electronic structures, that use a mathematical model to process information based on the communicative method in(Li et al., 2019; Simonyan & Zisserman, 2014)

computing; Thus, artificial neural networks are similar to the human brain in that they acquire knowledge by training and store this knowledge using interconnecting forces within neurons called synaptic weights(Zhang et al., 2018)

Artificial neural networks have been designed from computer programs to simulate in their structure and functions the human brain, with its billions of neurons (the number of human brain cells is estimated to be about 100 billion neurons), and each

cell has about 1,000 types of inputs, and it has connections and connections with other cells. These artificial neural networks acquire the intrinsic characteristics of the human brain in terms of their synaptic connectivity, distributed and parallel processing of information, which is the basis of Computing Neural; Neural networks consist of interconnected computer units, each unit carrying out processing operations and transmitting results to other units, so these networks can learn through training (Bejarbaneh et al., 2018; Garcelon et al., 2018).

So artificial neural networks; It is a software synthesis of instructions and commands formulated according to mathematical rules in the form of functions, whose goal is to replicate the work of the nervous system represented in the functions of the brain, and the various connections that connect the activities of these functions and their outputs to the rest of the vital organs responsible for the most important thing that distinguishes humans from other organisms; It is the thinking function, which is the main axis for which these simulated networks are designed, as it relies on the learning and training processes, the principles of processing and information processing, and the participatory method of transferring processing outputs and transforming them into knowledge outputs that simulate human experience; So this combination does not depend on the transfer of ready-made expertise, but rather its manufacture from databases based on the most important knowledge-making processes, from collecting raw data, learning to process it, and training to transfer and share it (He et al., 2016). The following model (Figure 1) illustrates the structure of a computerized neuron:

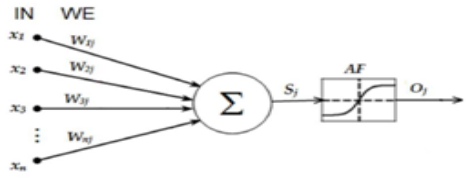

Figure 1. Structure of a computerized neuron

The neuron includes the input signals, and the processing element, which determines the level of activation of the accumulated strength of these signals by weighing the correlation given to each element or signal input and output of the neuron shown in numerical values (0,1). The following figure (Figure 2) represents a comparison between a biological neuron and an artificial neuron:

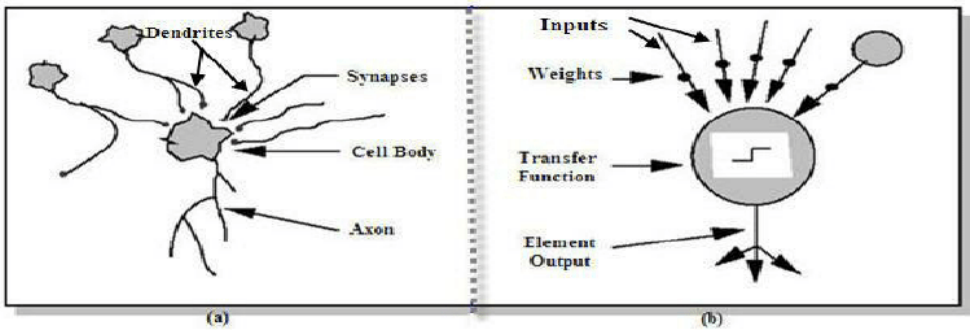

Figure 2. Comparison between a biological neuron and an artificial neuron.

(Hamdi & Aloui, 2015) Research and studies that dealt with the field of neural networks return to the work related to the concept of cybernetics, specifically what was done by the scientist Norbert Wiener, who worked at the Massachusetts Institute of Technology; In 1954, he published a book entitled "Human Use of Humanity: Information Control and Society." In this book, he indicated that the human system is similar in its function to the machine system. During the fifties, artificial intelligence scientists began trying to create an intelligent machine that could resemble the human brain(Silver et al., 2016). Because the computer industry

And its development in its beginnings at that period, the technology available at the time did not help them in making the required machine, and one of the most important attempts that characterized that period was that of Frank Rosenblatt in 1957, who made what he called the perception, a simplified model similar to the retina of the eye, and enabled him to teach This perceptual sensor has some specific forms, but it was criticized because of the simplicity of the model, which reduced the interest in research related to the field of neural networks until the eighties, when it began to work on the fifth generation of computers, and the interest returned to a greater degree in this field (Schmidhuber, 2015; Simonyan & Zisserman, 2014).

Characteristics of the artificial neural network

Artificial neural networks are characterized by capabilities and characteristics that make them one of the most important artificial intelligence systems, most notably: - The ability to distinguish patterns, self-learning, providing solutions to problems that require non-algorithmic solutions; After training and providing it with training data that enables it to determine and modify weights continuously, there are several rules for learning, including: (Schmidhuber, 2015) Herb rules, field Hop law, Delta rule, Kohomen's law - its use of the exploration approach, its search for optimal solutions, improvement of the proposed solution through training and learning, And its wide use in cases of prediction, classification, modelling, simulation, grouping, filtering,

abstraction, interpretation of solutions, in addition to its use in building simulation models for problems that we do not use in solving other artificial intelligence systems and techniques. The use of neural networks in various business activities; Especially in the field of operations management, financial analysis, control and control, stock and bond price forecasting, currency exchange rates and risk management, investment portfolio analysis, bank credit, e-commerce, and support for electronic management decisions (Li et al., 2019).

The architecture of the artificial neural network

An artificial neural network consists of several components, including:

Input Layer: It receives input signals from outside the neural network and corresponds to the dendrites in the vital neuron in humans.

Weights: represent the connections between layers in artificial neural networks, which correspond to natural neural networks (Yusri et al., 2018).

The middle layer is Hidden layer: It is the process of discovering and distinguishing characteristics, classifying and analyzing the inputs by giving certain weights to each of them, and using an analytical function to modify those weights, based on the comparison of the target results (Schmidhuber, 2015).

Output Layer: It is the last layer that gives the real output after a series of manipulations that take place through the previous layers.

Threshold: It is the limit that determines the extent and type of output to be compared with the desired output (Target Output).

Benefits of Artificial Neural Network

Among the most important benefits of using artificial neural networks are the following (Xiaosong et al., 2019)

• It deals with the non-linearity that exists in reality, ie it deals with the non-linear models.

• It deals with incomplete data, ie incomplete.

• Operates with a large number of variants.

• It gives general solutions with high predictive powers.

Artificial Neural Networks and the Regulatory Environment

Artificial neural network and expert systems

Expert systems are among the most prominent artificial intelligence systems applied in organizations, as they are systems based on knowledge bases, and fundamentally different from traditional database-based systems. Expert systems are based on the technology of representation and storage of knowledge, and accumulated human experience, In a specific scientific or applied field. The knowledge is represented by the knowledge engineer, who, through observation, interview and analysis, models the knowledge gained from the experts in the analysis, and writes it with a computer program or an algorithm through which the computer can implement it and meet the needs of the non-expert user later (Junio Guimarães et al., 2019). While neural networks are not based on knowledge modelling technology

Humanity, or human intelligence, and does not seek programmed solutions, and therefore does not need the intervention of knowledge engineers. They are subject to many variables, so the capabilities of these networks are described by the term layers of knowledge for their ability to cognitive analysis (Khan et al., 2020).

Artificial neural networks are not just simulation, modelling or prediction solutions only, but go beyond that to an attempt to search for solutions to the most complex problems, and the most prominent sudden phenomena (non-linear phenomena), relying on the process of learning and training, by focusing on the exact software and physical aspects of the computing process, It aims to establish an intelligent system that transcends the mathematical and programming operations of the computer to create experienced hardware that can deal with these intelligent mathematical software, and the complex human brain structure transcends the precise anatomical aspect to the external morphological aspect. Among the environments that have tried to implement this type of application, we find the organizational and administrative environment, where the organizations' strategies are looking for solutions to take their organizational decisions, which are considered as supportive of their work process and continuity (Egrioglu et al., 2013). There are two important types of artificial neural networks applied in organizational environments:

A- Single-layer networks: They are considered one of the simplest types of neural networks and consist of an input layer and an output layer, which represents the function of the neuron. Ie there is no input (X1 X2.....Xn) affects weights (w1, w2,...Wn), to produce a final output, let it be 7 as follows: [v = F [2xi wi]

B- Multi-layer networks: They consist of three layers; An input layer, a hidden middle layer) and an output layer, and the middle layer may be one layer, or several layers, depending on the nature of the problem under study, and the development has been in training multi-layer networks using the reverse propagation method. That is, there are inputs (X1.X2,..,Xn) that affect the weights (W1, w2, wn) to produce an output (Y1.Y2....,YM), which in turn affects the weights (01,02...,0m), to produce a final output Z as follows:

$$Z=F\ [\Sigma Oj\ Yj]=F\{\ \Sigma Oj\ F[\Sigma\ Xi\ Wi]\}\ (4\text{-}5).$$

The multi-layer network model is considered one of the best models applied in the organizational environment. The following figure (Figure 3) shows a model of a multi-layer neural network

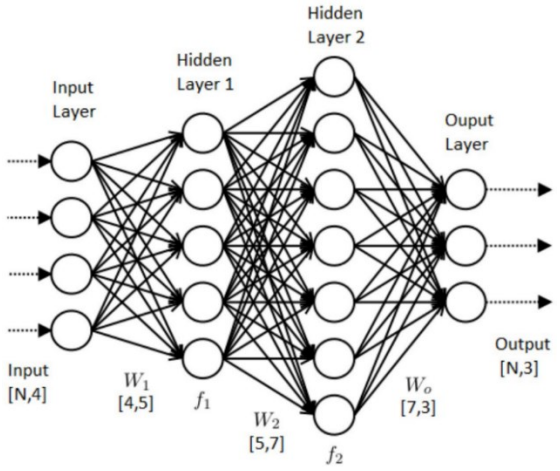

Figure 3. Model of a multi-layer neural network

The neural network in this model consists of three levels; input level, hidden level, output level; Each level contains a simple processing unit or element associated with the processing elements and units in the subsequent level, and because of this structure, the artificial neural network can provide an easy and efficient way to find a solution to the problem studied, i.e. a relatively easy way to model or predict the behaviour of non-linear phenomena, making it The best methods applied in the two currencies of modelling and forecasting compared to the traditional statistical models and methods applied in the fields of management and organization (Nord et al., 2019).

Artificial Neural Networks and Nonlinear Phenomena

Linear Organizational Phenomenon

The organizational phenomenon is considered one of the human phenomena in which the human directly intervenes in its occurrence, which makes it characterized by the character of privacy and uniqueness, and the characteristic of kinetic dynamics in the sense that it is not fixed, as it is difficult to study it in isolation from the conditions of its occurrence due to the overlap of several elements and aspects in it, the most important of which are the socio-cultural and geo-environmental aspects. Even economic and political (Lin et al., 2016; Peng et al., 2018). The organization, as the most important units forming the social structure and the most important interactive forms within it, faces many challenges, to draw up its organizational strategy that it is supposed to follow to continue within its context organizational without drifting or going back, in order to achieve the goals and gains for which these strategies were developed, and for which this organization was established, which makes it classified in the category of nonlinear phenomena. The term nonlinear may be a mathematical term; It refers to a state of heterogeneity and non-overlap between numerical variables, which are difficult to enumerate and express with a linear mathematical function, but the non-linear organizational phenomenon from an administrative perspective; It is everything that happens intentionally or suddenly and unexpectedly in the organizational environment and affects the rest of the organization, and requires intervention to find solutions. Finding solutions to them, and one of the most important solutions for dealing with such phenomena is simulations, modelling and prediction (Njitacke & Kengne, 2018).

The difference between the concept of simulation, modelling, and prediction
Simulation has multiple concepts, many in different epistemological contexts that include simulation activity. necessary, to describe the behaviour of a phenomenon, and the simulation process begins with building a model for the problem under discussion and then implementing experiments and solutions for the complex model in digital computers." Modelling is not very different from simulation but is one of the basics of simulation; It means a description of a specific situation or topic, where this situation or topic is expressed by a mathematical equation, which includes in its composition a set of variables, and the modeling process depends on many statistical methods and laws, which make it necessary for the modelling user to be familiar with statistical methods and theories. Forecasting in general is "an expectation and estimation of future events under uncertain conditions" or "constructing a perception of what the phenomenon will be like in the future, in a more accurate sense; a process of intelligent and thoughtful estimation and estimation based on the nature of the phenomenon, its development and growth in its current situation, The degree,

directions, extent and strength of growth after all these have been subjected to the appropriate measuring tools (Jaensch & Polifke, 2017).

Computerized or artificial neural networks are considered one of the most effective ways to predict the behaviour of the organizational phenomenon, as it is not fixed. This prediction includes tracking the changes that occur to it, since it began to occur, even trying to predict the results that you will reach, and make predictions about the solutions that can pass them depending on the education algorithms that we mentioned previously with the reverse propagation algorithm, which is used with multi-layer neural networks, as it includes two layers Inputs, outputs and hidden layers, called middle layers, are connected to the rest of the layers by ganglia or neurons; As each layer in the neural network contributes its work, the input layer receives all the data related to the phenomenon or problem under study, in its digital form, where the human resource responsible for decision-making and searching for effective solutions for this, collects all indicators about the phenomenon and enters them, so that the middle layer receives the inputs The reception takes place at the level of the neuronal ganglia, where the connection of each neuron node with its predecessor through weighted connections contributes to receiving these inputs. Assembling and transforming calculates the weights of the inputs and determines the quality of the outputs. As for the process of processing the input data, it is done by multiplying each input from the neuron of the previous layers, with the weights of the weighted communication links with the neurons so that the products of the multiplication are collected, where the conversion function intervenes in the process of producing the output that will be transmitted to the neurons of the other layers.

Since artificial neural networks depend on the principle of learning, to identify problems, learning methods have been developed that are compatible with the nature of the neural network (Goldt et al., 2019).

The multi-layered neural network, which can interact with the three layers of the network, is the Generalized Delta Rule, also known as the back propagation rule.

This rule was dealt with in a book published under the title Distributed Parallel Processing, and this learning rule is considered complex compared to the simple learning rule of a neuron (Schädler et al., 2021).

Conclusion

The great development witnessed by all technology-based fields with its various achievements; It allowed the emergence of the process of exchanging roles between

humans as innovators, achievers and manufacturers, and between what they invented, manufactured and accomplished, as learning and training were no longer the preserve of humans, but extended to even machines and software, so that the matter turned from mere learning to a thinking project, inventing systems that think instead of humans, And mimic his most unique behaviours. The need to match technology to human life, and to focus on the smallest details related to various tasks and activities with a cognitive dimension, requires a great effort by researchers and scholars, to develop these technical systems, because the matter goes beyond the idea of innovation, to the idea of innovation success and come out in a similar way to the bio-mental system, and this What cannot be completely and completely, due to the complex set of characteristics and features that the respondent enjoys about his similarity. The space of human knowledge is growing and aspiring to control the advanced techno-informational development at an accelerating pace. It is the era of artificial intelligence; And who is trying to compete with the human intelligence system, even though the latter is its main source, and because it is the source, the degree of its control may decrease and weaken, and it may increase and strengthen, and the conflict remains between what humans really need, and what can be accomplished, paralleling this limit of development and accelerating with it. Since the field of administration and administrative organizations is not immune from this conflict, the human resource needs to enter the fray of confrontation, and search for ways to seize the opportunities for progress.

References

Bejarbaneh, B. Y., Bejarbaneh, E. Y., Fahimifar, A., Armaghani, D. J., & Abd Majid, M. Z. (2018). Intelligent modelling of sandstone deformation behaviour using fuzzy logic and neural network systems. *Bulletin of Engineering Geology and the Environment*, *77*(1), 345–361.

Butcher, J., & Beridze, I. (2019). What is the state of artificial intelligence governance globally? *The RUSI Journal*, *164*(5–6), 88–96.

Chui, M. (2017). Artificial intelligence the next digital frontier. *McKinsey and Company Global Institute*, *47*(3.6).

Dick, S. (2019). *Artificial intelligence*.

Egrioglu, E., Aladag, C. H., & Yolcu, U. (2013). Fuzzy time series forecasting with a novel hybrid approach combining fuzzy c-means and neural networks. *Expert Systems with Applications*, *40*(3), 854–857.

Garcelon, N., Neuraz, A., Salomon, R., Faour, H., Benoit, V., Delapalme, A., Munnich, A., Burgun, A., & Rance, B. (2018). A clinician friendly data warehouse oriented toward narrative reports: Dr. Warehouse. *Journal of Biomedical Informatics*, *80*, 52–63.

Goldt, S., Mézard, M., Krzakala, F., & Zdeborová, L. (2019). *Modelling the influence of*

data structure on learning in neural networks.

Hamdi, M., & Aloui, C. (2015). Forecasting crude oil price using artificial neural networks: a literature survey. *Econ Bull*, *3*(2), 1339–1359.

He, K., Zhang, X., Ren, S., & Sun, J. (2016). Deep residual learning for image recognition. *Proceedings of the IEEE Conference on Computer Vision and Pattern Recognition*, 770–778.

Jaensch, S., & Polifke, W. (2017). Uncertainty encountered when modelling self-excited thermoacoustic oscillations with artificial neural networks. *International Journal of Spray and Combustion Dynamics*, *9*(4), 367–379.

Junio Guimarães, A., Vitor de Campos Souza, P., Jonathan Silva Araújo, V., Silva Rezende, T., & Souza Araújo, V. (2019). Pruning fuzzy neural network applied to the construction of expert systems to aid in the diagnosis of the treatment of cryotherapy and immunotherapy. *Big Data and Cognitive Computing*, *3*(2), 22.

Khan, A., Sohail, A., Zahoora, U., & Qureshi, A. S. (2020). A survey of the recent architectures of deep convolutional neural networks. *Artificial Intelligence Review*, *53*(8), 5455–5516.

Khrais, L. T. (2020). Role of Artificial Intelligence in Shaping Consumer Demand in E-Commerce. *Future Internet*, *12*(12), 226.

Li, Y.-H., Huang, P.-J., & Juan, Y. (2019). An efficient and robust iris segmentation algorithm using deep learning. *Mobile Information Systems*, *2019*.

Lin, C., Wang, P., Song, H., Zhou, Y., Liu, Q., & Wu, G. (2016). A differential privacy protection scheme for sensitive big data in body sensor networks. *Annals of Telecommunications*, *71*(9–10), 465–475.

Nishida, K., Sadamitsu, K., Higashinaka, R., & Matsuo, Y. (2017). Understanding the semantic structures of tables with a hybrid deep neural network architecture. *Proceedings of the AAAI Conference on Artificial Intelligence*, *31*(1).

Njitacke, Z. T., & Kengne, J. (2018). Complex dynamics of a 4D Hopfield neural networks (HNNs) with a nonlinear synaptic weight: Coexistence of multiple attractors and remerging Feigenbaum trees. *AEU-International Journal of Electronics and Communications*, *93*, 242–252.

Nord, J. H., Koohang, A., & Paliszkiewicz, J. (2019). The Internet of Things: Review and theoretical framework. *Expert Systems with Applications*, *133*, 97–108.

Peng, X., Wu, H., & Cao, J. (2018). Global nonfragile synchronization in finite time for fractional-order discontinuous neural networks with nonlinear growth activations. *IEEE Transactions on Neural Networks and Learning Systems*, *30*(7), 2123–2137.

Schädler, M., Böcherer, G., Pittalà, F., Calabrò, S., Stojanovic, N., Bluemm, C., Kuschnerov, M., & Pachnicke, S. (2021). Recurrent neural network soft-demapping for nonlinear isi in 800gbit/s dwdm coherent optical transmissions. *Journal of Lightwave Technology*, *39*(16), 5278–5286.

Schmidhuber, J. (2015). Deep learning in neural networks: An overview. *Neural Networks*, *61*, 85–117.

Silva Araújo, V. J., Guimarães, A. J., de Campos Souza, P. V., Rezende, T. S., & Araújo, V. S. (2019). Using resistin, glucose, age and BMI and pruning fuzzy neural network for the construction of expert systems in the prediction of breast cancer.

Machine Learning and Knowledge Extraction, *1*(1), 466–482.

Silver, D., Huang, A., Maddison, C. J., Guez, A., Sifre, L., Van Den Driessche, G., Schrittwieser, J., Antonoglou, I., Panneershelvam, V., & Lanctot, M. (2016). Mastering the game of Go with deep neural networks and tree search. *Nature*, *529*(7587), 484–489.

Simonyan, K., & Zisserman, A. (2014). Very deep convolutional networks for large-scale image recognition. *ArXiv Preprint ArXiv:1409.1556*.

Thierer, A. D., Castillo O'Sullivan, A., & Russell, R. (2017). Artificial intelligence and public policy. *Mercatus Research Paper*.

Vinuesa, R., Azizpour, H., Leite, I., Balaam, M., Dignum, V., Domisch, S., Felländer, A., Langhans, S. D., Tegmark, M., & Nerini, F. F. (2020). The role of artificial intelligence in achieving the Sustainable Development Goals. *Nature Communications*, *11*(1), 1–10.

Wall, L. D. (2018). Some financial regulatory implications of artificial intelligence. *Journal of Economics and Business*, *100*, 55–63.

Xiaosong, L., Ting, J., Tian, L., & Zenghua, L. (2019). Research on Weapon Equipment Acquisition Benefit Evaluation Based on Artificial Neural Network. *Proceedings of the 2019 10th International Conference on E-Business, Management and Economics*, 123–127.

Yusri, I. M., Majeed, A. P. P. A., Mamat, R., Ghazali, M. F., Awad, O. I., & Azmi, W. H. (2018). A review on the application of response surface method and artificial neural network in engine performance and exhaust emissions characteristics in alternative fuel. *Renewable and Sustainable Energy Reviews*, *90*, 665–686.

Zhang, Y.-D., Zhang, Y., Hou, X.-X., Chen, H., & Wang, S.-H. (2018). Seven-layer deep neural network based on sparse autoencoder for voxelwise detection of cerebral microbleed. *Multimedia Tools and Applications*, *77*(9), 10521–10538.

Khazar Journal of Science and Technology Volume 6 №1 2022, 78-84
© Khazar University Press 2022 DOI: 10.5782/2520-6133.2022.6.1.78

Assessment of Drilling Operation, and Efficiency of Multilateral Wells (Based on the West Absherov Field)

Elvin Hajiyev, Elvin Ahmadov
Khazar University, SOCAR "Azneft PU" Azerbaijan
Corresponding author: elvin.haciyev@khazar.org

Abstract

The article provides a detailed justification for the improvement of traditional technologies for drilling wells and development systems in accordance with the development plan of the West Absheron field. It is noted that the most optimal option for modern technologies and approaches to field development is drilling horizontal and multilateral wells in order to effectively develop recoverable oil and gas reserves and stimulate field production. Drilling and exploitation such wells has also been found to be more cost-effective. Thus, the optimal number and type of wells from existing and new platforms have been determined to ensure effective field development.

Keywords: reservoir, horizontal wells, production, drilling, multilateral wells, well completion

Introduction

The Western Absheron field is located in the north-western part of the Absheron archipelago. Industrial oil in the field was first extracted in 1985 during the testing of exploration well No. 35. In 2006, wells 57, 173, 174, 175, and 176 were drilled by the Khazar-6 floating drilling rig and put into conservation because the transmission lines were not ready. The wells were put into operation on 12.01.2011 after the completion of the construction of jacket No. 57 in 2011 and the construction of lines to transport oil to the consumers. Wells drilled from rig No. 120 were put into conservation in 1989. After the overhaul of the jacket, wells 120, 123, 124, 126, 127, and 128 were reconstructed and put into operation on 02.02.2012. At present, 80 wells have been drilled in the field, of which 50 are in operation. The field produces 810 tons of oil per day. The processing rate is up to 1% (Figure 1). The

main exploitation objects are QD and QA formation groups. As of 01.01.2021, 495.8 thousand tons of oil were extracted from the QD formation and 254.8 thousand tons from the QA formation. The total residual oil reserves of the GD formation are 6750.2 thousand tons, dissolved gas reserves are 1133.8 million m^3. The total residual oil reserves of the QA formation are 4,858,200 tons, and the dissolved gas reserves are 875.3 million m^3.

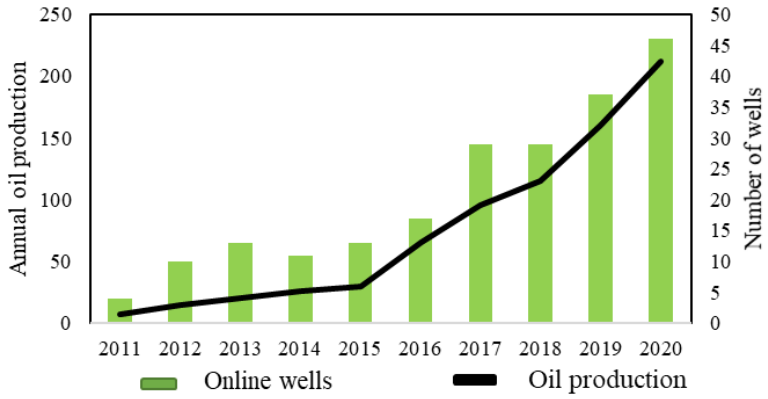

Figure 1 . Number of wells and production dynamics over the field

As can be seen, the resource utilization rate in the field is 6.8% for the QD formation, 5% for the QA formation, and only 6.1% for the field. This shows that, given the future growth of oil reserves, it will take a long time to complete the development of the field at this production rate (Ehlig-Economides et al., 1996; Yusufzade, 1995). From this point of view, there is a need to apply a new development system and technologies to ensure the efficient development of the field (Yusufzade, 1995; Hariri et al., 2012).

To intensify production and increase the efficiency of development from the central block of the field horizontal wells were drilled in 2015 from rigs No. 20, No. 54, and No. 10. A total of 50 wells were drilled from these fixed platforms, including 45 horizontal and 1 multilateral well. At present, 24 wells produce QA formation, 25 wells produce QD formation, and 1 multilateral well produce both QA + QD formation. The length of the horizontal filter on the wellbore is 80-100 m. The average daily oil production of these wells is 16.2 tons/day. This stage can be marked as the beginning of the period of innovation in the development of the field. Thus, compared to 2015, production in the field has increased 7.3 times over 5 years (Figure 1).

Materials and methods

The beginning of the second innovative phase of the field development is the multilateral well No. 19 drilled in February 2021 which has been noted for its high production rate. Thus, after it was determined that the formation pressure at QD and QA formations was equal to 1160.3 psi, multilateral well No. 19 was drilled in the central block of the field with two laterals and designed for joint development of QA and QD formations (Figure 2). The main well was drilled to a depth of 786 m with a deviation of 321,265° azimuth to the QA formation, the lateral well was drilled from 608 m depth with 240° azimuth, and deviation of 249 m to the QD formation to a depth of 722 m. The completion filter on the QA formation was set at 772-662 m (110 m), and the filter on the QD formation was set at 692-630 m (62 m) depth.

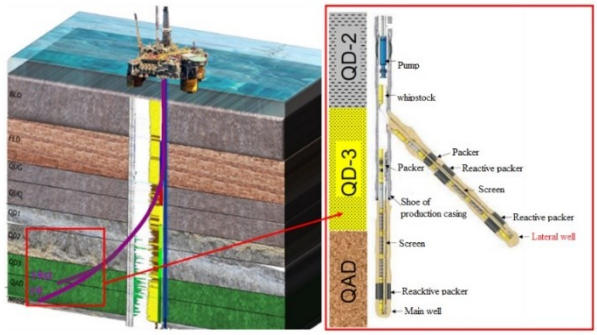

Figure 2 . Schematics of well No19

The production rates for the first well in the field are described in the graph below (Figure 3). As can be seen from the graph, the well operates with a stable oil production of 28-29 tons/day. However, it should be noted that according to the results of production analysis of surrounding wells (wells 8, 17, 22, 64, 144, 146), the average daily oil production of wells from the QD formation is 15 tons/day, the average daily oil production from wells from the QA formation equal to 12 tons/day. Multilateral well No. 19 produced an additional 1,200 tons of oil during its operation compared to the surrounding wells. Taking into account the actual production figures of the well, the production forecast until 2040 was calculated in the three-dimensional model of the field and compared with other completion options (Figure 4).

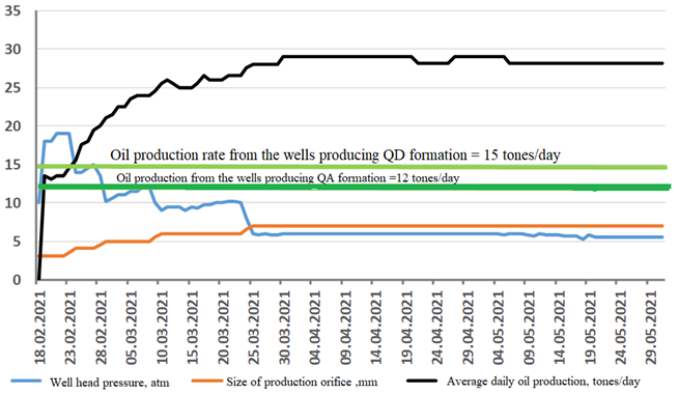

Figure 3. Development parameters of multilateral well 19.

With the current method of completion, the total oil production of the well by 2040 is 114,000 tons, the total oil production is 86,000 tons if both wells are operated from the QD formation, and the total oil production is 84,000 tons if the well is completed from the QA formation and returned to the QD formation, in the case of completion of two horizons (QA + QD) with one lateral, the total oil production is projected at 100 thousand tons. At the same time, the capital costs of the well do not differ significantly from other options, and the income from the well is projected to be 1.5-3 times higher than other options, which indicates that diversified wells to be drilled in the field in the future will have higher economic efficiency (Neskoromnykh, 2012; Salas et al., 1996).

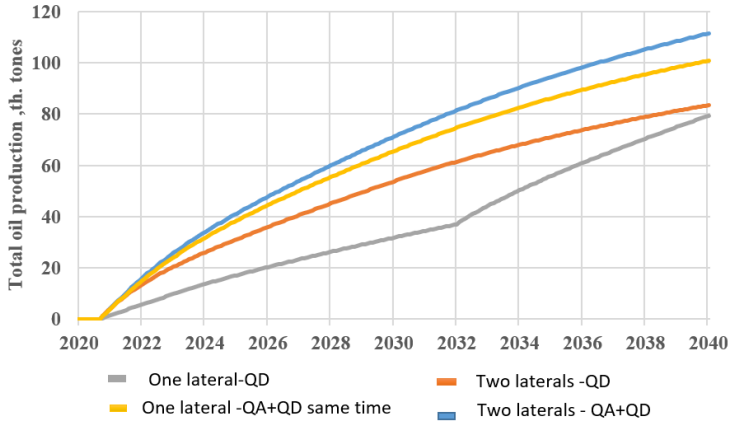

Figure 4. Comparison of the production forecast in the multilateral well 19

Taking into account the above, it is proposed to drill this type of multilateral wells from existing and future foundations to ensure the efficient development of the Western Absheron field (Figure 5).

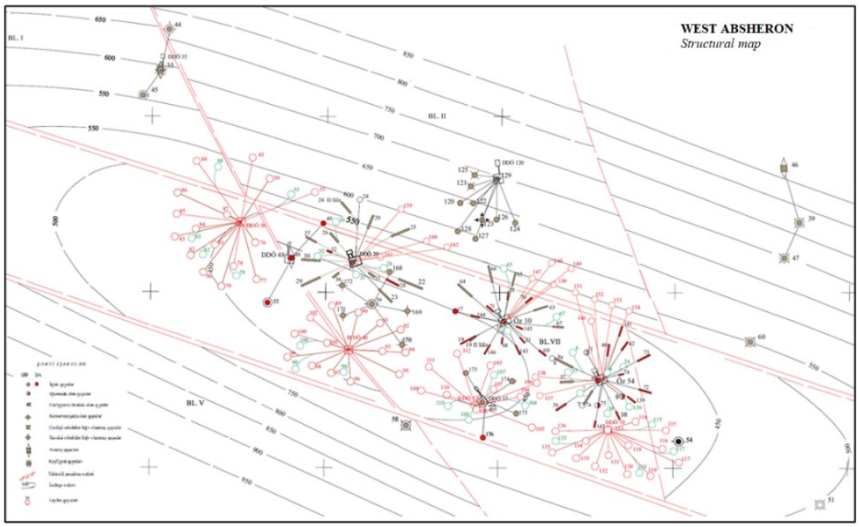

Figure 5. Perspective drilling map of the Western Absheron field.

To ensure full-scale development of the field, a new development scenario has been developed based on a three-dimensional model and based on the development results of well No. 19. In addition to the existing foundations, it was considered to build and put into operation 3 new foundations (50, 60, 70) in the field and to drill a total of 31 horizontal and 12 multilateral wells from these foundations. It is proposed to expand rig No. 57 by drilling an additional 6 horizontal and 4 multilateral wells, and an additional lateral well from 15 existing horizontal and 14 drilled wells. This development strategy is considered the most optimal option for current technologies and modern development systems (Golenkin et al., 2017; Salas et al., 1996; Eliseev et al., 2016).

Results and discussions

From the results of the comparative analysis, it was determined that the drilling of multilateral wells is more efficient to ensure the efficient development of the Western Absheron field. The production performance of multilateral well No. 19 drilled in the field is twice higher than the production performance of other wells. This will increase the intensity of production and increase the efficiency of

development. In this regard, it is proposed to drill this type of multilateral wells from existing and future offshore platforms in the field. At the same time, it is recommended to consider the possibility of drilling a lateral well in existing operational wells where geological and technological aspects allow to do so. Drilling laterals reduce the number of casing strings lowered in upper sections thus noticeably the expenses for well constructions and field development reduce.

Acknowledgments

I would like to express my gratitude to each person who helped me throughout the research. First of all, I am thankful to my supervisor Mr Elvin Ahmadov for giving me valuable advice and suggestions. Secondly, I would like to thank other professors and engineers for their priceless explanations to my questions. Finally, I would like to thank my workmates and my groupmates for their help.

References

Ahmadov, E.H. (2012). On ways to complete the effective development of the Gunashli field GUG formation. Materials of the II International scientific-practical conference. "New technologies in oil and gas production". Baku, p. 67-69.

Ahmadov, E.H. (2020). ”Geological-technological, technical-economic analysis and risk assessment of oil and gas field development projects”. News of the Azerbaijan Academy of Engineering, №2, p. 98-104.

Bagirov, B.A, Salmanov A.M, &Nazarova S.A. (2007). Effective ways of development and completion of offshore fields of Azerbaijan.News of Azerbaijan Higher Technical Schools, №2, Baku 13-18.

Ehlig-Economides, C.A., Mowat, G. R. & Corbett, C. (1996). Techniques for multibranch well trajectory design in the context of a three-dimensional reservoir model.SPE European 3-D Reservoir Modeling Conference.

Eliseev, D., Golenkin, M., Bulygin, I., Ruzhnikov, A., & Kashlev, A. (2016). TAML5 Wells on Caspian Offshore.Reasons,Implementation and Results.Socielty of Petroleum Engineers, 1-7.

Hariri N., & Al Sabuhi I. (2012). Multilateral Drilling Under Challengnig Conditions.SPE, Schlumberger.International Petroleum Exhibition. Abu Dhabi, UAE. p 1-7.

Hill, A.D., Ding Zhu, Economides, & Michael. J. (2008). Society of Petroleum Engineers.USA, California. 65-105.

Golenkin., M.Y., & Latypov., A.S. (2017). First Intelligent Multilateral TAML5 Wells on Filanovskogo Field.SPE Annual Caspian Technical Conference. Baku, Azerbaijan.

Mattew Jabs. (1997). Expanding the Options For Complex Multilateral Completions. SPE Annual Technical Conference.Richardson,USA.

Neskoromnykh., V.V. (2012). Destruction of rocks during drilling of wells: textbook. allowance / VV Neskoromnykh. Infra-M,p 336.

Nettleship D., Palmer,A., & Eshtewi, A. (2014).Installation of Complex Multilateral Wells With Sand Screens . Society of Petroleum Engineers. 1-5.

Povalikhin, A. S., Kalinin A. G., & Bastrikov S. N. (2012). Drilling of directional, horizontal and multilateral wells.p. 645.

Rosen, J.B. (1961). The gradient projection method for nonlinear programming: Part II nonlinear constraints. SIAM J. Appl. Math., 9, 514-532.

Salmanov, A.M. (2008). Justification of the ways of rational development of oil reserves by geological and mathematical models, Baku., 304.

Salas, J.R., Clifford, P.J., & Jenkins, D.P. (1996). Multilateral Well Performance Prediction.Society of Petroleum Engineers. 2-8.

Smith, K.M., & Redrup, J.P. (2002). Use of a Fullbore-Access Level 3 Multilateral Junction in the Orinoco Heavy Oil Belt,Oil & Gas Journal's International Multilateral Well Conference, Galveston, Texas.

Stalder J.L., York, G.D., Kopper, R.J., Curtis, C.M., Cole, T.L., & Copley, J.H. (2001). Multilateral Horizontal Wells Increase Rate and Lower Cost Per Barrel in the Zuata Field, Faja, Venezuela. SPE International Thermal Operations and Heavy Oil Symposium, Porlamar, Margarita Island, Venezuela, 12–14 March, 2-8.

Stokley, C.O., & Seale, R. (2000). Development of an openhole Sidetracking System.SPE Drilling Conference, New Orleans.

Yusufzade, Kh. B. (1995). Features of the development of oil and gas fields in the Caspian Basin. Azerbaijan Oil Industry, No. 1-2,45-53.

Yoshioka, K., Zhu, D., Hill, A.D., & Lake, L.W. (2005). Interpretation of Temperature and Pressure Profiles Measured in Multilateral Wells Equipped with Intelligent Completions. SPE Europec Annual Conference, Madrid, Spain.

Khazar Journal of Science and Technology Volume 6 №1 2022, 85-91
© Khazar University Press 2022 DOI: 10.5782/2520-6133.2022.6.1.85

QD2 in the III Tectonic Block of the Neft Dashlari Field Ways of Efficient Use of Residual Resources of the Usage Object

Huseyn Novruzov[1*], Elvin Ahmadov[2]
Department of Petroleum Engineering, Khazar University[1], SOCAR[2]
Corresponding author: Huseyn.Novruzov@khazar.org

Abstract

Like many other oil and gas fields in Azerbaijan, as well as we have faced the problem of efficient development of residual resources at the QD2 production facility in the III tectonic block of the Oil Rocks field. The article explores ways to solve this problem. The proposal is to increase the number of production wells and apply new methods to increase oil production. Using the field classification model, it was proposed to apply a physical and chemical method in accordance with the geological and technological parameters of the QD2 production facility in tectonic block III. The efficiency to be obtained after the application of the method has been calculated.

Keywords: tectonic block, exploitation object, injection, cracking analysis, classification model

Introduction

Offshore oil and gas fields have been intensively and rapidly exploited in our country more than 50 years. the volume of hard-to-recover residual resources in the balance of total resources is growing in Azerbaijan, as in the whole world. Efficient use of these residual resources remains as actual problem.

Most of the oil and gas fields in Azerbaijan are in the final stages of usage. In many of these fields, we face the problem of efficient use of residual resources. In IV stage of the usage, satisfactory results can be obtained by artificially influencing the layers (irrigation, new methods, etc.). In order to design the process of artificial impact to the layer, it is expedient to consider the issue of ensuring the compatibility of their geological and technological conditions.

The problem of efficient development of residual resources is also related to the QD2 production facility in the tectonic block III of the Neft Dashlari field. From this point of view, first of all, the distribution of residual resources of the facility in the field, etc. issues should be considered.

Determining the distribution of resources of the facility by field is associated with the collection, application and integrated use of multidimensional geological-geophysical and mining data. Mining and geophysical data for each well are collected, processed and the values of effective thickness, porosity and oil saturation parameters are determined. Determination of the distribution of linear resources in the field is carried out using a complex method of cracking and volume (Ahmadov, 2014; Bagirov, 2001; Nazarova, 1996). The methodology used is implemented on the basis of a special algorithm, program and the following maps are compiled:

- distribution maps of linear resources, taking into account the values of geological and geophysical parameters for wells;

- field distribution maps of accumulated oil production;

- Field distribution maps of residual (geological and extractable) oil resources.

Material and Methods

Using the cracking mapping method, a static geological model of the explored III tectonic block QD2 facility was constructed (Figure 1 a) and field differentiation maps were developed and analyzed (Figure 1 b, c, d, e, f). According to the maps of the first balance and distribution of the first recoverable resources of the QD2 production facility, the main resources are related to the bedrock areas of the field. However, in some limited areas, 23-25 thousand tons of oil was extracted around wells 1756, 1761, 2040, 1758 and 542 (Figure 1 d). Based on the distribution maps of the remaining reserves, it can be determined that there are 330-350 thousand tons of oil reserves around the wells in the arched areas of the III tectonic block (Figure 1 e and f).

In general, it was determined that the rate of development of recoverable oil reserves did not exceed about 20%. The optimal density of the well network has been determined for the efficient use of residual resources and the application of new methods has been considered. For this purpose, the fund of inactive wells in tectonic block III was investigated, injection wells were selected. Thus, the commissioning of wells 446, 711, 1754, 1766 in the stock of inactive wells and the commissioning

of wells 475, 526, 527, 1765 as injection wells should be based on economic indicators.

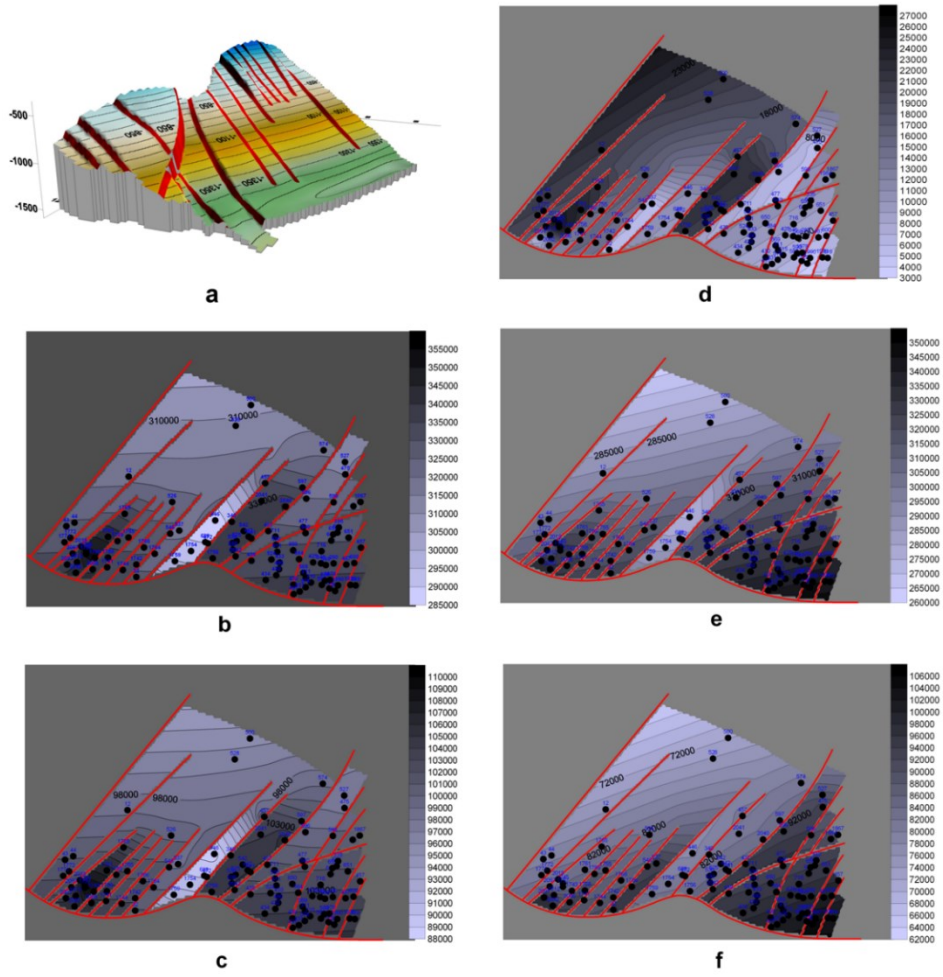

Figure 1. Cracking maps of the III tectonic block QD2 exploitation object: three-dimensional model of the "a"-III block (according to the ceiling of the QD2 exploitation object); "b"-initial balance reserve; "c"-first removable reserve; "d"- accumulated production; "e"-balance balance reserve; "f"-residual removable resource.

The results of the research show that one of the ways to efficient usage the residual resources of the objects is to apply new methods that increase the oil production of

the layers. These methods include physical and chemical, heating, thermic, microbiological and etc. methods apply (Salmanov et al., 2012; Surguchev, 1991). These methods have been widely used in various production objects of the world's oil fields and have been highly effective. Their geological and technological conditions have been identified for the effective application of each of these methods (Bagirov, 2001). It is noted in the classification model of Baghirov (2001) that geological-technological characteristics of the effective application of impact methods that increase the oil production of layers (Figure 2).

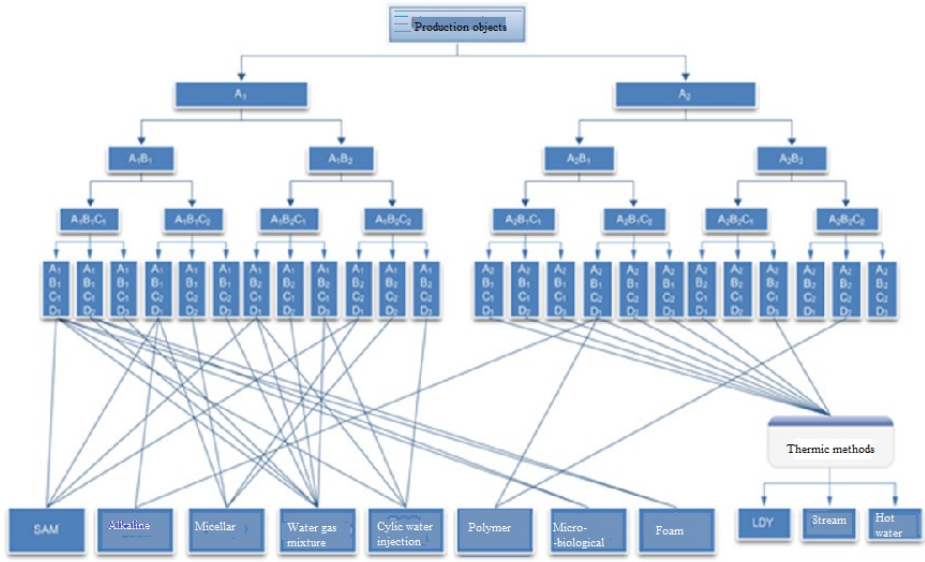

Figure 2. Classification model of methods to increase oil production (according to Baghirov B.A.) A- viscosity of oil, A1 <10m Pas, A2> 10m Pas; Depth of bed of B-layer, B1 <2000m, B2> 2000m; C- conductivity of rocks, C1 <0.1m km2, C2> 0.1m km2; Rate of use of D-resources, D1 <20%, D2 = 20-40%, D3> 40%.

Experience shows that four parameters play an important role in the application of these methods. These parameters include the viscosity of the oil in the formation conditions, the depth of the production object, the conductivity of collector rocks and the degree of use of oil resources. Based on the values of these parameters, a classification model has been developed, which allows to identify the scope of impact methods that increase the oil production of objects.

1) Oil viscosity under layer conditions (A) A1 <10m Pas, A2> 10m Pas;

Here, in the conditions of A1-layer, the layers are characterized by light oil with viscosity of less than 10m Pas and heavy oil with A2-10m Pas. The value of this parameter is considered very important because it determines beforehand the possibility of applying physical and chemical, and thermal methods in the layers. Thus, more effect can be achieved by using physical and chemical methods in facilities with low viscosity of oils. In this regard, it is proposed to divide all operating facilities into two groups: the first group of physical and chemical facilities, and the second group of objects which are suitable for the application of thermal methods.

2) Depth of exploitation objects bedding (B) B1 <2000 m, B2> 2000 m;

Here B1 and B2 are bedding depth according to the 2,000 m and more than 2,000 m, exploitation objects.

It should be noted that the application of thermal methods that increase the oil production of the layers is more effective in the layers up to 2000 m depth. However, the application of physical and chemical methods is not limited by the depth of deposition of objects.

3) Conductivity of collector rocks (C) C1 <0.1 μm2, C2> 0.1 μm2;

As can be seen, according to the values of these parameters, the development objects are divided into weak and high-quality collectors.

4) Rate of resource use (D) D1 <20%, D2 = 20-40%, D3> 40%;

The value of this parameter is very important to determine the sequence of application of methods that increase the oil production of layers.

The classification model, consisting of 24 homogeneous groups reflects all the possible application conditions of the methods that increase the oil production of the layers according to the values of the four selected parameters (Figure 2). The values of the relevant parameters of the QD2 operating facility have been determined and given in the table below (Table1).

The benefit of applying the method is calculated as follows:

$$Qs = \frac{Qqbe}{100} \times E\,ef$$

Here Qs is the efficiency obtained after the application of the method, Qqbe is the residual balance resource, Eef is the efficiency of the method.

Table 1. The values of the relevant parameters of the QD2 operating facility

Object of operation Additional,	Oil viscosity, m Pas (A)	Depth of bedding, m (B)	Conductivity of rocks, m km2 (C)	Rate of resource use,% (D)	Belonged grade	Applied Method,	Effect of the method %	Gained extra oil production thousand tones
QD2	5.7	1300	0.105	20	A1B1C2D1	SAM	3-5	77-129
	5.7	1300	0.105	20	A1B1C2D1	Alkaline	5-10	129-257
	5.7	1300	0.105	20	A1B1C2D1	micellar	8-15	206-386

It was determined that according to the classification scheme, the QD2 object is more suitable for the application of physical and chemical (SAM, alkaline and micellar) methods. The table gives the forecast estimates of the growth of additional oil reserves calculated for the QD2 production object. In tectonic block III, the value of this indicator is 77-386 thousand tons. The choice of the appropriate development option should be based on economic indicators.

Results and discussion

Ways of efficient development of residual resources of QD2 exploitation object in tectonic block III of Neft Dashlari field have been studied. With the help of cracking analysis, resource distribution maps were compiled and layer differentiation of residual resource was determined.

Residual resource in tectonic block III have been identified mainly in the bedrock areas of the field. From this point of view, it is important to cover the QD2 production object in these areas with a network of wells for the efficient use of residual resources. Therefore, the commissioning of wells 446, 711, 1754, 1766 in the stock

of inactive wells and the commissioning of wells 475, 526, 527, 1765 as injection wells should be based on economic indicators.

In addition, the application of methods to increase oil production has been identified as a main solution for the efficient use of residual resources.

As a result of the research, it was found that as a result of the application of physical chemical (SAM, alkaline and micellar) methods in accordance with the geological and technological parameters of the QD2 production object, it is possible to increase 77-386 thousand tones of residual oil resource.

References

Ahmadov, E. H. (2014). Selection of new methods for the efficient use of residual resources / Proceedings of the XIX Republican Annual Scientific Student Conference. Baku, p. 19-20

Bagirov, B. A. (2001). Oil and gas mining geology. Baku: ADNA, 311 p.

Bagirov, B. A., Narimanov, A. A., Nazarova, S. A. & Salmanov, A. M. (2001). Calculation of recoverable oil reserves of fields. Baku: ADNA, 57 p.

Bagirov, B. A., Nazarova, S. A. & Salmanov, A. M. (2005). Method of detection of field distribution of residual reserves in oil fields, Scientific Works of AzNQSDETLI, №5, p. 3-8

Bagirov, B. A., Khismetov, T. V., Aliev, R. M. & Shabanov, S. F. (1989). Identification of local zones by the area of deposits in order to apply thermal methods of influencing reservoirs, Azerbaijan Oil Industry, No. 2, p. 16.

Nazarova, S. A. (1996). Estimation of geological reserves by means of kriging, Uchenye zapiski, No. 3, p. 17-22

Salmanov, A. M. (2007). Geological and mathematical aspects of the selection of promising areas for the application of enhanced oil recovery methods, Natural and Technical Sciences, No. 5, p. 7-11

Salmanov, A. M., Karimov, N. S. & Ahmadov, E. H. (2012). Results of irrigation in the objects of the Girmaki formation in the Neft Dashlari field // News of Azerbaijan Higher Technical Schools, №5, p. 20-

Surguchev, M. L. (1991). Methods of extraction of residual oil. M .: Nedra, 347 p.

Khazar Journal of Science and Technology Volume 6 №1 2022, 91-95
© Khazar University Press 2022 DOI: 10.5782/2520-6133.2022.6.1.91

Development of an Ultrasonic Measuring Instrument in the Oil Industry

Tural Kishizada*, Elchin Hasanov
Department of Physics and Electronics of Khazar University
**Corresponding author: tural.kishizada@khazar.org*

Abstract

The article discusses the development of new methods and tools for the use of ultrasonic devices in the oil industry. It should be noted that ultrasonic level measuring devices make it possible for us to measure liquids in tanks up to 5 meters high. Determination of liquid level measurement in different types of tanks can be done using industrial electronics and automation, the principle of operation of such measuring systems is generally the same - one of the main differences when entering information from a measuring sensor into a data processing device based on optical computers is the choice of sensor type. stops. The article analyzes the main technical characteristics of the ultrasonic sensor used in the devices to measure the filling level of the reservoirs. The principles of processor selection are shown. Thus, the article will be about the development of an ultrasonic device.

Introduction

PIC microcontrollers include a RISC-processor with a symmetrical command system that allows you to perform operations with any register using the free method of addressing (Evtikheev, et al. 1990). This microcontroller is able to store the results of the operation in the Register-accumulator itself or in the second register used for the operation. High-speed execution of commands on PIC microcontrollers is achieved through the use of Horvart architecture instead of the traditional Fonneyman technique (Salamova & Binnatov, 2017).

Harvard architecture is based on stacking registers with address fields and tires for command and information (Evstifeev, 2005; Ivanov et al., 2009; Ivanov et al., 2004). The input of the microcontroller (all resources, means, reserves, such as the output portal, memory window and timer) consists of physically implemented hardware registers. Let's choose microcontrollers from PIC18FXXX series.

PIC18FXXX is a family of high-efficiency microcontrollers with a wide command system (75 commands) and a 10-degree analog-to-digital converter (ADC) operating at frequencies up to 40 MHz. They have the ability to address up to 32 words of code and 4 Kbytes of data memory installed in the 31-level hardware memory command, and up to 2 MB of external memory software. The extensive RISC core of the microcontrollers from that family has been optimized for use with the new C compiler. When designing the device, PIC 18F252 28-output high-speed FLASH microcontrollers are grade 10 ADC (Farzana et al., 2000).

Results

The output information signal of the sensor is a constant voltage + 0 ÷ 10V, the maximum input voltage is equal to the supply voltage (V_n) of the controller АЦП ОЭВМ PIC18F252, it means 5V. Thus, the task of the input converter is to reduce the output voltage (V_a) of the sensor by a factor of two.

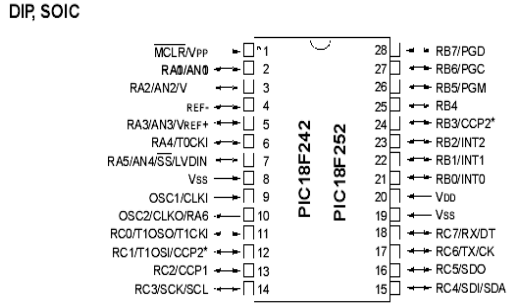

Figure 1. Location of microcontroller outputs

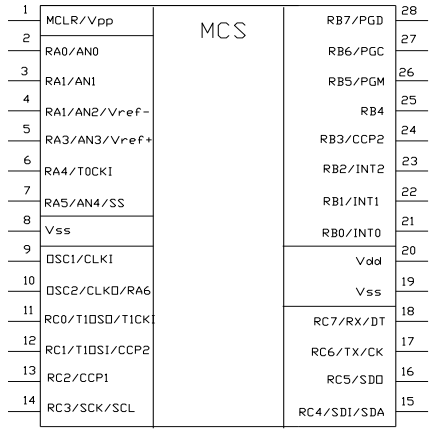

Figure 2. Conventional geographical indication PIC18F252

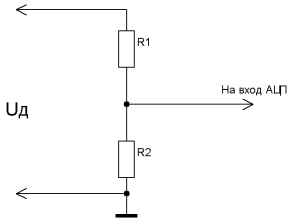

Figure 3. Schematic of the input changer

From the expressions (3.1) and (3.2) we find the nominals of resistors R1 and R2.

$$V_{out} = 2M_{ADC} \tag{3.1}$$

$$(R1 + R2) \cdot I = 2 \cdot R2 \cdot I \rightarrow R1 + R2 = 2 \cdot R2 \rightarrow R1 = R2 \tag{3.2}$$

Let's choose the nominals of resistors R1 and R2 at 100 kOhm. In this circuit, it is necessary to use the most accurate dividing resistors of the type C5-53Ф-0.125-100kOhm ± 0.05% to ensure the accuracy of the converter.

The indication block should provide information on the level of filling of the tanks in the form of decimal digits in the format X, XX meters. Thus, as can be seen from the problem, it is important to use an indicator consisting of three LED seven-segment dot indicators. The indication is dynamic.

The A-H segments of the LED seven-segment indicators are connected to the outputs of the microcontroller post RB7-RBO B, respectively, and the indicators are transmitted to the ports that serve the display and are packaged in BCD format. To implement the circuit of the indication block, select the seven-segment LED indicators with red light emission ALC333A. The choice of LED indicators is due to the fact that they have a number of advantages over liquid crystal and vacuum luminescences - a good degree of visibility of indicators at a considerable distance and in the dark. This shows that liquid crystal indicators, as well as indicators with lower energy consumption, are not able to meet the expected potential, unlike vacuum luminescence indicators. ALC333A height is 12 mm, current consumption of each segment is I_cs = 20mA, supply voltage is V_qg = 2V. The ports of the PIC18F252 microcontroller have a large enough load capacity, so the segments of the indicators are connected directly to the MK outputs without any amplifying elements. Resistors R5-R13 give the required V_qg = 2V for each segment. VI1-VT3 biopolar transistors are used as switches from the RCO-RCO2 ports to select a specific indicator with a control signal, thus fulfilling the dynamic mode of

indication. We choose KT814A transistors to implement the circuit. We choose resistors R5-R13. The denominations of resistors R5-R13 are calculated as follows (Figure 3):

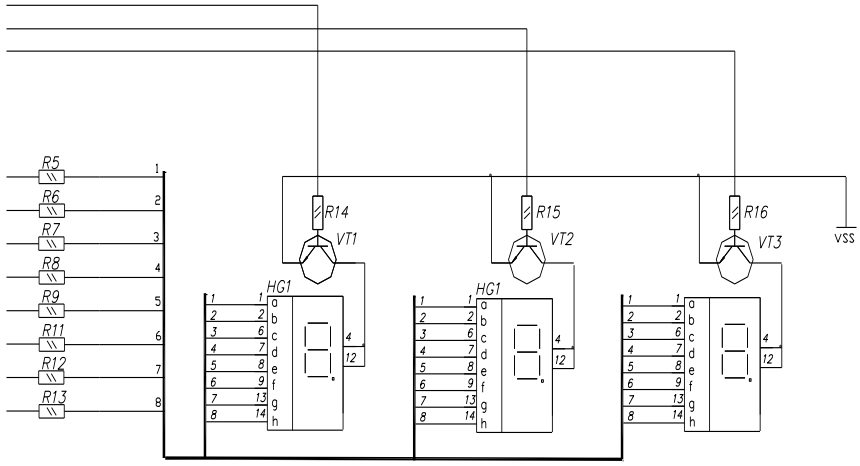

Figure 3. Schematic of the indication block

$$V_R = U_{MKout} - V_{ke} - V_{vd}, \quad (3.3)$$

Here,

Log unit voltage at U_{MKout}-MK outputs, voltage drop in V_R-resistor, voltage drop in V_{vd} indicator segment.

Considering the value of $V_R = 1V$

$$R = \frac{V_R}{I_{cs}} \quad (3.4)$$

Where I_cs is the voltage dissipated by the segment of the indicator. Thus R = 50 Ohm. C2-33-0,125-50 Ohm ± 1% resistor is selected.

R14-R16 resistors in the base circuits of transistor switches are distinguished by a nominal value of 470 Ohm, type: C2-33-0,125-470 Ohm ± 1%.

Then the parameters to be selected by the keyboard, communication unit and, finally, the process of calculating the power supply are taken into account, and thus the selection of RISC-processor components with a symmetrical command system that allows to perform operations for the operation of ultrasonic devices is considered complete.

References

Evstifeev, A.V. (2005). Tiny and Mega family AVR microcontrollers from ATMEL. 2nd edition. M.: Dodeka-XXI.

Evtikheev, N.N., Skugorov, V.N., & Papulovsky, V.F. (1990). Measurement of electrical and non-electric quantities (textbook for universities). M., Energoatomizgat, 349 p.

Ivanov, Yu.I. & Yugai, V.Ya. (2009). Microprocessor technology in control systems. Part II: Tutorial. - Taganrog: TTI SFU Publishing House.

Ivanov, Yu.I. & Yugai, V.Ya. (2004). Microprocessor devices of control systems: Methodological guide to laboratory work. - Taganrog: Publishing House of TRTU.

Farzana N.H. (2005). Technological measurements and devices (textbook).Baku, ADNA, 310 s.

Farzanə N.H., Jəfərov H.C., & Abbasova S.M. (2000). Basics of metrology. Baku, ADNA, 212 s.

Klassen, K.B. (2000). Fundamentals of measurements. Electronic methods and devices in measuring technology. M., Postmarket, 352 p.

Mammədov R.Q., Tagiyev F.K., Mutallimova A.S. (2013). Basics of measurement techniques. Baku, ADNA, -250 s.

Salamova Kh.E., & Binnatov M.F. (2017). Materials of the Republican Scientific-Technical Conference on "Youth and Scientific Innovations", Baku, AzTU, 82-184.

Khazar Journal of Science and Technology Volume 6 №1 2022, 96-104
© Khazar University Press 2022 DOI: 10.5782/2520-6133.2022.6.1.96

Experimental Investigation of the Projectile type on Sound Pressure Levels Fired with 9 mm Gun

Onur Gurdamar[1], Seyda Ozbektas[2], Bilal Sungur[3]*

[1]Samsun Yurt Savunma, Samsun, Turkey

[2] Faculty of Engineering, Department of Mechanical Engineering
Ondokuz Mayis University, Samsun, Turkey

[3]Faculty of Engineering, Department of Mechanical Engineering
Samsun University, Samsun, Turkey

[*]Corresponding author: bilal.sungur@samsun.edu.tr

Abstract

Throughout of the firing process, too much noise is occurred in the form of an blast wave caused by the discharged gas. An instantaneous and high amplitude sound pressure is created by the explosion and this pressure causes a harmful noise to the human ear. The main sources of the generated sound can be categorized as the explosion at the barrel exit, projectile velocity and the sound produced when the projectile hits the target. Subjects such as subsonic and supersonic projectiles, projectiles with different geometries, silencer systems are very important to reduce this explosion noise created by gun systems. Within the scope of this study, the peak sound pressure levels after firing the subsonic and supersonic projectiles from a 9 mm gun were experimentally measured at different positions. The measurements were realized at 23 different positions. The results of this study showed that in all measurement positions, supersonic projectiles have higher peak sound pressure levels (db) than subsonic projectiles. The peak sound pressure levels decreased with increasing distance from the gun barrel exit a as expected. Also, it has been determined that subsonic and supersonic projectiles give close results to each other in the measurements made at the same level with the barrel at y-axis direction.

Keywords: Sound pressure level; subsonic projectile; supersonic projectile; gun**.**

Introduction

Gun ammunition, also known as cartridges consists of four basic parts: the cartridge case, the ignition system (primer), the propellant powder and the projectile (bullet). The cartirdge case mainly keeps the gunpowder filler and the primer, and holds the

projectile. The primer is located behind the cartridge case and provides ignition. The main parts of a cartridge shown in Figure 1.

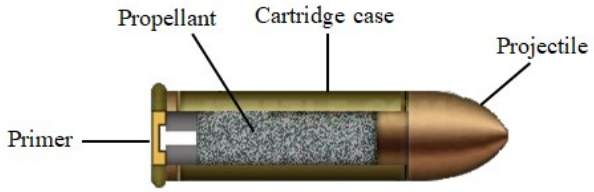

Figure 1. The main parts of the gun cartridge (Anonymus-a, 2022)

In firearms, with the combustion of gunpowder in the case, the transition from solid phase to gas phase and chemical energy is converted into heat energy. With the heating of the gunpowder gases, there is an expansion in the barrel, and this causes an increase at temperature and pressure inside the barrel. As a result, the initial movement of the projectile is ensured and it continues its movement by accelerating along the barrel. The movement of the bullet inside and outside the weapon and the effect on the target as a result of this movement is known as ballistics. While the internal ballistics field is related to all the events that occur from the start of firing until the projectile leaves the gun barrel, the events that occur during the time that the projectile leaves the barrel and reach the target are related to the external ballistics. Experimental testing of internal and external ballistics are difficult, expensive and time consuming.

With firing a gun, two main sources of noise occurred. These are the muzzle blast (impulse) and sonic boom (bow shock). Muzzle blast occurs when the projectile uncorks the high-pressure propellant gases and caused by many factors such as turbulent fluctuation in the mixing zone of the expanded jet at high speeds or the unstable shock wave in muzzle flow. Most of this kind of noise attenuates and disappears in the early stage of muzzle flow field formation. It is known that the main impulse noise in the muzzle system is generated by the propelled gas turbulent jet. The second source is sonic boom and this occurs with supersonic projectiles (Pater & Shea, 1981; Zhao et al., 2019).

Many studies have been conducted in the literature on the projectile motion on the flow field and the noise after explosion. Jiang Z et al. (Jiang, 2003) used a flat-nosed projectile to investigate the shock-wave and jet-flow interactions of the flow field. Zhuo et al. (Zhuo, Feng, Wu, Liu, & Ma, 2014) used a cone nose projectile and numerically analyzed the non-equilibrium Euler equations with dynamic overlapped grids. Trabinski et al. (Czyżewska & Trębiński, 2015) analyzed the dynamic

characteristics of the flow field around a cone-nose projectile exited the barrel with and without the muzzle device, respectively. The instability and production mechanism of the bow shock wave (BSW) at the projectile front both experimentally and numerically investigated by Kikuchi (Kikuchi, Ohnishi, & Ohtani, 2017). Kang et al. (Kang, Ko, & Lee, 2008) carried out a numerical study on the attenuation of sound propagated from a shock tube to the surrounding environment for a high pressure explosion. In this study, a numerical analysis is developed for high pressure explosion flow field analysis.

Studies in the literature have generally focused on projectile geometry. In this study, the effects of subsonic and supersonic projectiles on the sound pressure level of the 9 mm gun were investigated. In this context, shots were made for each projectile and the results were evaluated by taking measurements from 23 different points.

Materials and Methods

One of the basic measurement for the pressure fluctuations made by sound waves as they propagate in the air is the Sound Pressure Level (SPL), which is given in db units (Zhao et al., 2019). The SPL for the gun muzzle noise generally determined by peak sound pressure level. All the results given in this study are the results obtained in the case of a peak sound pressure level. The general formula of SPL is given in Eq. (1):

$$SPL = 20log\frac{p'}{p_{ref}} \qquad (1)$$

where p' is the sound pressure, p_{ref} is the reference sound pressure ($p_{ref} = 2\ x\ 10^{-5}\ Pa$).

A number of arrangements and planning are required to realize shooting tests and obtain the results. The experimental system mainly consist of sound pressure level measurement device with microphone, table, gun and gun stabilizer as illustrated in Figure 2. The photo of the experimental setup was given in Figure 3. To measure the sound pressure level Larson Davis LXT model was used with its microphone. Before the experiments, the calibration of this device checked with CAL200 sound level calibrator. The microphone was mounted on a tripod vertically and the height of the tripod was in level with the gun barrel axis in all experiments. The height of the table where the shooting test realized was 1 m above the ground level to prevent the sound reflection.

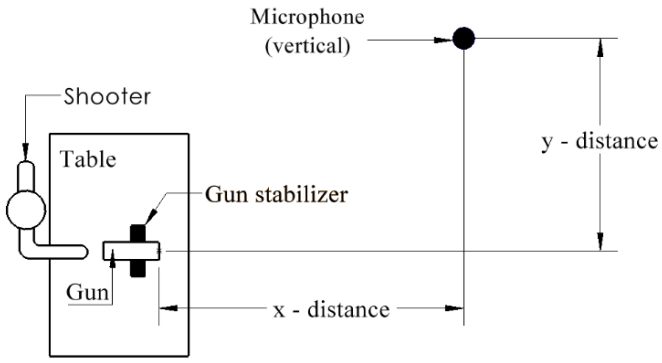

Figure 2. Schematic diagram of the experimental setup

Figure 3. A photo of the experimental setup

For each projectile type, sound levels were measured at 23 different points. These measurement points were illustrated in Table 1. A shooter was required to perform the firing process. The shots were carried out with 6 projectiles for each point at intervals of 10 seconds.

In addition, the velocities of subsonic and supersonic projectiles at the exit of the muzzle were also measured and Labradar Ballistic Velocity Doppler Radar Cronograph was used for velocity measurement.

Table 1. Sound pressure level measurement positions

Measurement number	X (m)	Y (m)
1	0.0	0.2
2	0.0	0.4
3	0.0	0.8
4	0.0	1.0
5	0.0	1.5
6	0.0	2.0
7	0.0	2.5
8	0.0	5.0
9	0.2	0.2
10	0.4	0.2
11	0.8	0.2
12	1.0	0.2
13	1.5	0.2
14	2.0	0.2
15	2.5	0.2
16	5.0	0.2
17	10.0	0.2
18	20.0	0.2
19	30.0	0.2
20	0.8	0.8
21	1.5	1.5
22	2.5	2.5
23	5.0	5.0

Table 2. Technical properties of the subsonic and supersonic cartridges (Anonymus-a, 2022; Anonymus-b, 2022)

Properties	Subsonic	Supersonic
Maximum pressure (bar)	1500	2850
Bullet weight (g)	9.50	12.15
Mean radius (cm)	Max 5.0 @ 25 meters	Max 7.6 @ 46 meters
Velocity (m/s)	290±10 @ 16 meters	370 ± 10 @ N/A

As said before two types of cartridge was used in the experiments which were named as subsonic projectile and supersonic projectile. The technical properties of these cartridges were given in Table 2.

Results and Discussions

In this study, the effects of projectiles with subsonic and supersonic characteristics on the sound pressure level of a 9 mm pistol were studied. In this context, shots were taken for each case and measurements were taken from 23 different points. For the measurement at each point, 6 shots were taken and the average of the values obtained from these shots was given. In this sense, a total of 276 projectiles were used for both cases (subsonic and supersonic). Figure 4 illustrates the SPL values varying with distance along the x-axis direction. Higher SPL values were obtained in experiments with supersonic projectiles at every distance. The highest SPL values were obtained at nearly 0.2 m positions with both projectiles which was 178 db at supersonic projectile and 176 db at subsonic projectile. Then, the SPL values decreased with increasing distance. In addition, the differences between subsonic and supersonic projectiles increased with increasing distance. At a distance of 30 m, the SPL value that appeared in experiments with subsonic projectiles was about 133 db, while this value was about 143 db in the case of using supersonic projectiles.

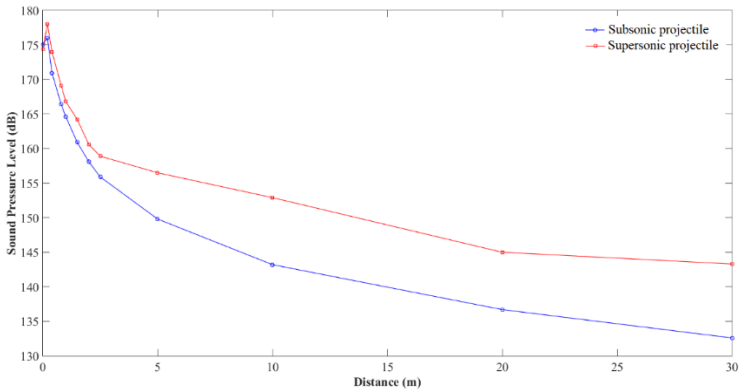

Figure 4. Sound pressure level varying with distance along the x-axis direction

The SPL values varying with distance along the y-axis direction was given in Figure 5. Unlike the measurement results taken at x-axis direction, the experiments performed with both projectiles gave similar results at y-axis direction. This can be explained by the projectile bow shock noise only occurs forward of the gun, in a region determined by the supersonic velocity of the projectile (Rehman, Hwang,

Tamtomo, Chung, & Jeong, 2011). However, with increasing distance, it is seen that the supersonic projectile has relatively higher results than the subsonic projectile. Especially after neraly 0.8 m, the differences between the results obtained from both projectiles increase.

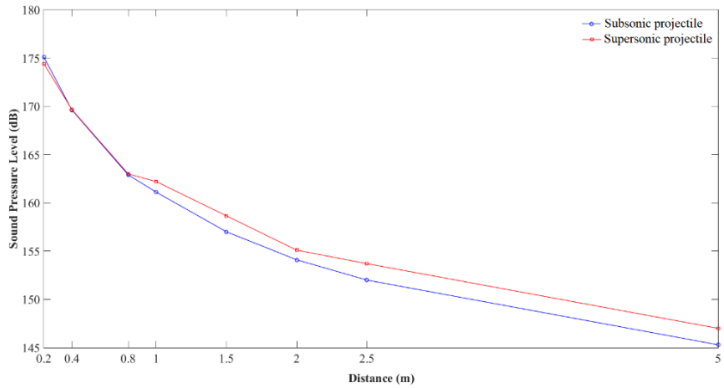

Figure 5. Sound pressure level varying with distance along the y-axis direction

Figure 6 shows the SPL values varying with distance along the 45° angle directions. As shown from this figure, in all distances supersonic projectile has higher SPL values than subsonic projectile. The SPL values were lower than the results of x-direction in all cases.

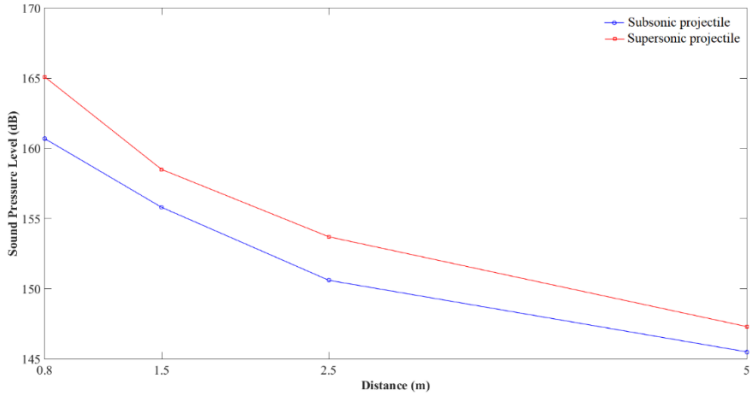

Figure 6. Sound pressure level varying with distance along the 45° angle directions

As stated before, velocity measurements were also made within the scope of the experiments. For each projectile type, 6 shots were made and the results were taken

in level with the gun barrel axis and the average of these results were recorded. Results showed that the subsonic projectile velocity was 317 m/s and the supersonic projectile velocity was 382 m/s.

Conclusion

Basically, it is required of a gun is to have a destroying effect and when the destruction effect is desired to be increased, the sound levels also increase and this situation needs to be examined. This study aims to investigate the effect of subsonic and supersonic projectiles on SPL at 9 mm gun. In this context microphones inserted to 23 different positions and the results of these measurements evaluated.

From the results of this study it was concluded that,

- Supersonic projectiles have higher peak sound pressure levels than subsonic projectiles in all measurement positions.
- The peak sound pressure levels decreased with increasing distance from the gun barrel exit.
- The highest SPL values were obtained at nearly 0.2 m positions with both projectiles which was 178 db at supersonic projectile and 176 db at subsonic projectile.
- Subsonic and supersonic projectiles give close results to each other at the same level with the barrel in the y-axis direction.
- With increasing distance, it is seen that the supersonic projectile has relatively higher results than the subsonic projectile at y-axis direction.
- Especially after neraly 0.8 m, the differences between the results obtained from both projectiles increase at y-axis direction.
- The subsonic projectile velocity was 317 m/s and the supersonic projectile velocity was 382 m/s in level with the gun barrel axis.

In future studies, to reduce the SPL values, projectiles with different geometries, shapes and properties can be experimentally analzed. Also, the numerical calculations of these systems can be realized and comparison of the experimental and numerical results can be made.

Acknowledgments

The authors would like to express their appreciation to the Samsun Yurt Savunma company for supports provided to this experimental study.

References

Anonymus-a. (2022). Available from: https://www.buckeyefirearms.org/5-things-about-personal-defense-ammunition [Accessed 21 February 2022].

Anonymus-b. (2022). Available from: http://www.sterling.com.tr/en/Urunler/Detay/66/sterling-9x19-mm-subsonic-fmj-tabanca-fisegi.

Anonymus-c. (2022). Available from: https://urunler.mke.gov.tr/Urunler/9-mm-x-19-Tabanca-Fi%C5%9Fe%C4%9Fi-(115-gr)/30/441.

Czyżewska, M., & Trębiński, R. (2015). Wpływ urządzenia wylotowego lufy na przyrost prędkości pocisku w okresie balistyki przejściowej. *Problems of Mechatronics. Armament, Aviation, Safety Engineering*, *6*, 87–98. https://doi.org/10.5604/20815891.1157779

Jiang, Z. (2003). Wave dynamic processes induced by a supersonic projectile discharging from a shock tube. *Physics of Fluids*, *15*(6), 1665–1675. https://doi.org/10.1063/1.1566752

Kang, K.-J., Ko, S.-H., & Lee, D.-S. (2008). A study on impulsive sound attenuation for a high-pressure blast flowfield. *Journal of Mechanical Science and Technology*, *22*, 190–200. https://doi.org/10.1007/s12206-007-1023-8

Kikuchi, Y., Ohnishi, N., & Ohtani, K. (2017). Experimental demonstration of bow-shock instability and its numerical analysis. *Shock Waves*, *27*(3), 423–430. https://doi.org/10.1007/s00193-016-0669-5

Pater, L., & Shea, J. (1981). *Techniques for Reducing Gun Blast Noise Levels: An Experimental Study*. 61.

Rehman, H., Hwang, S., Tamtomo, B., Chung, H., & Jeong, H. (2011). Analysis and attenuation of impulsive sound pressure in large caliber weapon during muzzle blast. *Journal of Mechanical Science and Technology*, *25*. https://doi.org/10.1007/s12206-011-0731-2

Zhao, X. Y., Zhou, K. D., He, L., Lu, Y., Wang, J., & Zheng, Q. (2019). Numerical Simulation and Experiment on Impulse Noise in a Small Caliber Rifle with Muzzle Brake. *Shock and Vibration*, *2019*, 5938034. https://doi.org/10.1155/2019/5938034

Zhuo, C., Feng, F., Wu, X., Liu, Q., & Ma, H. (2014). Numerical simulation of the muzzle flows with base bleed projectile based on dynamic overlapped grids. *Computers & Fluids*, *105*, 307–320. https://doi.org/https://doi.org/10.1016/j.compfluid.2014.08.006

Khazar Journal of Science and Technology Volume 6 №1 2022, 105-120
© Khazar University Press 2022 DOI: 10.5782/2520-6133.2022.6.1.105

Comparative Analysis of Effectiveness in the Implementation of Natural Drive and Artificial Lift Methods for Hydrocarbon Production

Samir Muzaffarov[1*], Elvin Ahmadov[2]
[1] Faculty of Graduate School of Science, Art, And Technology, Khazar University, Baku, Azerbaijan
[2] Modeling and Production Forecasting Department, SOCAR Azneft PU, Baku, Azerbaijan
[*]Corresponding author: samir.muzaffarov@khazar.org

Abstract

There are different production techniques that can be applied to produce hydrocarbons from subsurface formations. Reservoir fluids can be lifted to surface by either means of natural energy available within the reservoir or by applying artificial lift methods. Even though hydrocarbons are generally produced by natural drive mechanisms at the initial stage of field development where reservoir pressures are strong enough to push hydrocarbons to surface and then suitable artificial lifting techniques are implemented when wells cannot flow naturally, artificial lifting can also be applied to maximize production rate when individual well production rate is low due to lower reservoir pressure available in the system. The main objective of this research is to do comparative analysis of effectiveness in implementation of natural drive and artificial lift methods (gas – lift and pumps) for hydrocarbon production acceleration and optimization in West Absheron oil field, which is in the Caspian Sea, by using PROSPER software package based on a fictitious well data, namely Well WA-1. The Nodal Analysis is done for natural drive case and artificial lift techniques, specifically said, electrical submersible pump method and continuous gas lifting on PROSPER. Calculated oil production rates for natural drive, ESP and continuous gas lift cases are equal to 17.6 sm^3/day, 53.8 sm^3/day and 50.8 sm^3/day respectively. Comparative analysis of the outputs obtained from this research show that implementation of artificial lift methods significantly increases oil production rate. However, considering that source for lift gas is the main challenge for gas lift application in West Absheron oilfield, it is concluded that ESP implementation in West Absheron oilfield wells is the most favorable choice.

Keywords: Production techniques, Nodal Analysis, Natural Drive, Artificial Lift.

Introduction

It is generally true that in newly developed fields, the hydrocarbons can flow naturally to the earth's surface through the production tubing due to sufficient available reservoir pressure to push reservoir fluids. However, through time the reservoir pressure may drop due to depletion if pressure maintenance actions have not been taken in the field. In these cases, reservoir fluids may not flow naturally to the surface because of insufficient reservoir pressure, or hydrocarbon production rates may not be high enough to be considered economically viable. In that case to lift hydrocarbons to the surface, artificial lift techniques can be applied. Therefore, artificial lifting helps production engineers make the “dead” wells alive and achieve increased hydrocarbon production in the producing wells (Nguyen, 2020).

The fundamental objective of this research is to comparatively analyze the implementation of natural drive and artificial lift techniques, specifically said Electrical Submersible Pump (ESP) and Continuous Gas Lift for hydrocarbon production maximization and optimization in West Absheron oilfield, which is in Absheron archipelago, the Caspian Sea. To make this comparison, a mathematical model including various sub models are created in a special computer software package, namely PROSPER, to predict the achievable hydrocarbon production rates for three different cases (natural drive case, ESP, and continuous gas lifting) based on a fictitious well data, namely Well WA-1.

Natural Drive Mechanisms

Primary hydrocarbon recovery refers to the production of hydrocarbons with the help of natural energy available in the reservoir without supplementary aid from other sources like fluid injection into the reservoir. This natural energy is also known as “natural drive mechanism”. As (Tarek & D.Nathan, 2012) states, knowledge of reservoir drive mechanism plays a vital role in understanding fluid behavior within the porous medium and future fluid production forecasting. This drive mechanism is the main energy source to push hydrocarbons towards the producing wells. Generally, six reservoir drive mechanisms are present, which provide the available natural energy support for hydrocarbon recovery: Gap gas drive; water drive; gravity drainage drive; solution gas drive; rock and liquid expansion drive; combination drive(Tarek & D.Nathan, 2012):

Artificial Lifting

Depending on the natural energy available in the reservoir, hydrocarbons naturally flow to the surface at the early stages of the field development because the reservoir pressure is high enough to support natural flow. These naturally flowing wells have sufficient energy to push hydrocarbons to the surface. However, when the wells are not capable of flowing naturally since bottom hole pressure is inadequate to overwhelm the total pressure losses along the fluid flow path or the production rate is not high enough to be economical, then artificial lift (AL) is required to be implemented (Takacs, 2015). The well cannot flow naturally because reservoir pressure is less than the hydrostatic pressure due to the liquid column in the wellbore and the well is only capable of pushing hydrocarbons up to some level. Thus, an artificial lifting must be deployed to "initiate" fluid flow in this well (Figure 1).

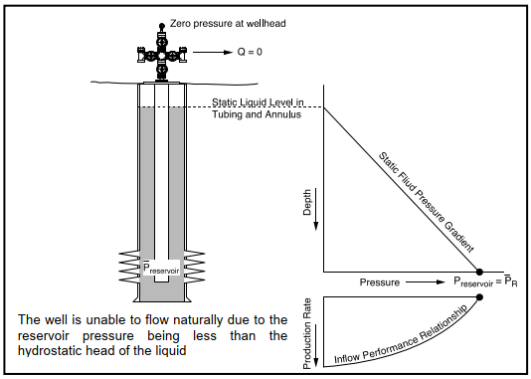

Figure 1.Typical well profile which is naturally unable to flow (Production Technology - 1, 2015)

There are mainly two artificial lift methods in production engineering. It can be either downhole pumping or gas lifting (Michael & Curthis H, 1991). In the case of downhole pumping a specially designed pump is lowered into the well and it operates at the bottom. This downhole pump aids the movement of hydrocarbons from the bottom hole to the wellhead by eliminating the back pressure when the fluids flow through the production tubing. In case of gas lifting, natural gas is injected into the tubing/casing annulus and from the annulus, injected gas flows into production tubing through gas lift valves inserted into the production tubing, and this injected gas mixes with the fluid column within the tubing, reduces its density and thus hydrostatic pressure at the formation rock.

A general definition for reservoir deliverability is the fluid (oil or gas) production rate can be achieved from a reservoir at a determined bottom hole pressure. Reservoir deliverability is a key element in petroleum production engineering, and it plays a

fundamental role in the selection of well completion type and artificial lift methods. In reservoir deliverability modelling, the relationship between bottom hole pressure and fluid production rate is analyzed, and this relationship in petroleum engineering is also called the "Inflow Performance Relationship (IPR)" (Guo, 2007).

Wellbore flow performance is an essential tool to evaluate the performance of the production tubing by plotting the fluid production rate versus flowing bottom hole pressure. In literature outflow performance relationship is also called tubing performance relationship (TPR) or vertical lift performance (VLP). VLP is used to determine required bottom hole flowing pressure to transfer fluids flowing at different flow rates to the surface. (Lyons, 2016) There are eight pressure drops in the flow path of formation fluid and the fluid must overcome all pressure losses present within the system to move to the surface facility equipment (Figure 2; (Economides & Nolte, 2000). VLP allows the production engineers to minimize pressure losses along the flow path and maximize the well production. To plot VLP for a typical well, either wellhead pressure or flowing bottom hole pressure is fixed at a given flow rate. Then the pressure drop along the production tubing is calculated based on correlations or engineering charts. Then flowing bottom hole pressure is plotted against production rate and the resultant relationship gives VLP curve (Michael & Curthis H, 1991).

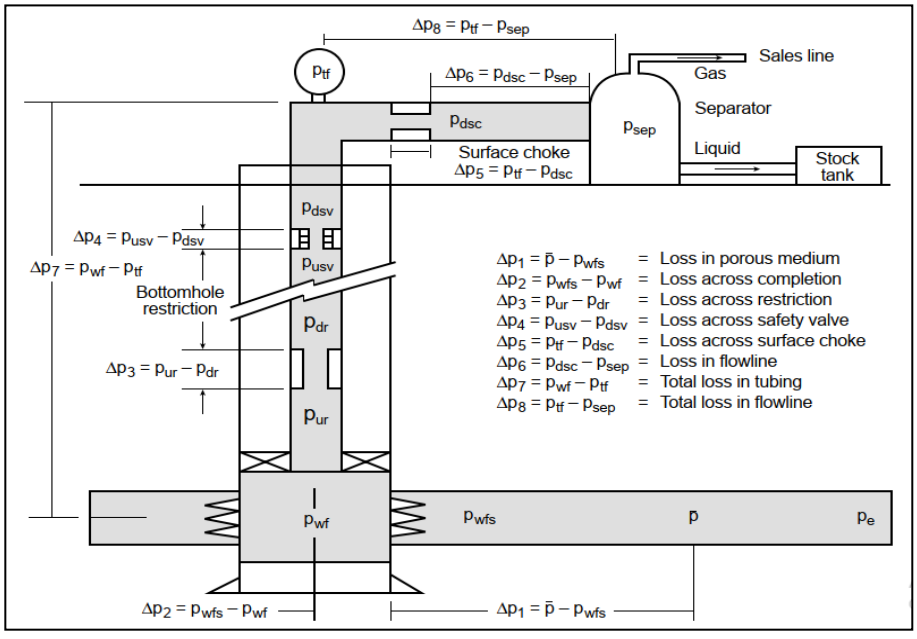

Figure 2. Pressure losses along the system (Economides & Nolte, 2000)

IPR and VLP curves are used to evaluate production capacity of a well. This evaluation in production engineering is known as Nodal Analysis where the well deliverability is analyzed based on reservoir performance and well performance. In the nodal analysis a solution node is selected within the system (Tetoros, 2015). At the solution node the system is divided into two sections. Either bottom hole or wellhead can be selected as a solution node. If for example, bottom hole is selected as a solution node that means fluid flow from reservoir into the bottom hole of the well is regarded as inflow, that is reflected in IPR curve, and the fluid flow from the bottom hole to the wellhead through the production tubing is regarded as outflow, which is displayed in VLP curve. The intersection point of IPR and VLP curves provide the stabilized flow rate which is also the natural flow point or operating point. It should be noted that when these two curves are not intersecting, that means the well will not naturally flow and some artificial lifting should be taken into consideration (Economides & Nolte, 2000).

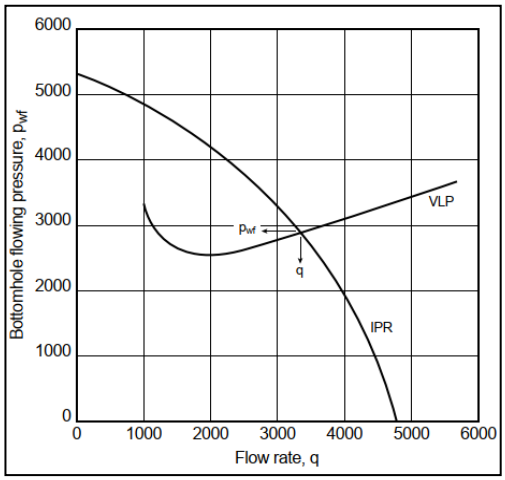

Figure 3. Typical IPR and VLP curves to predict natural flow (Economides & Nolte, 2000)

Study Area

The study area of this research is West Absheron oil field, which is located in the Caspian Sea, 40 km north of the Absheron Peninsula (Figure 4.). Structurally it is an anticline uplift in the north-west-south-east direction, and its core is composed of sediments of the Balakhany Unit of the Productive Series (PS). Productive Series is the main hydrocarbon bearing rock succession in South Caspian Basin and based on the microfauna composition, it is divided into Lower Productive Series and Upper

Productive Series. On the basis of lithological composition, Lower Productive Series include Kala Suite, Pre-Kirmaki Suite, Kirmaky Suite, Kirmaky Suite, Post-Kirmaky Sand Suite and Post-Kirmaky Clay Suite.

Figure 4. Location of West Absheron Oilfield

Upper Productive Series is subdivided into Fasila Suite, Balakhany Suite, Sabunchy Suite and Surakhany Suite (Abdullayev & Leroy, 2016). The dimensions of the main reservoir rock are 11x4 km. Stratigraphic succession of West Absheron field was discovered and studied through drilled wells and seismic works and it has turned out that, from Cretaceous sedimentary complex till Quaternary sediments are present in sedimentary succession of West Absheron field. Main hydrocarbon bearing rock successions are Kirmaky Suite and Pre-Kirmaky Suite of PS. In the West Absheron oilfield, the first oil was extracted in 1985, when Post-Kirmaki Suite was perforated in Well#35 (initial production rate was 61 tons of oil per day). The field has been in production since 1985. Initial reserve estimation in the West Absheron field based on Russian Federation Classification Scheme has revealed that commercial reserves under C1&C2 category was 64635 thousand tons of crude oil, 2587 million m^3 of dissolved gas and volume of recoverable reserves was 12359 thousand tons of crude oil, 2035.5 million m^3 of dissolved gas. Updated reserve estimation in 01.01.2022 has revealed that commercial reserves under C1&C2 category is 63884.4 thousand tons of crude oil, 2561.1 million m^3 of dissolved gas and volume of recoverable reserves is 11608.4 thousand tons of crude oil, 2009.1 million m^3 of dissolved gas. In total, 74 wells were drilled in the field as of 01.01.2022 and from these wells 750.6 thousand tons of crude oil, 25.9 million m^3 of dissolved gas and 27.6 thousand m^3 of water has been produced. 3.1% of recoverable crude oil reserves under C1&C2 category has been extracted.

Methodology

Generation of inflow performance relationship (IPR) and vertical lift performance (VLP) curves for this study is achieved using PROSPER software package that is designed to obtain inflow/outflow performance curves, create IPR and VLP models, select best artificial lift method, do well perforation design and so on based on the minimum required input data. The software also enables to input real production history data to increase the accuracy of models generated on. The software is a product of Petroleum Experts Limited (PETEX), located in UK and one of most widely used software in the petroleum industry (IPM PROSPER User Manual,Version 11.5, January 2010).

Required Data

The data needed to perform calculations and make final decision is as follows:

- PVT data
- Reservoir Data
- Equipment data: this includes downhole equipment, deviation survey, geothermal gradient, and average head capacities
- Gas lift data for gas lift case
- ESP data for ESP case

Summary of required input data is given in Table and Table 2.

Table 1. PVT data

PVT properties	Value	Unit
Solution GOR	31.632	m^3/m^3
Oil gravity	806.509	kg/m^3
Gas gravity	0.65	sg
Water salinity	76580.7	ppm
Mole percent H2S	0	%
Mole percent CO2	0.2	%
Mole percent N2	0	%

Table 2.Reservoir and wellbore properties

Properties	Value	Unit
Reservoir pressure	82	atm.
Reservoir temperature	34	°C
Water cut	5	%
Total GOR	31.632	m^3/m^3
Reservoir permeability	30	mD
Reservoir thickness	13	m
Drainage area	750000	m^2
Dietz shape factor	31.6	unitless
Skin factor	3	unitless
Wellbore radius	6	inches

Model Setup

To do simulations for natural drive and artificial lift techniques in PROSPER software, a fictitious offshore well named WA-1, in the West Absheron field is modelled. Based on the offset wells data and reservoir data provided, 750 meters deep, deviated wellbore is designed. To produce IPR and VLP curves and get the intersection point (which is stable flow point) between these curves based on input data for Well WA-1, the following steps are followed in the software for Natural Drive Case, Electrical Submersible Case and Gas Lift Case.

Building Natural Drive Model

IPR and Equipment Data

To generate inflow performance relationship curve that represents reservoir performance PVT data is required to accurately predict how the properties of reservoir fluid change as a function of pressure and temperature. It should be noted that in the PROSPER software either the basic fluid properties can be inserted and based on some traditional black oil model correlations (e.g., Glaso, Beggs, Petrosky etc.) the software can calculate fluid properties or basic fluid data and PVT laboratory readings can be introduced into the software and PROSPER can choose the best correlation to match the measured laboratory data. For this research basic PVT input data including GOR, API gravity, Gas gravity, water salinity and impurities present in reservoir fluid is introduced into the software and then laboratory measurement data taken from offset wells are entered to match PVT test data to the Black Oil correlations that are available on PROSPER. It is found that the best correlation with respect to Well WA-1 input data for Bubble point pressure,

GOR and Oil FVF is Glaso correlation which has the smallest standard deviation. For the oil viscosity, the best correlation is Beal et al which has the smallest standard deviation based on the available data provided. Then to construct IPR curve Darcy Model is selected due to its simplicity and ease of convergence. Then the software applies Darcy's flow equation when the flowing bottom hole pressure is above the bubble point pressure and the Vogel's solution when the flowing bottom hole pressure is equal or below the bubble point pressure. IPR curve is generated on software and it is obvious that absolute open flow (AOF) is 76.3 sm^3/day, and the formation productivity index (PI) is 1.76 sm^3/day/bar (Figure 5). Then equipment data including deviation survey, surface equipment, downhole equipment, geothermal gradient, and average heat capacity values are entered to make calculations of pressure and temperature profiles along the modelled well.

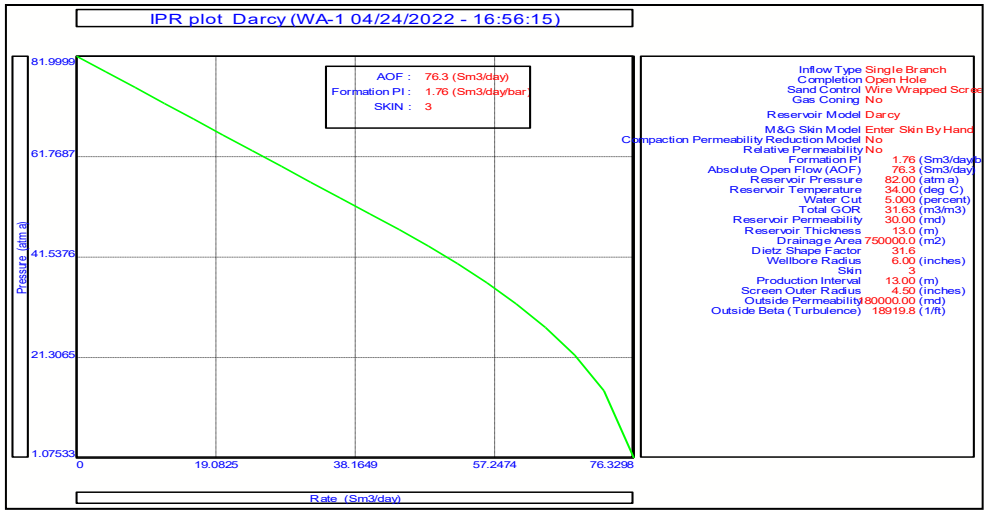

Figure 5.IPR plot based on reservoir Darcy model

Building ESP model

To model ESP artificial lift method on PROSPER, several input parameters should be entered into the software. In the system summary window firstly ESP method is selected as an artificial lift technique. Because IPR and PVT modelling is same as the natural drive case, ESP designing is directly followed by inserting required input parameters on design menu of PROSPER and then considering the best efficiency of the pump, a combination of appropriate pump, downhole motor, and cable from the list that PROSPER suggests achieving the target flow rate is selected.

Building Continuous Gas lift model

Modelling of continuous gas lift system on PROSPER starts with selecting gas lift (continuous) option on system summary menu. Here again IPR and PVT data remain same as for the Natural Drive Case and ESP Case. Then on the design menu of PROSPER required parameters for continuous gas lift system are introduced. A gas lift valve is selected from the PROSPER database which is visible on the right-hand side of the data input screen. For this scenario, Camco R-20 Normal Valves with port sizes in a range of 8 to 32 64 ^{ths} inch are selected. It should be stated that PROSPER tries to define which port sizes will deliver the optimal production rate and it means that the type of valve included on the software is not a big issue if the valves are casing sensitive.

Results

Natural Drive Model

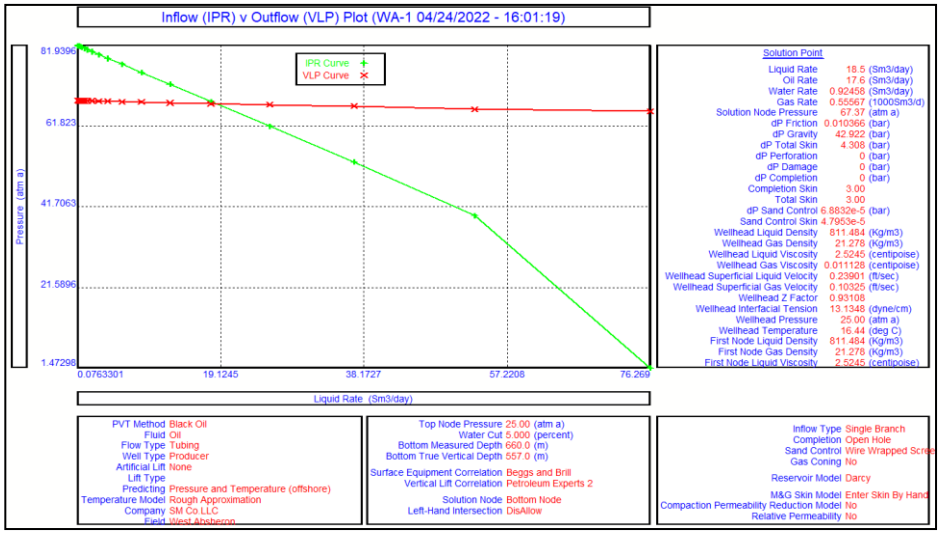

Figure 6. IPR and VLP curves plot for natural drive case

Input parameters for natural drive case generate a production profile without artificial lift technique for WA-1 well with an oil production rate equal to 17.6 sm^3/day. The relationship between IPR and VLP curves and these two curves are intersecting at one point, meaning that this well can flow naturally (Figure 6). However, the calculated flow rate is low and the main reason for that is having high pressure drop due to gravity (Figure 6). Sensitivity analysis on changing reservoir

pressure values is performed to see how well production rate is affected. While the reservoir pressure decreases, well production rate decreases as well (Figure 7). However, if the reservoir pressure falls to 65 atm., then the well will not flow naturally and the intersection points between IPR and VLP curves will not be achieved.

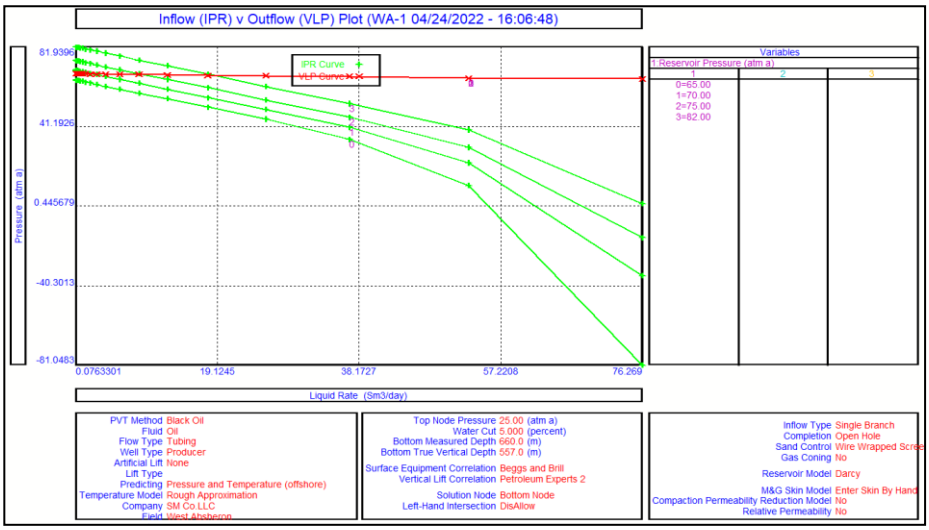

Figure 7. Sensitivity analysis based on changing reservoir pressure

ESP Model

Obtained design results are included in the software to perform system calculations and create IPR and VLP curves. To do that on PROSPER System ESP data menu should be filled up by obtained design results and then the vertical lift performance curve is generated, and intersection point between Pump Discharge Pressure (PDP) curve and VLP curve is achieved which shows the solution point of ESP-lifted well (Figure 8). It should be noted that Pump Performance should be examined to see if the operating point lies at or near the Best Efficiency Line. The pump performance is highest when the operating rate corresponds to the Best Efficiency Line. If the operating point is above or below the Best Efficiency Line, then the pump efficiency decreases (Oilfield Review, 2016). For this reason, care must be given to select the best combination of pump, motor, and cable to be sure that we are at the Best Efficiency Line. By this way we are sure that the pump will deliver highest efficiency. Taking the best performance of the pumps into consideration, REDA DN440 (101.6 mm OD) pump which is manufactured by Schlumberger is selected

to achieve the best efficiency. The performance curve of this pump is given, and it is obvious that operating point given as a red dot perfectly lies on the Best Efficiency Line (Figure 9).

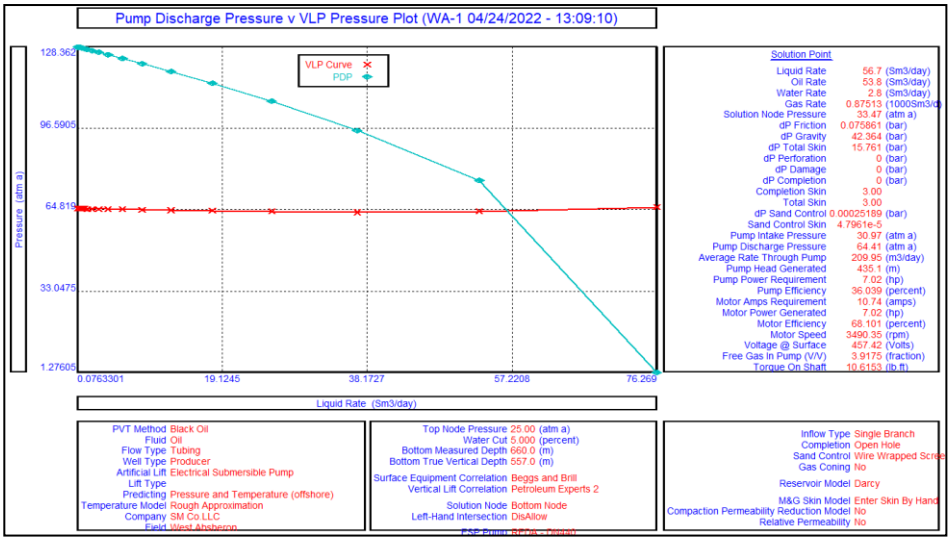

Figure 8. Pump Discharge Pressure vs VLP plot for ESP-lifted well

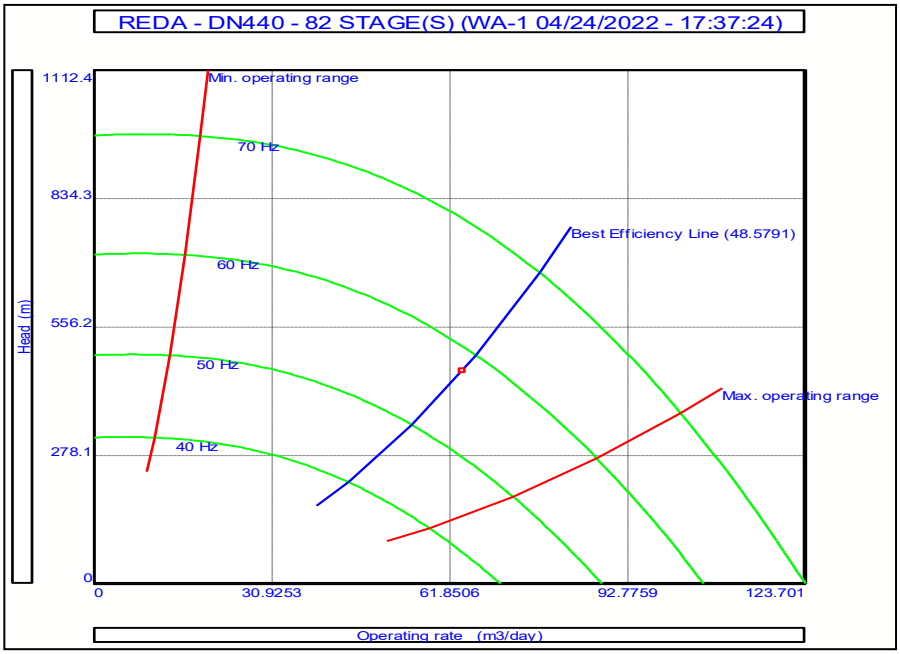

Figure 9. Performance Curve of REDA DN440 ESP

Pump Discharge Pressure is given in blue curve and VLP is shown in red curve, from wellhead to the pump discharge (Figure 8). It is obvious that the calculated liquid rate and oil rate by PROSPER for this case is 56.7 sm^3/day and 53.8 sm^3/day respectively (Figure 8).

Continuous Gas Lift Model

The obtained results on continuous gas lift method show that there is a significant increase on well production rate compared to natural drive case as well (Figure 10). It becomes clear that 2 unloading valves and one orifice type valve are required for this gas lift design. During the valve positioning calculations, the oil rate is checked for the conformance with the IPR and if necessary, the design rate is reduced by the software. It is worth mentioning that PROSPER checks the available gas injection rate to achieve designed rate and if the amount of available gas is less than required gas injection rate, then target oil production is reduced. All calculation results related to the gas lift valve positioning procedure were shown in Table 3:

Table 3.Gas lift valve positioning results

Valve Number	*Valve Type*	*Measured Depth (m)*	*True Vertical Depth (m)*	*Valve Opening Pressure (atm)*	*Valve Closing Pressure (atm)*	*Gas Lift Gas Rate (10000 sm^3/d)*	*Port Size (64^{ths} inch)*
1	Valve	222.103	219.114	61.1765	60.6364	1.56207	8
2	Valve	429.575	392.181	58.6963	57.7194	8.94982	12
3	Orifice	600	515			15.6208	11

As a final step, obtained design results are included in the software to perform system calculations and create IPR and VLP curves. To do that on PROSPER System Gas Lift data menu should be filled up with lift gas properties, determined gas lift valve depths and designed injection pressure values. Finally, the vertical lift performance curve is generated, and intersection point between IPR curve and VLP is achieved:

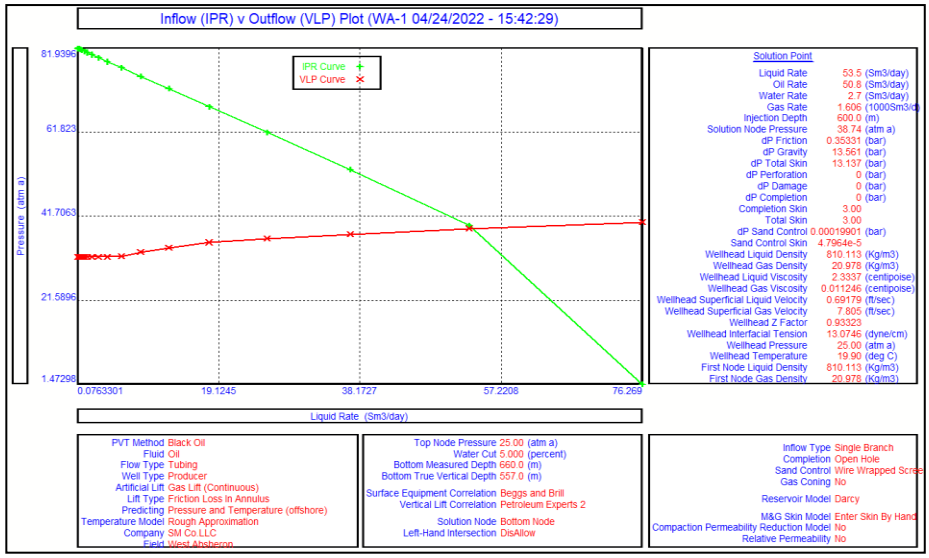

Figure 10. IPR and VLP plot for gas lift case

IPR is given in green curve and VLP is shown in red curve, and it is obvious that the calculated liquid rate and oil rate by PROSPER for this case is 53.5 sm^3/day and 50.8 sm^3/day respectively (Figure 10).

Discussion and Conclusions

The obtained results show that in case of natural drive case the modelled well oil production rate is equal to **17.6 sm^3/day**. However, if artificial lift techniques are applied, the production rate is significantly increased. So that for ESP case REDA DN440 pump which is manufactured by Schlumberger is modelled on PROSPER and the system calculations yield that oil production rate is equal to **53.8 sm^3/day**. Finally designing of continuous gas lift is modelled on PROSPER and it turns out that continuous gas lift system with 2 unloading valves and 1 operating valve with 15620.8 sm^3/day injection rate and 53.1954 atm injection pressure can produce oil equal to **50.8 sm^3/day**. From the obtained results, it is obvious that application of ESP and continuous gas lifting yields higher production rates and by this way production enhancement and optimization can be achieved in West Absheron oilfield. However, for the application of continuous gas lifting, the biggest obstacle is the unavailability of source gas for West Absheron oilfield. That means gas should be obtained from somewhere else, possibly from a nearby gas producing field that requires much more investment before the system goes online. What is more, a gas lift compression station, pipeline network and required surface facilities should be

installed in the field as well, leading to increased CAPEX of this plan and in this case, application of gas lift system seems unfavorable. ESP implementation for hydrocarbon production enhancement and optimization in West Absheron oilfield among the three cases seems the most suitable choice. However, for the ESP case, a detailed planning is highly demanded to realize this project because ESPs have a limited lifetime, and there will be a need to change the downhole completion (workover, maintenance) in ESP lifted wells when they experience failure, leading to increased OPEX later in the project. Comparing this factor to that of gas lifting system, it should be noted that gas lifting is a very simple, commonly applied artificial lift method where little can go wrong. From the obtained results and specifically unavailability of source gas and required infrastructure in the study area, it can be deduced that implementation of ESPs to maximize and optimize hydrocarbon production in West Absheron oilfield seems to be superior choice.

Recommendations

It should be emphasized that although the modelling done on PROSPER for this research is successful and the most suitable option to optimize and maximize the hydrocarbon production in West Absheron oilfield can be concluded which is ESP implementation, in reality this planning is far too complex and production optimization should be done for every well individually considering the available input data for each well. In case of field production optimization and enhancement, more sophisticated software is required to make an integrated approach considering the surface network of present wells and available subsurface data.

References

Abdullayev, E., & Leroy, S. (2016). Provenance of clay minerals in the sediments from the Pliocene Productive Series, western South Caspian Basin. *Marine and Petroleum Geology*.

Economides, M. J., & Nolte, K. G. (2000). *Reservoir Stimulation* (3rd ed.). England: Wiley.

Guo, B. (2007). *Petroleum Production Engineering, A Computer-Assisted Approach.* Gulf Professional Publishing.

IPM PROSPER User Manual,Version 11.5*.* (January 2010). United Kingdom: Petroleum Experts.

Lyons, W. P. (2016). *Standard Handbook of Petroleum and Natural Gas Engineering,* (3rd ed.). Gulf Professional Publishing, Elsevier.

Michael, G., & Curthis H, W. (1991). *Well Performance.* Prentice Hall.

Nguyen, T. (2020). *Artificial Lift Methods: Design, Practices, and Applications* (1st ed.). Switzerland: Springer. doi:https://doi.org/10.1007/978-3-030-40720-9

(2016). ***Oilfield Review***. USA: Schlumberger. Retrieved April 2022, from https://www.slb.com/-/media/files/oilfield-review/jan2016-oilfield-review.ashx

Production Technology - 1. (2015). Edinburgh, United Kingdom: Heriot Watt University, Institute of Petroleum Engineering.

Takacs, G. (2015). *Sucker-Rod Pumping Handbook* (1st ed.). Gulf Professional Publishing.

Tarek, A., & D.Nathan, M. (2012). *Advanced Reservoir Management and Engineering* (2nd ed.). Gulf Professional Publishing.

Tetoros, I. E. (2015). *Design of a continuous gas lift system to initiate production in a dead well.* Master Thesis, Technical University of Crete, Chania.

Khazar Journal of Science and Technology Volume 6 №1 2022, 121-136

DOI: 10.5782/2520-6133.2022.6.1.121

On a Boundary Value Problem for a Fourth Order Partial Differential Equation with Non-Local Conditions

Khanim Huseynova[1], Tahir Mammadov[2]
[1]*Baku State University, Baku, Azerbaijan*
[2]*Ganja State University, Ganja, Azerbaijan*
**Corresponding author:* xanimh77@gmail.com

Abstract

A boundary value problem for a fourth order partial differential equation with an integral boundary condition is studied. At first the initial problem is reduced to the equivalent problem, for which a uniqueness and existence theorem is proved. Then, using these facts, the existence and uniqueness of the classic solution of the original problem is proved.

Keywords: boundary value problem, differential equation, existence, uniqueness, classic solution.

Introduction

Mathematical modeling of many processes, taking place in the real world, leads to the study of boundary value problems for partial equations. Therefore, theory of boundary value problems at present is one of the important sections of theory of differential equations. Forth order differential equations are of great interest in terms of physical applications. Modern problems of natural science lead to the need for generalizing classic problems of mathematical physics and also to statement of qualitatively new problems which include non-local problems for differential equations. The problems with integral conditions are of great interest among non-local problems. Nonlocal integral conditions describe the behavior of solutions at the internal points of the domain in the form of some average. This kind of integral conditions are encountered in the study of physical phenomena in the case when the boundary of the process behavior domain is not available for direct measurements. The problems arising in the study of particle diffusion in a turbulent plasma (Samarskii, 1980; Smirnov, 1957), of heat propagation processes (Cannon, 1963; Ionkin, 1977) of moisture transfer process in capillary-porous media (Nakhushev,

1982), and in the study of some inverse problems of mathematical physics can be shown as examples.

Problem statement and its reduction to an equivalent problem

Let us consider the equation

$$u_{tt}(x,t)-\alpha u_{ttxx}(x,t)+u_{xxxx}(x,t)=f(x,t) \tag{1}$$

in the domain $D_T=\{(x,t):0\le x\le 1, 0\le t\le T\}$ and set for it a boundary value problem with non-local integral conditions

$$u(x,0)+\delta u(x,T)=\varphi(x),\ \ u_t(x,0)+\delta u_t(x,T)=\psi(x)\ \ (0\le x\le 1), \tag{2}$$

with periodic conditions

$$u(0,t)=u(1,t),\ u_x(0,t)=u_x(1,t),\ u_{xx}(0,t)=u_{xx}(1,t)(0\le t\le T) \tag{3}$$

with a non-local integral condition

$$\int_0^1 u(x,t)dx=0 \quad (0\le t\le T), \tag{4}$$

where $\delta\neq\pm 1,\ \alpha>0$ are the given numbers, $\varphi(x),\psi(x),f(x,t)$ are the given functions, $u(x,t)$ is desired function.

Definition. Under the classic solution of the problem (1)-(4) we understand the function $u(x,t)$, continuous in the closed domain D_T together with all its derivatives included in equation (1) and satisfying the conditions (1)-(4) in the usual sense.

The following lemma is valid.

Lemma 1. Let

$$\delta\neq\pm 1,\ \varphi(x)\in C[0,1],\ \int_0^1\varphi(x)dx=0,\ \psi(x)\in C[0,1],\ \int_0^1\psi(x)dx=0,$$

$$f(x,t) \in C(D_T), \ \int_0^1 f(x,t)dx = 0 \ (0 \le t \le T).$$

Then the problem of finding a classical solution of the problem (1)-(4) is equivalent to the problem of definition of functions $u(x,t)$ from (1)-(3),

$$u_{xxx}(0,t) = u_{xxx}(1,t) = 0 \ \ (0 \le t \le T), \tag{5}$$

Proof. Let $u(x,t)$ be a classic solution of problem (1)-(4). We integrate the equation (1) from 0 to 1 with respect to x T and have:

$$\frac{d^2}{dt^2}\int_0^1 u(x,t)dx - \alpha(u_{ttx}(1,t) - u_{ttx}(0,t)) + u_{xxx}(1,t) - u_{xxx}(0,t) =$$

$$= \int_0^1 f(x,t)dx \ (0 \le t \le T). \tag{6}$$

Hence, allowing for $\int_0^1 f(x,t)dx = 0$ and (3), we easily come to the fulfillment of (8).

Now, we suppose that $u(x,t)$ is the solution of problem (1)- (3), (5).

Then, from (6), allowing for (3), (5), we have:

$$y''(t) = 0 \quad (0 \le t \le T), \tag{7}$$

where

$$y(t) = \int_0^1 u(x,t)dx \ \ (0 \le t \le T). \tag{8}$$

By (2) and $\int_0^1 \varphi(x)dx = 0$, $\int_0^1 \psi(x)dx = 0$, we get:

$$y(0) + \delta y(T) = \int_0^1 (u(x,0) + \delta u(x,T))dx = \int_0^1 \varphi(x)dx = 0,$$

$$y'(0)+\delta y'(T)=\int_0^1 (u_t(x,0)+\delta u_t(x,T))dx=\int_0^1 \psi(x)dx=0 \qquad (9)$$

From (7), allowing for (9) it is obvious that $y(t)\equiv 0$ $(0\le t\le T)$. Hence, by (8), we easily come to the fulfillment of (4).

The lemma is proved.

Uniqueness of the solution of the problem

Theorem 1. If $\delta\neq\pm 1$, the problem (1)-(3), (5) can not have more than one solution.

Proof. Assume that there exist two solutions of the problem under consideration:

$$u_1(x,t),\ u_2(x,t)$$

and consider the difference $v(x,t)=u_1(x,t)-u_2(x,t)$.

The function $v(x,t)$, obviously satisfies the homogeneous equation

$$v_{tt}(x,t)-\alpha v_{ttxx}(x,t)+v_{xxxx}(x,t)=0 \qquad (10)$$

and the conditions:

$$v(0,t)=v(1,t),v_x(0,t)=v_x(1,t),v_{xx}(0,t)=v_{xx}(1,t),v_{xxx}(0,t)=v_{xxx}(1,t) \quad (11)$$

$$(0\le t\le T),\ v(x,0)+\delta v(x,T)=0,v_t(x,0)+\delta v_t(x,T)=0\ (0\le x\le 1). \quad (12)$$

Prove that the function $v(x,t)$ is identically equal to zero.

We multiply the both sides of the equation (10) by the function $2v_t(x,t)$ and integrate the obtained equality with respect to x from 0 to 1:

$$2\int_0^1 v_{tt}(x,t)v_t(x,t)dx-2\alpha\int_0^1 v_{ttxx}(x,t)v_t(x,t)dx+2\int_0^1 v_{xxxx}(x,t)v_t(x,t)dx=0. \quad (12)$$

Using the boundary conditions (11), we have:

$$2\int_0^1 v_{tt}(x,t)v_t(x,t)dx = \frac{d}{dt}\int_0^1 v_t^2(x,t)dx;$$

$$2\int_0^1 v_{ttxx}(x,t)v_t(x,t)dx = 2(v_{ttx}(1,t)v_t(1,t) - v_{ttx}(0,t)v_t(0,t)) -$$

$$-2\int_0^1 v_{ttx}(x,t)v_{tx}(x,t)dx = -\frac{d}{dt}\int_0^1 v_{tx}^2(x,t)dx;$$

$$2\int_0^1 v_{xxxx}(x,t)v_t(x,t)dx = 2(v_{xxx}(1,t)v_t(1,t) - v_{xxx}(0,t)v_t(0,t)) -$$

$$-2\int_0^1 v_{xxx}(x,t)v_{tx}(x,t)dx = -2\int_0^1 v_{xxx}(x,t)v_{tx}(x,t)dx =$$

$$= -2(v_{xx}(1,t)v_{tx}(1,t) - v_{xxx}(0,t)v_{tx}(0,t)) + 2\int_0^1 v_{xx}(x,t)v_{txx}(x,t)dx =$$

$$= \frac{d}{dt}\int_0^1 v_{xx}^2(x,t)dx.$$

Then from (12) we have:

$$\frac{d}{dt}\int_0^1 v_t^2(x,t)dx + \frac{d}{dt}\int_0^1 v_{tx}^2(x,t)dx + \frac{d}{dt}\int_0^1 v_{xx}^2(x,t)dx = 0$$

or

$$y(t) \equiv \int_0^1 v_t^2(x,t)dx + \int_0^1 v_{tx}^2(x,t)dx + \int_0^1 v_{xx}^2(x,t)dx = C.$$

Hence, allowing for (12), we obtain:

$$y(0) - \delta^2 y(T) = \int_0^1 (v_t^2(x,0) - \delta^2 v_t^2(x,T))dx +$$

$$+\int_0^1 (v_{tx}^2(x,0) - \delta^2 v_{tx}^2(x,T))dx + \int_0^1 (v_{xx}^2(x,0) - \delta^2 v_{xx}(x,T))dx = 0.$$

Thus,

$$y(0)-\delta^2 y(T)=C(1-\delta^2)=0.$$

Since $\delta \neq \pm 1$, then $C=0$. Consequently,

$$\int_0^1 v_t^2(x,t)dx+\int_0^1 v_{tx}^2(x,t)dx+\int_0^1 v_{xx}^2(x,t)dx\equiv 0.$$

Hence we conclude that

$$v_t(x,t)\equiv 0, v_{tx}(x,t)\equiv 0, v_{xx}(x,t)\equiv 0,$$

Whence, allowing for (11), the identity

$$v(x,t)=const=C_0.$$

follows.

Using local conditions (6), we have:

$$v(x,0)+\delta v(x,T)=C_0(1+\delta)=0.$$

Consequently, $C_0=0$, because $\delta \neq -1$.

Thereby it is proved that

$$v(x,t)\equiv 0.$$

Thus, if there exist two solutions $u_1(x,t)$ and $u_2(x,t)$ of the problem (1)-(3), (6), then $u_1(x,t)\equiv u_2(x,t)$. Hence it follows that if there is a solution to problem (1)-(3), (6), then it is unique. The Theorem is proved.

By means of lemma 1, the uniqueness of the initial problem (1)-(5) follows from the last theorem.

Theorem 2. Let the conditions of theorem 1 be fulfilled, and

$$\varphi(x)\in C[0,1],\ \int_0^1 \varphi(x)dx=0,\ \psi(x)\in C[0,1],\ \int_0^1 \psi(x)dx=0,$$

$$f(x,t) \in C(D_T),\ \int_0^1 f(x,t)dx = 0\ \ (0 \le t \le T).$$

The problem (1)-(5) can not have more than one classic solution.

Existence of the solution to the problem

We consider the spectral problem:

$$X''(x) + \lambda^2 X(x) = 0, 0 \le x \le 1, \tag{13}$$

$$X(0) = X(1), X'(0) = X'(1). \tag{14}$$

It is known (Budak B.M., et al., 1972) that eigen values of the problem (8), (9) consist of the numbers $\lambda_k = 2\pi k\ \ (k = 0,1,2,...)$, and for $k \ge 1$ each eigen value λ_k corresponds to two linearly independent eigen functions $\cos\lambda_k x, \sin\lambda_k x;$ furthermore, the system

$$1, \cos\lambda_1 x, \sin\lambda_1 x, ..., \cos\lambda_k x, \sin\lambda_k x, ...$$

forms in $L_2(0,1)$ an orthogonal basis.

The classic solution of the problem (1)-(3), (5) will be sought in the form

$$u(x,t) = \sum_{k=0}^{\infty} u_{1k}(t)\cos\lambda_k x + \sum_{k=1}^{\infty} u_{2k}(t)\sin\lambda_k x, \tag{15}$$

where

$$u_{10}(t) = \int_0^1 u(x,t)dx,\ \ u_{1k}(t) = 2\int_0^1 u(x,t)\cos\lambda_k x dx\ (k = 1,2,...),$$

$$u_{2k}(t) = 2\int_0^1 u(x,t)\sin\lambda_k x dx\ (k = 1,2,...).$$

Applying the Fourier formal method, from (1), (2) we obtain:

$$(1 + \alpha\lambda_k{}^2)u''_{1k}(t) + \lambda_k{}^2 u_{1k}(t) = f_{1k}(t)\ \ (k = 0,1,2,...,0 \le t \le T), \tag{16}$$

$$\begin{aligned} u_{1k}(0)+\delta u_{1k}(T)&=\varphi_{1k}, \quad (k=0,1,2,...),\\ u'_{1k}(0)+\delta u'_{1k}(T)&=\psi_{1k} \quad (k=0,1,2,...), \end{aligned} \tag{17}$$

$$(1+\alpha\lambda_k^2)u''_{2k}(t)+\lambda_k^2 u_{2k}(t)=f_{2k}(t) \quad (k=1,2,...;0\le t\le T), \tag{18}$$

$$\begin{aligned} u_{2k}(0)+\delta u_{2k}(T)&=\varphi_{2k} \quad (k=1,2,...),\\ u'_{2k}(0)+\delta u'_{2k}(T)&=\psi_{2k} \quad (k=1,2,...), \end{aligned} \tag{19}$$

where

$$\varphi_{10}=\int_0^1 \varphi(x)dx,\ \psi_{10}=\int_0^1 \psi(x)dx \ ,\ f_{10}(t)=\int_0^1 f(x,t)dx \ ,$$

$$\varphi_{1k}=2\int_0^1 \varphi(x)\cos\lambda_k x dx,\ \psi_{1k}=2\int_0^1 \psi(x)\cos\lambda_k x dx \ ,\ (k=1,...)$$

$$f_{1k}(t)=2\int_0^1 f(x,t)\cos\lambda_k x dx \ \ (k=1,2,...) \ ,$$

$$\varphi_{2k}=2\int_0^1 \varphi(x)\sin\lambda_k x dx,\ \psi_{21k}=2\int_0^1 \psi(x)\sin\lambda_k x dx \ \ (k=1,2,...) \ ,$$

$$f_{2k}(t)=2\int_0^1 f(x,t)\sin\lambda_k x dx \ \ (k=1,2,...) \ .$$

From (16)-(19) we have:

$$\begin{aligned} u_{10}(t)&=(1+\delta)^{-1}\varphi_{10}+(1+\delta)^{-1}(t-(1+\delta)^{-1}\delta T)\psi_{10}-\\ &-\delta(1+\delta)^{-1}\int_0^T (T(1+\delta)^{-1}+t-\tau)f_{10}(\tau)d\tau+\\ &+\int_0^t (t-\tau)f_{10}(\tau)d\tau \ \ (0\le t\le T), \end{aligned} \tag{20}$$

$$u_{ik}(t)=\frac{1}{\rho_k(T)}\left\{(\cos\beta_k t+\delta\cos\beta_k(T-t))\varphi_{ik}+\frac{1}{\beta_k}(\sin\beta_k t-\delta\sin\beta_k(T-t))\psi_{ik}-\right.$$

$$\left.-\frac{\delta}{\beta_k(1+\alpha\lambda_k^2)}\int_0^T f_{ik}(\tau)(\sin\beta_k(T+t-\tau)+\delta\sin\beta_k(t-\tau))d\tau\right\}+$$

$$+\frac{1}{\beta_k(1+\alpha\lambda_k^2)}\int_0^t f_{ik}(\tau)\sin\beta_k(t-\tau)d\tau\quad i=1,2,\quad (k=1,2,...,0\le t\le T),\ (21)$$

where

$$\beta_k=\frac{\lambda_k^2}{\sqrt{1+\alpha\lambda_k^2}},\ \rho_k(T)=1+2\delta\cos\beta_k T+\delta^2\ \ (k=1,2,...).$$

Obviously,

$$u'_{ik}(t)=\frac{1}{\rho_k(T)}\{\beta_k(-\sin\beta_k t+\delta\cos\beta_k(T-t))\varphi_{ik}+(\cos\beta_k t+\delta\cos\beta_k(T-t))\psi_{ik}-$$

$$\left.-\frac{\delta}{1+\alpha\lambda_k^2}\int_0^T f_{ik}(\tau)(\cos\beta_k(T+t-\tau)+\delta\cos\beta_k(t-\tau))d\tau\right\}+$$

$$+\frac{1}{1+\alpha\lambda_k^2}\int_0^t f_{ik}(\tau)\cos\beta_k(t-\tau)d\tau\quad (i=1,2,\quad k=1,2,...,\ (0\le t\le T)),\ (22)$$

$$u''_{ik}(t)=\frac{1}{1+\alpha\lambda_k^2}f_{ik}(t)-\frac{\beta_k^2}{\rho_k(T)}\{(\cos\beta_k t+\delta\cos\beta_k(T-t))\psi_{ik}+$$

$$+\frac{1}{\beta_k}(\sin\beta_k t-\delta\sin\beta_k(T-t))\psi_{ik}-$$

$$\left.-\frac{\delta}{\beta_k(1+\alpha\lambda_k^2)}\int_0^T f_{ik}(\tau)(\sin\beta_k(T+t-\tau)+\delta\sin\beta_k(t-\tau))d\tau\right\}-$$

$$-\frac{\beta_k}{1+\alpha\lambda_k^2}\int_0^t f_{ik}(\tau)(\sin\beta_k(t-\tau)d\tau \quad (i=1,2,\ k=1,2,...;\ 0\le t\le T), \quad (23)$$

$$u_0'(t)=(1+\delta)^{-1}(\psi_{10}-\delta\int_0^T f_{10}(\tau)d\tau)+\int_0^t f_{10}(\tau)d\tau \quad (0\le t\le T). \quad (24)$$

Theorem 3. Let $\delta \neq \mp 1$ and

1. $\varphi(x)\in C^4[0,1], \varphi^{(5)}(x)\in L_2(0,1)$ and

$$\varphi(0)=\varphi(1), \varphi'(0)=\varphi'(1),\ \varphi''(0)=\varphi''(1),\ \varphi'''(0)=\varphi'''(1), \varphi^{(4)}(0)=\varphi^{(4)}(1).$$

2. $\psi(x)\in C^3[0,1], \psi^{(4)}(x)\in L_2(0,1)$ and

$$\psi(0)=\psi(1),\ \psi'(0)=\psi'(1),\ \psi''(0)=\psi''(1),\ \psi'''(0)=\psi'''(1).$$

3. $f(x,t), f_x(x,t)\in C(D_T),\ f_{xx}(x,t)\in L_2(D_T)$ and

$$f(0,t)=f(1,t), f_x(0,t)=f_x(1,t).$$

Then the function

$$u(x,t)=(1+\delta)^{-1}\left\{\int_0^1\varphi(x)dx+(t-\delta(1+\delta)^{-1}T)\int_0^1\psi(x)dx+\right.$$

$$\left.-\delta\int_0^T\int_0^1(T(1-\delta(1+\delta)^{-1})+t-\tau)f(x,t)dxdt\right\}+\int_0^t\int_0^1(t-\tau)f(x,t)dxd\tau+$$

$$+\sum_{k=1}^{\infty}\left\{\frac{1}{\rho_k(T)}\{(\cos\beta_k t+\delta\cos\beta_k(T-t))\varphi_{1k}+\frac{1}{\beta_k}(\sin\beta_k t-\delta\sin\beta_k(T-t))\psi_{1k}-\right.$$

$$\left.-\frac{\delta}{\beta_k(1+\alpha\lambda_k^2)}\int_0^T f_{1k}(\tau)(\sin\beta_k(T+t-\tau)+\delta\sin\beta_k(t-\tau))d\tau\right\}+$$

$$\left.+\frac{1}{\beta_k(1+\alpha\lambda_k^2)}\int_0^t f_{1k}(\tau)\sin\beta_k(t-\tau)d\tau\right\}\cos\lambda_k x+$$

$$+\sum_{k=1}^{\infty}\left\{\frac{1}{\rho_k(T)}\{(\cos\beta_k t+\delta\cos\beta_k(T-t))\varphi_{2k}+\frac{1}{\beta_k}(\sin\beta_k t-\delta\sin\beta_k(T-t))\psi_{2k}-\right.$$

$$-\frac{\delta}{\beta_k(1+\alpha\lambda_k^2)}\int_0^T f_{2k}(\tau)(\sin\beta_k(T+t-\tau)+\delta\sin\beta_k(t-\tau))d\tau\Big\}+$$

$$\left.+\frac{1}{\beta_k(1+\lambda_k^2)}\int_0^t f_{2k}(\tau)\sin\beta_k(t-\tau)d\tau\right\}\sin\lambda_k x \tag{25}$$

is the solution of the problem (1)-(3), (5).

Proof. It is easy to see that

$$\frac{\lambda_k^2}{\sqrt{\alpha+1}}<\beta_k<\frac{\lambda_k^2}{\sqrt{\alpha}},\ |\rho_k(T)|\geq 1+\delta^2-2|\delta|\equiv 1/\rho.$$

Taking them into account, from (21), (22), (23) we find:

$$|u_{ik}(t)|\leq\rho(1+\delta)|\varphi_{ik}|+\frac{\sqrt{\alpha+1}}{\lambda_k}\rho(1+\delta)\psi_{ik}+$$

$$+\frac{\sqrt{\alpha+1}}{\alpha}\frac{1}{\lambda_k^3}(1+\rho\delta(1+\delta))\sqrt{T}\left(\int_0^T|f_{ik}(\tau)|^2d\tau\right)^{\frac{1}{2}},(i=1,2)$$

$$|u'_{ik}(t)|\leq\rho(1+\delta)\frac{\lambda_k^2}{\sqrt{\alpha}}|\varphi_{ik}|+\rho(1+\delta)\psi_{ik}+$$

$$+\frac{1}{\alpha\lambda_k^2}(1+\rho\delta(1+\delta))\sqrt{T}\left(\int_0^T|f_{ik}(\tau)|^2d\tau\right)^{\frac{1}{2}},\ (i=1,2)$$

$$\left|u''_{ik}(t)\right| \le \frac{1}{\alpha\lambda_k^2}\left|f_{ik}(t)\right| + \frac{\lambda_k^2}{\sqrt{\alpha}}\rho(1+\delta)\left|\varphi_{ik}\right| + \sqrt{\frac{\alpha+1}{\alpha}}\lambda_k\left|\psi_{ik}\right| +$$

$$+ \frac{\sqrt{(\alpha+1)T}}{\alpha^2\lambda_k}(1+\rho\delta(1+\delta))\left(\int_0^T\left|f_{ik}(\tau)\right|^2 d\tau\right)^{\frac{1}{2}} \ (i=1,2)$$

$$\left|u''_{ik}(t)\right| \le \lambda_k^{-2}\left|f_{ik}(t)\right| + \rho(1+\left|\delta\right|)(\left|\varphi_{ik}\right| + \left|\psi_{ik}\right|) +$$

$$+ (1+\rho\left|\delta\right|(1+\left|\delta\right|))\sqrt{T}\lambda_k^{-2}\left(\int_0^T\left|f_{ik}(\tau)\right|^2 d\tau\right)^{\frac{1}{2}} \ (i=1,2).$$

Hence we have:

$$\left(\sum_{k=1}^{\infty}(\lambda_k^5\left\|u_{ik}(t)\right\|_{C[0,T]})^2\right)^{\frac{1}{2}} \le \sqrt{3}\rho(1+\rho)\left(\sum_{k=1}^{\infty}(\lambda_k^5\left|\varphi_{ik}\right|)^2\right)^{\frac{1}{2}} +$$

$$+ \sqrt{3(\alpha+1)}\rho(1+\rho)\left(\sum_{k=1}^{\infty}(\lambda_k^4\left|\psi_{ik}\right|)^2\right)^{\frac{1}{2}} +$$

$$+ \frac{\sqrt{\alpha+1}}{\alpha}(1+\rho\delta(1+\delta))\sqrt{T}\left(\int_0^T\sum_{k=1}^{\infty}(\lambda_k^2\left|f_{ik}(\tau)\right|)^2 d\tau\right)^{\frac{1}{2}} \ (i=1,2),$$

$$\left(\sum_{k=1}^{\infty}(\lambda_k\left\|u'_{ik}(t)\right\|_{C[0,T]})^2\right)^{\frac{1}{2}} \le \sqrt{3}\rho\frac{1}{\sqrt{\alpha}}(1+\delta)\left(\sum_{k=1}^{\infty}(\lambda_k^2\left|\varphi_{ik}\right|)^2\right)^{\frac{1}{2}} +$$

$$+ \sqrt{3}\rho(1+\rho)\left(\sum_{k=1}^{\infty}(\lambda_k\left|\psi_{ik}\right|)^2\right)^{\frac{1}{2}} +$$

$$+ \frac{1}{\alpha}(1+\rho\delta(1+\delta))\sqrt{T}\left(\int_0^T\sum_{k=1}^{\infty}\left|f_{ik}(\tau)\right|^2 d\tau\right)^{\frac{1}{2}} \ (i=1,2),$$

$$\left(\sum_{k=1}^{\infty}(\lambda_{ik}^3\|u_k''(t)\|_{C[0,T]})^2\right)^{\frac{1}{2}} \le \frac{2}{\alpha}\left(\sum_{k=1}^{\infty}(\lambda_k|f_{ik}(\tau)|)^2\right)^{\frac{1}{2}} +$$

$$+\frac{2}{\alpha}\rho(1+\rho)\left(\sum_{k=1}^{\infty}(\lambda_k^5|\varphi_{ik}|)^2\right)^{\frac{1}{2}} + \frac{\sqrt{\alpha+1}}{\sqrt{\alpha}}\rho(1+\rho)\left(\sum_{k=1}^{\infty}(\lambda_k^4|\psi_{ik}|)^2\right)^{\frac{1}{2}} +$$

$$+\frac{2\sqrt{\alpha+1}}{\alpha^2}(1+\rho\delta(1+\delta))\sqrt{T}\left(\int_0^T\sum_{k=1}^{\infty}\lambda_k^2|f_{ik}(\tau)|^2\,d\tau\right)^{\frac{1}{2}} \ (i=1,2),$$

or

$$\left(\sum_{k=1}^{\infty}(\lambda_k^5\|u_{ik}(t)\|_{C[0,T]})^2\right)^{\frac{1}{2}} \le \sqrt{3}\rho(1+\rho)\|\varphi^{(5)}(x)\|_{L_2(0,1)} +$$

$$+\sqrt{3(\alpha+1)}\rho(1+\rho)\|\psi^{(4)}(x)\|_{L_2(0,1)} +$$

$$+\frac{\sqrt{\alpha+1}}{\alpha}(1+\rho\delta(1+\delta))\sqrt{T}\|f_{xx}(x,t)\|_{L_2(D_T)} \ (i=1,2), \tag{20}$$

$$\left(\sum_{k=1}^{\infty}(\lambda_k\|u_{ik}'(t)\|_{C[0,T]})^2\right)^{\frac{1}{2}} \le \sqrt{3}\rho\frac{1}{\sqrt{\alpha}}(1+\delta)\|\varphi''(x)\|_{L_2(0,1)} +$$

$$+\sqrt{3}\rho(1+\rho)\|\psi'(x)\|_{L_2(0,1)} +$$

$$+\frac{1}{\alpha}(1+\rho\delta(1+\delta))\sqrt{T}\|f(x,t)\|_{L_2(D_T)}\, i=1,2), \tag{21}$$

$$\left(\sum_{k=1}^{\infty}(\lambda_{ik}^3\|u_k''(t)\|_{C[0,T]})^2\right)^{\frac{1}{2}} \le \frac{2}{\alpha}\|f_x(x,t)\|_{L_2(D_T)} + \frac{2}{\alpha}\rho(1+\rho)\|\varphi^{(5)}(x)\|_{L_2(0,1)} +$$

$$+\frac{\sqrt{\alpha+1}}{\sqrt{\alpha}}\rho(1+\rho)\|\psi^{(4)}(x)\|_{L_2(0,1)} +$$

$$+\frac{2\sqrt{\alpha+1}}{\alpha^2}(1+\rho\delta(1+\delta))\sqrt{T}\left\|f_{xx}(x,t)\right\|_{L_2(D_T)} \quad (i=1,2). \tag{23}$$

Further, from (15) and (19), we obtain:

$$\left|u_{10}(t)\right| \le \left|1+\delta\right|^{-1}(\left\|\varphi(x)\right\|_{L_2(0,1)} + T(1+\left|\delta\right\|1+\delta\right|^{-1}\left|\delta\right|)\left\|\psi(x)\right\|_{L_2(0,1)}) +$$

$$+T\sqrt{T}(2+\left|\delta\right|(3+\left|\delta\right\|1+\delta\right|^{-1}))\left\|f(x,t)\right\|_{L_2(D_T)}, \tag{24}$$

$$\left\|u_0'(t)\right\| \le \left|1+\delta\right|^{-1}\left\|\psi(x)\right\|_{L_2(0,1)} + \sqrt{T}(1+\left|\delta\right\|1+\delta\right|^{-1})\left\|f(x,t)\right\|_{L_2(D_T)} . \tag{25}$$

Obviously,

$$\left|u(x,t)\right| \le \left\|u_0(t)\right\|_{C[0,T]} + (\sum_{k=1}^{\infty}\lambda_k^{-6})^{1/2}\sum_{i=1}^{2}(\sum_{k=1}^{\infty}(\lambda_k^3\left\|u_{ik}(t)\right\|_{C[0,T]})^2)^{1/2}, \tag{26}$$

$$\left|u_t(x,t)\right| \le \left\|u_0'(t)\right\|_{C[0,T]+}(\sum_{k=1}^{\infty}\lambda_k^{-6})^{1/2}\sum_{i=1}^{2}(\sum_{k=1}^{\infty}(\lambda_k\left\|u_{ik}'(t)\right\|_{C[0,T]})^2)^{1/2} , \tag{27}$$

$$\left|u_{tt}(x,t)\right| \le \left\|u_0''(t)\right\|_{C[0,T]+}(\sum_{k=1}^{\infty}\lambda_k^{-6})^{1/2}\sum_{i=1}^{2}(\sum_{k=1}^{\infty}(\lambda_k^3\left\|u_{ik}''(t)\right\|_{C[0,T]})^2)^{1/2}, \tag{28}$$

$$\left|u_{xxxx}(x,t)\right| \le (\sum_{k=1}^{\infty}\lambda_k^{-2})^{1/2}\sum_{i=1}^{2}\ (\sum_{k=1}^{\infty}(\lambda_k^5\left\|u_{ik}(t)\right\|_{C[0,T]})^2)^{1/2}, \tag{29}$$

$$\left|u_{ttxx}(x,t)\right| \le (\sum_{k=1}^{\infty}\lambda_k^{-2})^{1/2}\sum_{i=1}^{2}\ (\sum_{k=1}^{\infty}(\lambda_k^3\left\|u_k''(t)\right\|_{C[0,T]})^2)^{1/2}. \tag{30}$$

From (26)-(30), allowing for (21)-(25), it follows that the functions $u(x,t)$, $u_t(x,t)$, $u_{tt}(x,t)$, $u_{xxxx}(x,t), u_{ttxx}(x,t)$ are continuous in D_T By direct verification it is easy to see that the function $u(x,t)$ satisfies the equation (1) and conditions (2), (3) in the usual sense. The theorem is proved.

By means of lemma 1 we prove the following theorem

Theorem 4. Let the conditions of theorem 3 be satisfied, and

$$\int_0^1 \varphi(x)dx = 0\,,\ \int_0^1 \psi(x)dx = 0\,,\ \int_0^1 f(x,t)dx = 0\ (0 \le t \le T)\,.$$

Then the function

$$u(x,t) = -\frac{\delta}{1+\delta}\int_0^T\int_0^1 (T(1-\delta(1+\delta)^{-1}) + t - \tau) f(x,t)dxdt + \int_0^t\int_0^1 (t-\tau) f(x,t)dxd\tau +$$

$$+\sum_{k=1}^{\infty}\left\{\frac{1}{\rho_k(T)}\{(\cos\beta_k t + \delta\cos\beta_k(T-t))\varphi_{1k} + \frac{1}{\beta_k}(\sin\beta_k t - \delta\sin\beta_k(T-t))\psi_{1k} -\right.$$

$$-\frac{\delta}{\beta_k(1+\alpha\lambda_k^2)}\int_0^T f_{1k}(\tau)(\sin\beta_k(T+t-\tau) + \delta\sin\beta_k(t-\tau))d\tau\Big\} +$$

$$\left. + \frac{1}{\beta_k(1+\alpha\lambda_k^2)}\int_0^t f_{1k}(\tau)\sin\beta_k(t-\tau)d\tau\right\}\cos\lambda_k x +$$

$$+\sum_{k=1}^{\infty}\left\{\frac{1}{\rho_k(T)}\{(\cos\beta_k t + \delta\cos\beta_k(T-t))\varphi_{2k} + \frac{1}{\beta_k}(\sin\beta_k t - \delta\sin\beta_k(T-t))\psi_{2k} -\right.$$

$$-\frac{\delta}{\beta_k(1+\alpha\lambda_k^2)}\int_0^T f_{2k}(\tau)(\sin\beta_k(T+t-\tau) + \delta\sin\beta_k(t-\tau))d\tau\Big\} +$$

$$\left. + \frac{1}{\beta_k(1+\lambda_k^2)}\int_0^t f_{2k}(\tau)\sin\beta_k(t-\tau)d\tau\right\}\sin\lambda_k x \qquad (25)$$

is the classic solution of the problem (1)- (5).

References

Budak B.M., Samarskii A.A., Tikhonov A.N. (1972) Collection of problems in mathematical physics. Moscow.

Cannon J.R. (1963) The solution of the heat equation subject to the specification of energy // Quart. Appl. Math., Vol. 5, № 21, p. 155–160.

Ionkin N.I. (1977) Solution of a boundary value problem of heat theory with a non-classic boundary // Diff. Uravnenia, vol. 13, № 2, p. 294–304.

Nakhushev A.M. (1982) On one approximate method for solving boundary value problems for differential equations and its approximation to measured moisture and groundwater dynamics// Diff. Uravnenia. vol. 18, № 1, p. 72–81.

Samarskii A.A. (1980) On some problems of theory of differential equations //Dif. Uravnenia, vol. 16, № 11, p. 1925–1935.

Smirnov V.I. (1957) Course of higher mathematics Moscow.

Khazar Journal of Science and Technology Volume 6 №1 2022, 137-143
© Khazar University Press 2022 DOI: 10.5782/2520-6133.2022.6.1.137

Normal Impact by The Dulled Wedge on the Viscous-Elastic String (a Subsonic Mode)

Tahir Mammadov
Ganja State University

In this paper is defined by a stess state of the linearly viscoelastic (Maxwell type) string on cross – section impact by a wedge having a flat forward part when the string material submits the linearly elastic Hook's law (Figure 1.). A similar problem was investigated in the paper (Mutallimov, 2001; Rahmatulin, 1945; Rahmatulin, 1947).

Let there is executed the transverse impact with constant speed V along the infinite long rectilinear flexible string by the above represented dulled wedge.

In the collision process the deflection part of the string clings the cheek of the «wedge», and the speed of the break point A is less than the sonic speed in the string $\left(b\,ctg\gamma < a_0\right)$. We use 2l for the length BB_1. (fig.1).

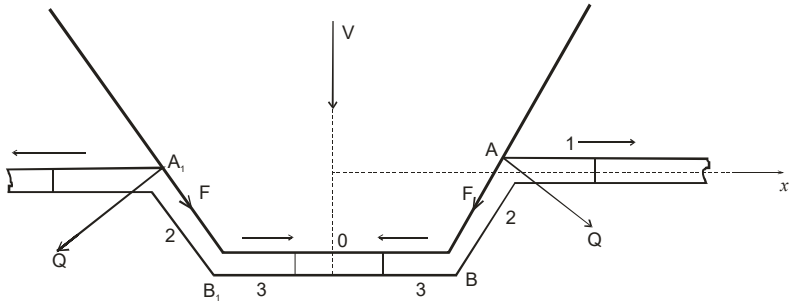

Figure 1. Above represented dulled wedge

The string behavior is symmetric with respect to the point «0».

The equation of the string motion ahead and behind the point of discontinuity A will be (Rahmatulin, 1961).

$$\rho \frac{\partial^2 u}{\partial t^2} = \frac{\partial \sigma}{\partial x} \tag{1.1}$$

The law of deformation by Maxwell type has the form [2]

$$\dot{\sigma} + \frac{E}{\mu}\sigma = E\dot{\varepsilon} \tag{1.2}$$

or

$$\sigma = \varepsilon - ke^{-kt}\int_0^t e^{k\tau}\varepsilon(x,\tau)d\tau \tag{1.3}$$

Herein, points above letters signify derivatives ε and σ with respect to time.

There is also taken the dimensionless notation in the form:

$$\overline{u} = uR^{-1};\ \overline{x} = xR^{-1};\quad \upsilon_i = \frac{\partial u_i}{\partial t};\ \overline{\upsilon_i} = \frac{\upsilon_i}{a_0},\ \ (i = 1,2),$$

$$\overline{b} = ba_0^{-1};\overline{b} = \frac{V\cdot ctg\gamma}{a_0};\overline{\sigma} = \sigma(\rho a^2)^{-1};a^2 = \frac{E}{\rho};\overline{t} = \frac{a_0 t}{R};k = ER(\mu a)^{-1}; \tag{1.4}$$

Further, we will omit dashes above letters.

R – const, having a dimension of a length, E- Young s modulus, ρ - density, other symbols are taken from the paper (Mutallimov, 2001; Mutallimov, 2001).

The motion equation (1.1) considering (1.3) has the form

$$\frac{\partial^2 u}{\partial t^2} = \frac{\partial^2 u}{\partial x^2} - k\frac{\partial u}{\partial x} \tag{1.5}$$

In solving the problem we will consider, that «k» is a small quantity, i.e. $k << 1$.

Conditions at the break point A (fig.1) in a dimensionless form will be (Mutallimov, 2001).

$$\frac{b-\upsilon_1}{1+\varepsilon_1} = \frac{b\sec\gamma - \upsilon_2}{1+\varepsilon_2} = z \tag{1.6}$$

$$z\cdot\left(\upsilon_2-\upsilon_1\cos\gamma-M\sin\gamma\right)=\sigma_1\cos\gamma-\sigma_2-F; \tag{1.7}$$

$$z\cdot\left(M\cos\gamma-\upsilon_2\sin\gamma\right)=\sigma_1\sin\gamma+Q. \tag{1.8}$$

The wavy motion scheme in the plane (x, t) is shown in the figure 2. We will denote by respective indexesAll parameters of a non- self – similar problem in domains 1,2,3…11, 21….

In the paper (Mutallimov, 2001). it was proved that there are two modes in the theory of transverse impact under the subsonic mode in a wave of the strong discontinuity. There is the condition (Mutallimov, 2001) in the first mode behind the wave front of a strong discontinuity,

$$F<\mu Q \tag{1.9}$$

i.e. a particle is closed to the point of discontinuity from the clinging side, is sticking to the cheek of the «wedge», therefore, the particle velocity equals to zero at this point.

$$\upsilon_2=0 \tag{1.10}$$

In the second mode, particles of the string are located in the wave front of a strong discontinuity, slipping along the wedge cheek, and it is consistent with the condition (Mutallimov Sh.M. 2001).

$$F=\mu_* Q. \tag{1.11}$$

Herein, F, Q – are concentrated force at the point of discontinuity, μ - is a friction coefficient in this point. We have a kinematic condition at the point B (fig.2).

$$\upsilon_3=\upsilon_2\cos\gamma. \tag{1.12}$$

From condition of the symmetry at the point 0 the particle velocity equals to zero too

2. The solution of the equation (1.5) in domains 1,2,3 may be written as the form

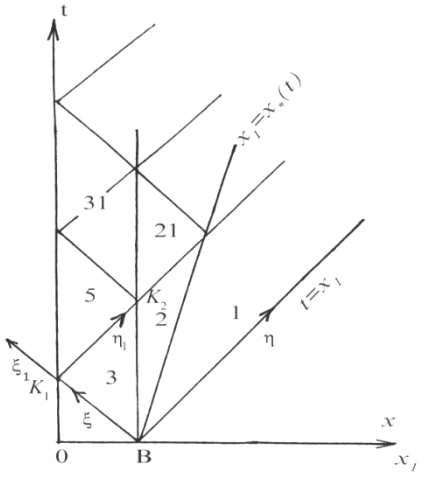

Figure 2. Kinematic condition at the point B

$$u_1 = \varepsilon_1^0 x_1 + \upsilon_1^0 t + k\left[a_{01}\varepsilon^2 + b_{01}\eta^2 - \frac{\upsilon_1^{(0)}}{4}\xi\eta \right], \tag{2.1}$$

$$u_2 = \left(\varepsilon_2^0 + 1\right)x_1 + \upsilon_2^{(0)} t + k\left[a_{02}\varepsilon^2 + b_{02}\eta^2 - \frac{\upsilon_2^0}{4} x_1\xi \right] \tag{2.2}$$

$$u_3 = \varepsilon_3^0 x_1 + \upsilon_3^0 t + k\left[a_{03}\xi^2 + b_{03}\eta^2 + \frac{\upsilon_3^0}{2} x_1\eta \right] \tag{2.3}$$

Where

$$x_1 = x - l;\ \ \xi = t - x_1;\ \ \ \eta = t + x_1 \tag{2.4}$$

An unknown wave trajectory of a strong discontinuity we will seek in the form

$$x_*(t) = z_0 t + k z_1 t^2 \tag{2.5}$$

Note that in the u(x,t), z(t) expansion with respect to a small parameter k, we will constraint by two terms .

We also have conditions

$$u_1(x_1, t) = 0,\ \varepsilon = 0 \tag{2.6}$$

$$u_3(x_1, t) = 0,\ \ \eta = 0 \tag{2.7}$$

Besides that, we have for the first mode

$$\upsilon_2 = \frac{\partial u_2}{\partial t} = 0,\ x = x_*(t). \tag{2.8}$$

In this way, considering solutions (2.1) – (2.4) in conditions (1.6), (1.10), (1.12), (2.6), (2.7), (2.8) we obtain

$$\upsilon_3^0 = a_{03} = b_{03} = 0;\ \ \upsilon_2^0 = 0;\ \ a_{02} = b_{02} = 0;$$

$$\upsilon_1^0 = -\varepsilon_1^0;\ \ \ b_{01} = 0;\ z_1 = 0;$$

$$\varepsilon_1^0 = \varepsilon_2^0 = b(\sec\gamma - 1);\ a_{01} = -\frac{\upsilon_1^0}{4}\cdot\frac{1+z_0}{1-z_0}$$

$$z_0 = b\left[(1-\cos\gamma)+\cos\gamma\right]^{-1};\quad b = Vctg\gamma;$$

Then parameters of the problem in domains 1, 2,3 (fig1, fig 2) are determined as the form

$$\left.\begin{aligned}
&\varepsilon_1 = \varepsilon_1^0 + k\varepsilon_1^0\cdot\frac{1}{2}\left[b_1(t-x_1)+x_1\right],\\
&\sigma_1 = \varepsilon_1^0(1-kt)+\frac{k}{2}\varepsilon_1^{(0)}\left[b_1(t-x_1)-x_1\right],\\
&\upsilon_1 = \upsilon_1^{(0)} - \frac{k}{2}\varepsilon_1^0\left[b_1(t-x_1)-t\right],
\end{aligned}\right\} \tag{2.9}$$

$$\varepsilon_2 = \varepsilon_2^0;\upsilon_2 = 0;\quad \sigma_2 = \varepsilon_2^0(1-kt);\quad \upsilon_1 = \frac{\partial u_1}{\partial t}; \tag{2.10}$$

$$\varepsilon_3 = 0;\upsilon_3 = 0;\quad \sigma_3 = 0;\quad \upsilon_2 = \frac{\partial u_2}{\partial t};\upsilon_3 = \frac{\partial u_3}{\partial t}, \tag{2.11}$$

$$b_1 = \frac{1+z_0}{1-z_0};\ b_3 = 1-\frac{1+z_0}{1-z_0}\cdot\frac{1}{2};\ b_4 = \frac{1}{2}\left(\frac{1+z_0}{1-z_0}-1\right);\ b_5 = b_1\cdot\frac{1}{2};$$

New domains arise as the form 5, 31, 21 (Fig 2) after reflection from the point B and gathering elastic waves at the point 0. We can easily show that the solution of the problem in domains 5, 31 will have the form (2.11) and in the domain 21 will have the form (2.10), respectively.

In this way, from the solutions found, it follows that if the first mode is satisfied in the wave front of a strong discontinuity then the string clings to the cheek of the impact wedge.

Let us now consider that the condition (1.11) is performed at the point A of discontinuity, i.e. there occurs slipping of the string particle at this point.

We should note that the slipping also occurs at the point B (fig. 1) and there is accepted the condition of deformation continuity at this point, i.e.it\s the condition

$$[\varepsilon] = 0, \quad x_1 = 0. \tag{2.12}$$

Then the solution of the problem in domains 1,2,3 once again is represented as the form (2.1), (2.2), (2.3), but constants, which take part in these solutions, are determined from conditions (1.6), (1.11), (1.12), (2.6), (2.7), (2.12).

It follows from conditions (2.6), (2.7) that

$$\upsilon_1^0 = -\varepsilon_1^0;\ b_{01} = 0; \tag{2.13}$$

$$\upsilon_3^0 = -\varepsilon_3^0;\ b_{03} = 0; \tag{2.14}$$

Considering solutions (2.1), (2.2), (2.3), (2.5) in conditions (1.6), (1.11), (1.12), (2.12) we define all unknown constants $\varepsilon_1^0, \varepsilon_2^0 = \varepsilon_3^0, \upsilon_2^0, z_0, z_1, a_{01}, a_{02}, b_{02}, b_{0,3}$ and we omit them because of their awkwardness.

Nevertheless, we note that a viscosity property of a material has an effect not only on stressful behavior of the material after impact but also it has visibly effect on the wave velocity of a strong discontinuity.

The wave velocity of a strong discontinuity is a diminishing time function.

We will construct below the solution of the problem for the time interval $1 \le t \le 2\ell$ i.e. there is emerge the domain 5, when the elastic wave reflects from the point «0» as the form K_1K_2 (fig.2). We have the condition

$$\upsilon_5 = \frac{\partial U_5}{\partial t} = 0, \quad x_1 = 0 \tag{2.15}$$

$$\upsilon_5(x,t) = U_3(x,t)\ 5-3 \tag{2.16}$$

We put new variables in the form down below for the solution of the problem in the domain 5

$$t - x_1 = \xi;\ t + x_1 = \eta \tag{2.17}$$

$$\xi_1 = \xi - 2l;\ \eta_1 = \eta \tag{2.18}$$

After some operations considering conditions (2.15), (2.16), the problem solution in the domain 5 has the form.

$$U_5(\xi_1,\eta)=\upsilon_3^0(\eta-\xi_1)+k\left[2b_{03}\frac{\eta^2-\xi_1^2}{2}+\frac{\upsilon_3^0}{2}\left(\frac{\eta^2-\xi_1^2}{2}-l(\eta-\xi_1)\right)\right] \qquad (2.19)$$

The solution of the $U_5(x,t)$ for variables x, t will be.

$$U_5(x,t)=2\ \varepsilon\ {}_3^0x+k\left[b_{03}.4(t-l)+\ \upsilon_3^0(t-2l)\right]x. \qquad (2.20)$$

then the particle velocity deformation ε_5 with respect to υ_5 and intensity σ_5 in the domain 5 will be in the form.

$$\left.\begin{aligned}&\varepsilon_5=2\varepsilon_3^0+k\left[4b_{03}(t-l)+\upsilon_3^0(t-2l)\right];\\&\upsilon_5=k\left(4b_{03}+\upsilon_3^0\right)x;\\&\sigma_5=\varepsilon_5-e^{-kt}\cdot k\int_0^t e^{kt}\varepsilon_5(x,t)dt\end{aligned}\right\} \qquad (2.21)$$

From the solutions received/gathered, it follows that a common feature of the research is that a viscosity property of a string has an effect on an increase of the deformation and on a decrease of velocity of the wave front particle of a strong discontinuity and on a stress in the string.

References

Mutallimov Sh.M. (2001) Wave dinamics of the flexible connectivity, Publ. «Elm», Baku, p. 267.

Rahmatulin H.A., Demyanov Yu. A. (1961) Strength on the intensity short – time loads, Phys. Math., M. p. 399.

Rahmatulin H.A, (1945) On cross secting impact on elastic string fir the great velocity, PMM,v.9, no.6, pp.449-462

Rahmatulin H.A., (1947) On the impact on elastic string, PMM, v.11, no.3, pp.379-386